Leonardo de Melo

POWDER JET PARTICLE DENSITY DISTRIBUTION ANALYSIS AND QUALIFICATION FOR THE LASER METAL DEPOSITION PROCESS

Dissertação submetida ao Programa de Pós-Graduação em Engenharia Mecânica da Universidade Federal de Santa Catarina para a obtenção do Grau de Mestre em Engenharia Mecânica.
Orientador: Prof. Dr. Ing. Walter Lindolfo Weingaertner.
Coorientador: Dipl. Ing. Stefan Mann.

Florianópolis
2015

Ficha de identificação da obra elaborada pelo autor,
através do Programa de Geração Automática da Biblioteca Universitária da UFSC.

de Melo, Leonardo
Powder jet particle density distribution analysis and qualification for the laser metal deposition process / Leonardo de Melo ; orientador, Walter Lindolfo Weingaertner ; coorientador, Stefan Mann. - Florianópolis, SC, 2015.
134 p.

Dissertação (mestrado) - Universidade Federal de Santa Catarina, Centro Tecnológico. Programa de Pós-Graduação em Engenharia Mecânica.

Inclui referências

1. Engenharia Mecânica. 2. Monitoramento de processos. 3. Deposição de metais a laser. 4. Metalurgia do pó. 5. Algoritmo e software. I. Weingaertner, Walter Lindolfo. II. Mann, Stefan. III. Universidade Federal de Santa Catarina. Programa de Pós-Graduação em Engenharia Mecânica. IV. Título.

Leonardo de Melo

POWDER JET PARTICLE DENSITY DISTRIBUTION ANALYSIS AND QUALIFICATION FOR THE LASER METAL DEPOSITION PROCESS

Dissertação submetida ao Programa de Pós-Graduação em Engenharia Mecânica da Universidade Federal de Santa Catarina para a obtenção do Grau de Mestre em Engenharia Mecânica.
Orientador: Prof. Dr. Ing. Walter Lindolfo Weingaertner.
Coorientador: Dipl. Ing. Stefan Mann.

Florianópolis
2015

Leonardo de Melo

ANÁLISE E QUALIFICAÇÃO DA DISTRIBUIÇÃO DE PARTÍCULAS EM FLUXO DE PÓ METÁLICO PARA O PROCESSO DE DEPOSIÇÃO DE METAIS A LASER

Este (a) Dissertação foi julgada adequada para obtenção do Título de "Mestre em Engenharia Mecânica", e aprovada em sua forma final pelo Programa de Pós-Graduação em Engenharia Mecânica.

Florianópolis, 26 de novembro de 2015

_____
Prof. Armando Albertazzi G. Junior, Dr. Eng.
Coordenador do Curso

Banca Examinadora:

_____
Prof. Walter Lindolfo Weingaertner, Dr.-Ing.
Orientador
Universidade Federal de Santa Catarina

_____
Prof. Rolf Bertrand Schroeter, Dr. Eng.
Universidade Federal de Santa Catarina

_____
Prof. Milton Pereira, Dr. Eng.
Instituto Federal de Santa Catarina

_____
Prof. Régis Henrique Gonçalves e Silva, Dr. Eng.
Universidade Federal de Santa Catarina

To my family and friends for all the support, motivation and love.

AKNOWLEDGEMENTS

I am very thankful to all the people who contributed to the development of this master thesis. I also would like to give special thanks:

To Prof. Dr. -Ing. Walter Lindolfo Weingaertner for the support, belief, advices and opportunities he gave me during all these years of co-working and friendship;

To Dipl. -Ing. Stefan Mann for the friendship we had during the years I worked at the Fraunhofer ILT and also for all the support and guidance he gave me – I express my sincere gratitude to him;

To Dipl. -Ing. Gehard Backes for the explanations, the good jokes and for sharing his vast experience in Laser Metal Deposition with me;

To Dipl. -Ing. Peter Abels and to all my colleagues of the Fraunhofer ILT for all the good moments we had;

To Dipl. -Ing. Christoph Franz who was one of my first friends in Germany and who helped me a lot during the time I was there;

To Prof. Dr. Eng. Rolf Schroeter and to all my colleagues at the Precision Engineering Laboratory – LMP for the support and motivation;

To my friends who were always with me (even when far away), for the motivation, the good times and the laughs we had and still have together.

Open the second shutter, so that more light can come in.

Johann Wolfgang von Goethe, 1832

RESUMO

A qualidade do processo de deposição de metais a laser depende de diversos fatores e componentes. Um dos componentes mais importantes é o fluxo de pó metálico. É necessário o monitoramento contínuo das diferentes variáveis e parâmetros que influenciam no fluxo de pó para se garantir os altos padrões de qualidade e estabilidade requeridos nas peças produzidas. Este monitoramento é realizado através de técnicas de controle de processos, onde o fluxo de pó metálico é iluminado lateralmente, por um laser de iluminação em formato de linha, e gravado por uma câmera coaxial ao bocal alimentador de pó. Simetria, geometria e posição de diferentes níveis do fluxo de pó podem ser analisados através de algoritmos relevantes. Tais algoritmos tornam possíveis também cálculos da distribuição das partículas no fluxo, através da sobreposição de imagens de todos os *frames* gravados no vídeo em cada nível do fluxo de pó. O processo de medição e análise foi testado com sucesso em diferentes bocais alimentadores de pó e com diferentes materiais e parâmetros do fluxo, tornando possível sua caracterização e qualificação.

Palavras-chave: deposição de metais a laser, distribuição de partículas em fluxo de pó, bocal alimentador de pó, controle de processos.

ABSTRACT

The quality of the Laser Metal Deposition process depends on several factors and components. One of them and also one of the most important is the powder jet. Regular monitoring of the different variables involved on the powder jet need to be performed in order to assure the demanded high stability and quality standards of the produced coating layers. This monitoring is done through process monitoring techniques, where the powder jet is illuminated from the side, by a laser line, and recorded by a coaxially aligned camera through the powder feed nozzle. Symmetry, geometry and position of different levels of the powder jet can be analyzed through relevant algorithms. They also provide calculations of the particle density distribution the recorded images. The spatial particle density distribution of the powder jet can be calculated by superimposing individual levels along the jet. The measurement and monitoring principle was successfully tested with various nozzles and powder properties, making it possible to fully characterize a powder jet.

Keywords: laser metal deposition, powder particle distribution, powder feed nozzle, process control.

RESUMO EXPANDIDO

INTRODUÇÃO

O processo de deposição de metais a laser (*Laser Metal Deposition* – LMD) é uma maneira eficiente de melhorar as propriedades mecânicas de determinados componentes, através da aplicação de materiais de propriedades superiores, visando reduzir a perda de material por corrosão e desgaste. É aplicado potencialmente na indústria aeronáutica, reduzindo custos de reparos ou manufatura de pás de turbinas e compressores.

As partes produzidas por este processo são em geral peças de alto valor, com geometrias complexas e altos padrões de qualidade e exigências funcionais e de segurança. Desta forma, para que se alcance tais padrões e requerimentos, o monitoramento e o controle preciso de parâmetros e condições do processo é fundamental. Uma das causas de erros de processo e também um dos componentes de maior importância nele é o fluxo de pó metálico, gerado pelo bocal alimentador de pó. A qualificação e uma maior confiabilidade destes alimentadores agrega valor ao processo e garante o alcance dos resultados desejados.

O desenvolvimento de um sistema de medição que possa caracterizar e qualificar ambos componentes (fluxo de pó e bocal alimentador) de maneira automatizada, confiável e reprodutível, representa um grande avanço nas técnicas de controle do processo de LMD e uma melhoria de sua qualidade e eficiência na indústria.

OBJETIVO

O fluxo de pó metálico junto do laser de trabalho e do bocal alimentador de pó são elementos cruciais para boa execução do processo de deposição de metais a laser. Tendo em vista os altos padrões de qualidade impostos sobre as partes produzidas por este processo, o monitoramento regular da eficiência e funcionalidade do sistema e seus componentes deve ser feito de maneira padronizada e reproduzível. Neste trabalho, um sistema de monitoramento capaz de reproduzir medições e caracterizar o fluxo de pó metálico e o bocal alimentador de pó é desenvolvido. Este sistema tem como objetivo melhorar a qualidade do processo e das partes produzidas, o tornando mais confiável e aumentando o valor de mercado dos bocais fabricados (são testados e qualificados para funcionar nas condições os quais foram especificados).

METODOLOGIA

A fim de se obter dados relevantes para análise do fluxo de pó, um sistema de medição foi desenvolvido utilizando-se de técnicas de monitoramento de processos. O sistema é composto de um conjunto óptico de lentes e filtros acoplados a uma câmera que monitora, de maneira coaxial, por através do bocal alimentador de pó, as partículas que formam o fluxo de pó metálico. Tais partículas são iluminadas por uma fonte de laser de iluminação com formato de linha, posicionada lateralmente ao fluxo de pó. As partículas são fornecidas por um sistema de alimentação de pó que é conectado ao bocal. As imagens gravadas por um software através da câmera e transmitidas para um computador industrial acoplado ao sistema.

O aparato é externo ao sistema de deposição de metais a laser, ele se utiliza de uma estrutura similar a deste processo, de forma que apenas o material (pó) e o bocal alimentador, que serão de fato utilizados no processo industrial, são trocados a cada nova medição.

A Figura 1 mostra na esquerda o modelo em CAD do sistema e na direita o sistema real após sua montagem. Para segurança do operador, o sistema fica enclausurado em uma caixa fechada por uma porta que filtra a radiação laser específica no comprimento de onda utilizado no laser de iluminação. Um sistema de exaustão também foi acoplado, de forma que as partículas de pó tenham um destino apropriado, visto que são nocivas à saúde do operador.

Figura 1 – Modelo do sistema (esquerda) e sistema real desenvolvido.

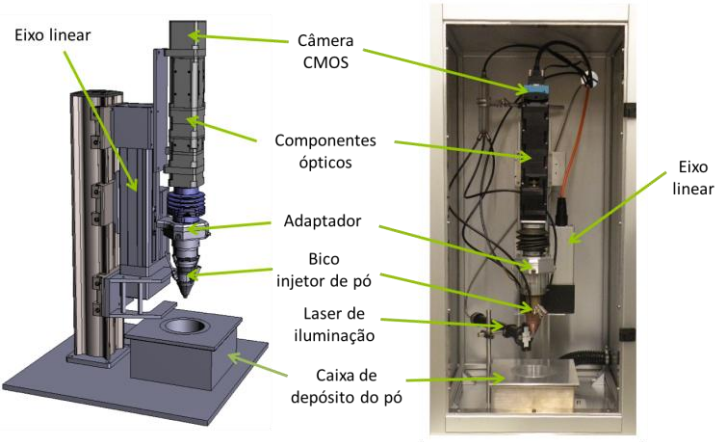

Fonte: Autor.

O procedimento de medição se inicia com a gravação de imagens das partículas de pó em fluxo de pó metálico de maneira coaxial. A Figura 1 mostra também o posicionamento coaxial da câmera CMOS em relação ao bocal e por consequência também o fluxo. Tal câmera monitora as reflexões do laser de iluminação na superfície das partículas. Após as imagens serem gravadas, os *frames* são processados por um algoritmo específico, desenvolvido para esta aplicação. Tal processamento se dá a partir uso do software MATLAB® e Simulink®, onde cada frame é convertido em imagens binárias e informações das partículas e do fluxo em geral são obtidas, como resultados de cada medição.

RESULTADOS

O sistema de medição desenvolvido tem como resultado principal imagens e parâmetros do fluxo de pó metálico necessários para sua avaliação e caracterização. A partir destes resultados, é possível de se qualificar o fluxo como apto ou não para o processo, de forma com que ele traga todas as características desejadas compatíveis com a qualidade requerida às peças e camadas produzidas.

Entre os principais parâmetros obtidos a partir da análise das imagens pelo algoritmo desenvolvido, estão o diâmetro e a posição do foco do fluxo de pó metálico. Estes têm forte influência nos resultados produzidos pelo processo de deposição de metais a laser.

A Figura 2 mostra exemplos de resultados apresentados pelo sistema, fundamentais para posterior análise dos parâmetros específicos do fluxo. A imagem superior mostra alguns níveis do fluxo logo após realizada uma medição, podendo-se identificar de antemão a posição do foco no nível 06 (menor diâmetro). A posição em milímetros do nível do foco até a saída do bocal alimentador de pó pode ser obtida correlacionando-se os parâmetros utilizados no software de medição. Ainda na Figura 2, a imagem em 3D (inferior) representa a distribuição da densidade de partículas no nível do foco. É notável a maior densidade na parte central do fluxo, onde as partículas se encontram e colidem.

Imagens e matrizes obtidas pelo software de medição após cada procedimento fornecem as informações necessárias sobre o fluxo de pó assim como garantem que o bocal utilizado está em condições de uso para reprodução dos resultados desejados.

Figura 2 – Exemplo de resultados apresentados pelo software de medição.

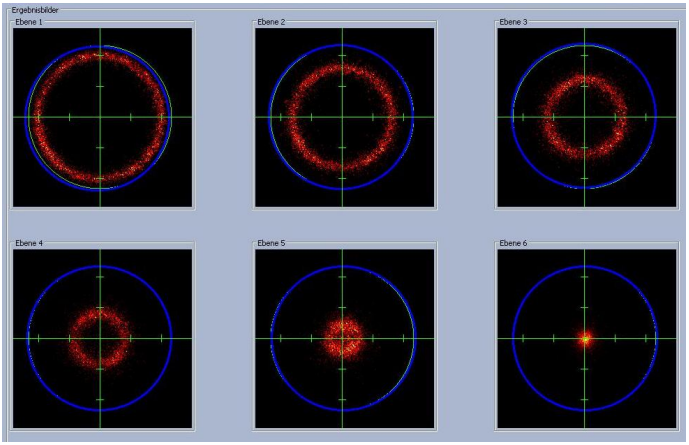

3D – distribuição da densidade de partículas

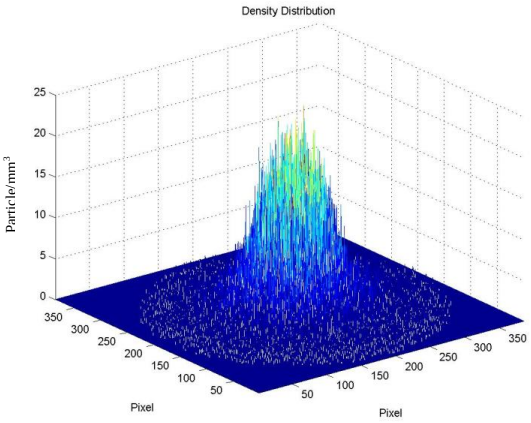

Fonte: Autor.

Os resultados obtidos neste trabalho promoveram um avanço nos estudos do processo de LMD, permitindo melhor conhecimento das variáveis e fatores que influenciam o processo, assim como aumento no valor agregado do bocal alimentador de pó, maior qualidade do fluxo de pó metálico e melhores resultados produzidos durante o processo na indústria.

LIST OF FIGURES

LIST OF TABLES

LIST OF ABBREVIATIONS

AKL	Aachener Kolloquium für Lasertechnik
BLISK	blade integrated disks
CAD	computer-aided design
CAM	computer-aided manufacturing
CD	compact disk
CG	carrier gas
CMOS	complementary metal-oxide-semiconductor
CO_2	Carbon dioxide
CPC	coaxial process control
CVD	chemical vapor deposition
DC	direct current
DLD	direct laser deposition
DLF	direct laser fabrication
DMD	direct metal deposition
DMLD	direct metal laser deposition
DSLR	digital single-lens reflex
EUV	extreme ultra violet
HAZ	heat-affected zone
HPDL	high-power diode laser
I/O	input and output
ICTM	International Conference on Turbomachinery Manufacturing
IEC	International Electrotechnical Commission
ILT	Institute for Laser Technology
LAM	laser additive manufacturing
LBAM	laser-based additive manufacturing
LDW	laser deposition welding
LED	light-emitting diode
LIBS	Laser induced breakdown spectroscopy
LMD	laser metal deposition
LMP	Precision Engineering Laboratory
LPD	laser powder deposition

P.E.	powder efficiency
PVD	physical vapor deposition
SDM	shape deposition manufacturing
SEM	scanning electron microscope
SFF	solid freeform fabrication
SG	shielding gas
SLL	solid state laser
SLM	selective laser melting
SLS	selective laser sintering
SLSM	selective laser sintering of metals
SSL	solid state laser
UFSC	Federal University of Santa Catarina

LIST OF SIMBOLS

ß	angle with vertical axis [˚]
d_p	core diameter of powder jet focus [mm]
f_p	distance from nozzle tip to focus point [mm]
l	standoff distance [mm]

CONTENTS

INTRODUCTION

There are many different processes involving laser technology, most of them well established in the international and Brazilian markets. When compared to similar conventional processes, some of the laser ones offer relevant advantages regarding material properties, consumption and process efficiency.

The Laser Metal Deposition process (LMD) is a cost-effective way to increase the mechanical properties of a part reducing its material loss by corrosion and wear. It is potentially applied in the aircraft industry, leading to cost reduction for the design or re-design, manufacturing and repair of new or existing aero engine parts such as compressors, turbine and combustor casings, static parts, centrifugal compressors, small INCONEL® parts, BLISKs (Blade Integrated Disks), vanes and blades. Essentially, the process uses a 3-dimensional CAD model, divided into layers of definite thickness that provides the geometrical data required to the fabrication of the desired parts. This geometrical information is transferred to each layer using the laser beam to melt the added material, in this particular case, powder material, by a repeating process of applying new layers [1, 2].

The produced parts are usually high-value parts, with complex geometry and high safety standards, fulfilling very high quality and documentation requirements. Therefore, it is necessary to ensure these quality standards monitoring the process, analyzing the parameters and equipment used. The properties of the powder jet, which is delivered to the melt pool via the nozzle, are crucial elements in the LMD process.

The nozzle has a tapered powder jet, which forms a focus and then widens again. It can be adjusted usually to change the focus diameter, the powder distribution in the beam and the spatial position and extent of focus from the exit. Nowadays, each adjustment or alignment is documented by photographing the powder jet laterally. Such visual inspection requires advanced experience in the area. Due to high process stability and quality requirements of the LMD, frequent processing result checking is mandatory. Nozzle wear can lead to deviations that cause several changes in the diameter and position of the powder focus, as well as a poor orientation of the powder jet with the laser beam. Until now, the only way of determining these changes was to use laser deposition welding to obtain reference samples. Correlating these samples with comparative deposition welds revealed the quality of the nozzle [3, 4].

The most important variables of the powder jet that need to be regularly monitored are:

- Powder jet symmetry;
- Powder jet focus position relatively to nozzle and laser beam;
- Diameter of powder jet focus (size);
- Powder jet density distribution.

This work is about a system able to perform a standardized and reproducible characterization of powder feed nozzles, measuring and monitoring the above-related variables. Process control techniques, with the appliance of sensors, high-speed cameras, proper illumination (using lasers) and relevant algorithms to evaluate the produced images are applied on these measuring process. Although this procedure is carried out in a pre-process stage, with no use of the working laser, parameters of the laser beam are considered.

The innovative scope of this measurement process made it more difficult to be accomplished due to limited practical information available in the literature.

The cooperation between the Fraunhofer Institute for Laser Technology ILT, in Aachen – Germany, and the Precision Engineering Laboratory LMP, from the Federal University of Santa Catarina UFSC, in Florianópolis – Brazil made this master thesis possible to be executed. The institute's structure and expertise were key points to the achievement of the desired results. The measurement process can fully characterize a powder jet, being experimented in different kinds of powder feed nozzles.

1.1 OBJECTIVES

1.1.1 General objectives

The main objective of this work is to develop a monitoring system able to qualify and characterize the powder jet and powder feed nozzle for the LMD process, allowing the manufacturing of more reliable nozzles, providing enough information and parameters to the improvement of process efficiency, material consumption and produced parts' quality.

1.1.2 Specific objectives

- Define a mechanical and optical setup for the monitoring system;
- Develop an automated measurement procedure with a mobile system – can be transported and execute measurements locally where the LMD process occurs;
- Develop an algorithm to evaluate relevant information from the powder jet, provided by the monitoring system;
- Develop a software able to control the system and to execute automated experiments;
- Specify and define quality parameters for the powder jet;
- Check methodology and system reliability (hardware and software);
- Develop a system able to reproduce experiments and results.

2 LITERATURE REVIEW

2.1 LASER TECHNOLOGY

The word laser is an acronym for “Light Amplification by Stimulated Emission of Radiation”. A laser is a device that amplifies light and produces a highly directional and high-intensity beam [5 ,6]. Radiation from a laser is amongst the purist spectral forms of radiation available. It is considered monochromatic, i.e. it is pure in color (wavelength or frequency) or, in other words, it has a narrow frequency bandwidth [7].

A laser beam is a light beam (electromagnetic radiation) with particular properties. The laser light has specific wavelengths, depending on the kind of laser, which varies from infrared, to visible or to the ultraviolet field, in the electromagnetic spectrum.

What differs the laser to other conventional light sources is the way it is generated, which brings numerous applications to laser systems.

[6] classifies the laser light into the following wavelength regions:

- Far infrared: 10000 to 1000000 nm;
- Middle infrared: 1000 to 10000 nm;
- Near infrared: 700 nm to 1000 nm;
- Visible: 400 to 700 nm;
- Ultraviolet: 200 to 400 nm;
- Vacuum ultraviolet: 100 to 200 nm;
- Extreme ultraviolet: 10 to 100 nm;
- Soft X-rays: 1 nm to approximately 20–30 nm (some overlap with EUV).

Industrial lasers for material processing, like Nd:YAG, Diode and Fiber lasers are in the range of 1000 nm. CO_2 lasers are in another wavelength range, at 10000 nm [6].

Figure 1 shows an illustrated version of the classification above.

Figure 1 – Spectrum of electromagnetic radiation.

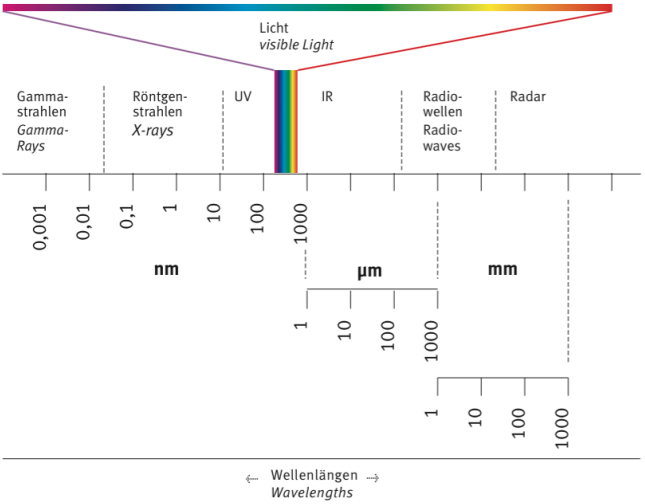

Source: [8].

One of the laser principles is the stimulated emission. It occurs when an incoming photon stimulates an excited atom or ion to undergo a transition from excited state to the ground state [9]. The stimulation of the excited atom or ion by the photon makes it to produce other photons, which have the same direction and wavelength [10].

Various processes occur inside the laser system to increase or amplify light signals, after those signals have been generated by other means. It consists basically of an active/gain (amplifying) medium, where stimulated emission occurs, and a set of mirrors to feed the light back into the amplifier for continued growth of the developing beam [6].

Figure 2 shows a schematic of a typical laser, with a pair of optically parallel mirrors, where one of them is highly reflecting and the other one partially transmitting. There is also an energy source to pump the active medium.

Figure 2 – Schematic of a typical laser.

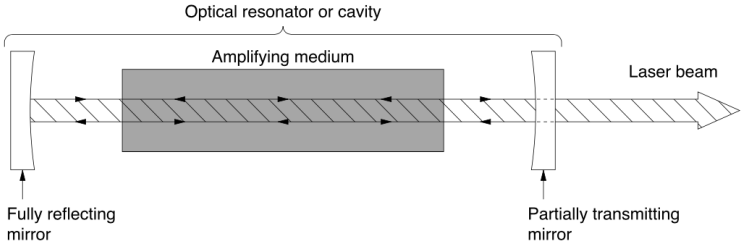

Source: [6].

The gain media may be solid, liquid, or gas and it has the property to amplify the amplitude of the light wave passing through it by stimulated emission. It is used to place between pair of mirrors in such a way that light oscillating between mirrors passes every time through it and after attaining considerable amplification emits through the transmitting mirror.

The optical resonator or cavity, as shown in Figure 2, is an arrangement of optical components which allows a beam of light to circulate in a closed path so that it retraces its own path multiple times, in order to increase the effective length of the media and also increase the beam energy. Combination of optical resonator with active medium is known as optical oscillator [11].

Considering all elements involved in a laser machine, there are many optical and electrical components involved. Figure 3 shows an assembly example of a Nd:YAG laser system, where diverse optical and mechanical components can be identified.

Figure 3 – Assembly of various components of a Nd:YAG laser system.

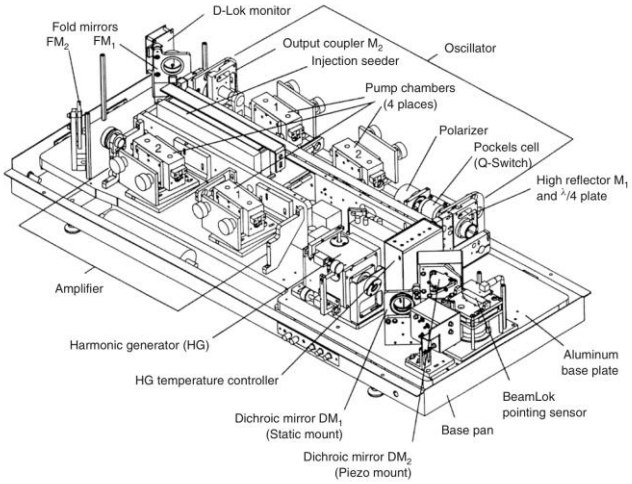

Source: [11].

Process, work piece and automation level can define how complex a laser system will be. The laser medium together with cooling and power supply generates the laser beam, which is just the heart of a laser system [10]. Focusing optics, working station, controlling and safety equipment complete the system, as shown in Figure 4.

Figure 4 – Schematic of a complete laser system.

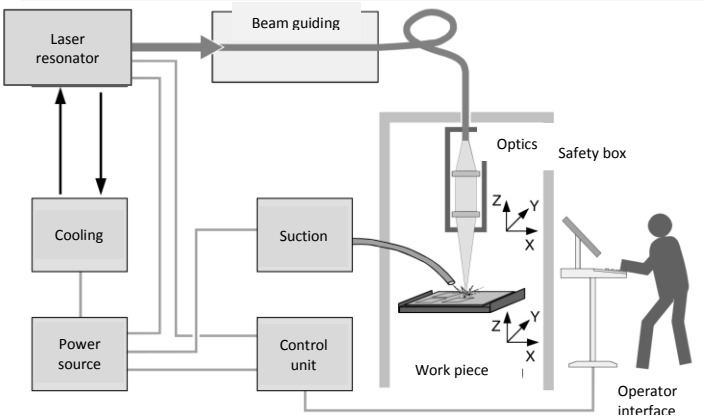

Source: [10].

2.1.1 Laser radiation properties

The light produced by lasers has several valuable characteristics different from other conventional light sources, which make it suitable for industrial, scientific and technological applications. These are some of the important properties of the laser light:

- **Monochromacity**: single color or monochromatic light sources are defined by waves of light in a single frequency of vibration or a single wavelength. Practically, there is no natural monochromatic source of light [11];

- **Divergence / Parallelism**: a laser beam is very directional, which implies laser light is of very small divergence. The laser output is in the form of an almost parallel beam, being able to carry, for example, energy and data for long distances for remote diagnoses and communication purposes. An ideal laser would have a perfectly parallel beam, and its diameter at the exit window should be same to that after traveling very long distances, although in reality, it is impossible to achieve [11, 12];

- **Coherence**: the laser light is called coherent because there is a fixed phase relationship between the electric field values at different locations or at different times. Its coherence can be spatial or temporal [9];

- **Brightness**: Lasers are more intense and brighter than other conventional sources, since it produces high levels of power in very narrowly collimated beams. Brightness is a measure of light intensity at a particular location, being defined as the power emitted per unit surface area per unit solid angle. It depends on the intensity of the source and the extent to which the light diverges after leaving the it [11, 12, 13];

Another important feature of the laser beam is that it can be focused to different sport sizes, with the use of lenses, varying its beam size and energy [11].

2.1.2 Types of lasers

There are different types of laser, with specific active media and a wide variety of applications. Laser type selection must be well performed so that the process results can be achieved. Each material to be worked with reacts in a specific way to the laser wavelength during process.

The main types of lasers are listed in Table 1, described with its active medium, wavelength and typical application.

Table 1 – Types of lasers and its common applications.

Type of laser	Active medium	Typical laser and wavelength	Typical application area
Gas	Gas or mix of gases	Carbon Dioxide (CO_2) – 10,6 µm	Cutting and welding of metals Also hardening and marking
Solid state	Doped crystals or glasses	Nd:YAG – 1,064 µm Yb:YAG – 1,03 µm Yb:Glas – 1,05 – 1,1 µm Nd:YLF – 1,047 µm	Welding, cutting, soldering and marking Also structuring, drilling and cleaning
Diode	Semiconductors	GaInP – 0,67 – 0,68 µm GaAs – 0,78 – 0,98 µm	Soldering, hardening and heat conduction welding Also used as pump source for solid state lasers
Fiber	Doped optical fiber	Ytterbium Fiber Lasers – 1,07 µm	Welding, cutting, micromachining, marking, sintering and soldering

Source: [10].

The table lists some of the most typical lasers in the industry and research areas.

2.1.3 Laser applications

Lasers are suitable for a wide variety of applications, interacting with materials in different ways, depending on wavelength and beam properties.

The following list shows some usual laser applications:

- Cutting;
- Welding;
- Heat Treatment;
- Marking and Scribing;
- Cleaning;
- Polishing;
- Drilling;
- Ablation
- Laser Metal Deposition;
- Rapid prototyping and manufacturing;
- Micro and Nano Structuring;
- Ultrashort Pulse Processing;
- Heat Treatment;
- Spectroscopy;
- Medical and biophotonics technology;
- Measurement technology.

Each application can be performed within a set of laser systems available in the market. Hybrid processes also takes the advantages of using the laser with conventional processes together.

Researches have also been carried on, in order to develop new laser types, improve power, modularibility and cover more types of applications. It is interesting to see the development of laser processes during several years, making the laser technology relevant in many current societal trends, such as mobility, health, energy or environment [14]. Figure 5 shows the growth of laser applications in the last 45 years.

Figure 5 – Growth of laser applications in the last 45 years.

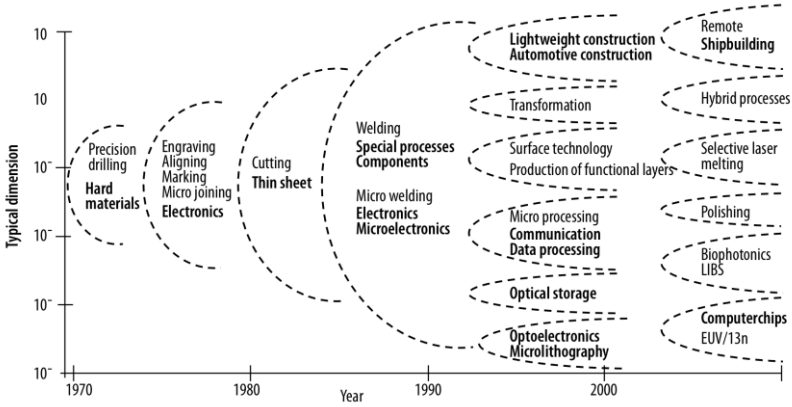

Source: [14].

2.1.4 Laser safety

Lasers are a universal tool, but they can also have a high complexity of possible hazards related with their use.

The ‘light’ from powerful lasers can be concentrated to power densities (power per area or watts/cm2) that are high enough to evaporate tissue, metal or ceramics. The eyes are at increased risk since they are more sensitive to the light. It is possible to cause irreversible damages to the eyes with just one glance into a direct or reflected laser beam [8].

A systematical approach to laser safety is not limited to the hazards of and the protection against laser radiation. It includes all parts of the laser installation – electric devices, laser gases, optics, handling devices, screens etc. Furthermore, emissions – such as fumes, gases or UV radiation generated by the interaction of the laser beam with materials or the atmosphere – must be taken care of [15].

There are primary and secondary hazard potentials related to the laser beam. Primary hazards are designated as laser-related hazards while secondary are subdivided in direct and indirect hazards.

Direct hazards caused by technical components of the laser installation and indirect hazards are generated by the interaction of the laser with materials or the atmosphere [15]. Figure 6 shows this classification and its related application and devices.

Figure 6 – Hazard potentials for laser-material interactions.

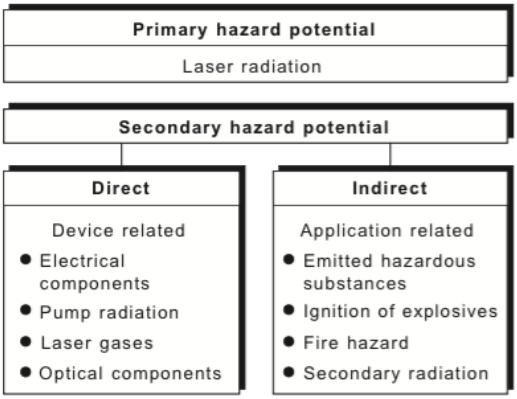

Source: [15].

There are many laser-related norms and standards, which describe a number of fundamental directives and guidelines about laser safety and a safe workplace.

The workplace must be properly signed and protected, informing internal and external users about the laser radiation that is being used.

Because of the wide ranges possible for the wavelength, energy content and pulse characteristics of a laser beam, the hazards arising in its use vary widely. Therefore, it is impossible to regard lasers as a single group to which common safety limits can apply [16]. According to EN 60825-1:2001 and ANSI Z136.1:2007 lasers are classified regarding its relative hazards [17]. The Table 2 provides a summary of this classification, also described in several sources available in the literature, as [8, 16, 17].

Table 2 – Classification of lasers and LED sources.

Class	Definition	Warning label
1	Intrinsically safe for continuous viewing. Includes embedded products that totally enclose a higher classification of laser, e.g., CD players, laser printers and most production industrial laser material processing machines	None
1M	Low risk to eyes. No risk to skin. Safe, provided binoculars, etc., are not used for viewing	"Laser radiation. Do not view directly with optical instruments"
2	Low risk to the eyes. No risk to the skin. Visible radiation in which protection is by blink reflex (0.25 s), <1 mW CW laser	"Do not stare into the beam"
2M	Low risk to the eyes. No risk to the skin. Same as for class 2 except binoculars and telescopes are not to be used to directly view the beam	"Do not stare into the beam or view directly with optical instruments"
3R	Low risk to eyes. Low risk to skin. Protection by blink reflex. The output accessible emission is up by a factor of 5 on that for class 1 or class 2 lasers	0.4-1.4-mm wavelengths: "avoid direct eye "exposure". Other wavelengths: "Avoid exposure to the beam"
3B	Medium risk to the eyes. Low risk to the skin. Direct or specular reflection exposure of the eyes is hazardous, even allowing for the blink reflex. Skin damage is prevented by natural aversion. Not a diffuse reflection or a fire hazard	"Avoid exposure to the beam"
4	High risk to the eyes and skin. May cause a fire. Standard safety precautions must be observed	"Avoid eye or skin exposure to direct or scattered radiation"

Source: [8, 16, 17].

2.2 LASER METAL DEPOSITION

Functional surfaces are a key factor for the quality, efficiency, and competitiveness of products and processes that are subject to complex strains and stresses. Tailor-made materials and procedures ensure resistance to abrasion, erosion, and corrosion, which are factors that significantly influence the service life and life cycle of plants and equipment [18].

Laser cladding or Laser Metal Deposition is an established standard for the specific adaptation of surface properties to the requirements of their specific fields of application [18]. Surface qualities, related to mechanical properties, can be improved, such as hardness, wear and erosion resistance, or chemical properties such as corrosion resistance [19].

Continuous wave lasers with power ranges up to 18 kW are used on automated machines with three or more axes, enabling 3D laser metal deposition. Examples are CO_2, solid state lasers SSL (either lamp-pumped Nd:YAG, fiber, or disc lasers) and high-power diode lasers (HPDL) [20].

LMD uses a laser beam to melt another material which has different metallurgical properties on a substrate, whereby only a very thin layer of the substrate has to be melted in order to achieve metallurgical bonding with low dilution of added material and substrate, in order to maintain the original properties of the coating material. Dilution is considered to be the mixing percentage of the substrate to the clad region [21, 22].

Essentially, a 3-dimensional CAD model, divided into layers of definite thickness, provides the geometrical data required to the fabrication of the desired parts. This geometrical information is transferred to each layer using the laser beam to melt the additive material by a repeating process of applying new layers [23].

A great variety of materials can be deposited on a substrate using laser cladding by powder injection to form a layer with thicknesses ranging from 0.05 to 2 mm and widths as narrow as 0.4 mm [24].

The literature shows several different nominations for this process technology, regarding the mechanisms of adding one or multiple thin layers of powder particles melted by a laser heat source on a substrate.

Ways of naming laser cladding for coating applications are exampled in [24], where researches use the term “laser coating”, “laser powder deposition” or “laser surfacing”.

Rapid prototyping applications or layered manufacturing applications show another range of names being used to describe the same technology. In prototyping by pre-placed powder the technology is called “selective laser sintering of metals (SLSM) or “direct metal laser sintering” [24].

Techniques of fabricating 3D items by progressively adding and consolidating progressive amounts of feedstock materials at precise locations, layer by layer, without any supporting preform or mask, by means of laser or other technologies, as Solid Freeform Fabrication (SFF) are described in [25]. Inside these techniques, when considering powder as feedstock material, two processes are mostly correlated: selective laser sintering (SLS) and laser cladding [25].

Other acronyms frequently used in the literature are:

- Direct Metal Deposition – DMD [26, 27, 28, 29];
- Direct Laser Deposition – DLD [28, 30];
- Direct Metal Laser Deposition – DMLD [31];
- Direct Laser Fabrication – DLF [32];
- Shape Deposition Manufacturing – SDM [33];
- Laser Metal Deposition – LMD [20, 34, 35, 36, 37, 38];
- Laser Powder Deposition – LPD [25];
- Laser-based Additive Manufacturing – LBAM [39];
- Laser Deposition Welding – LDW [40].

Although the diversity of names in use to describe the technology, the process will be named “Laser Material Deposition (LMD)” through this work.

Different literature sources, as an example of [37], show the LMD as a Laser Additive Manufacturing (LAM) technique, which involves near-net-shape processes with serial powder (or wire) material and no additives like binders. The current demand on energy efficiency, lightweight, wear and corrosion resistant high-value components offer a great opportunity to the development and implementation of LAM [23, 37].

Although LAM processes share the same material additive manufacturing philosophy, each LAM process has its specific characteristics in terms of useable materials, processing procedures and applicable situations [37].

LAM techniques are mainly classified in two kinds of processes:

- Two-stage process: with pre-placed adding material on site;
- One-stage process: the feed material is conducted simultaneously with the laser beam to the melt pool, on the form of powder or wire.

In both methods the laser moves and melts the additive material that rapidly re-solidifies to form a shape. In order to cover larger surfaces, overlapping tracks can be made [41].

2.2.1 Two-stage process

The first stage of the two-stage process, involves the application of an additional material powder layer on the substrate. In the second step of the process the laser beam melts the material creating a melt pool in the top surface. This melt pool expands to the interface with the substrate due to heat conduction. The heat penetrates the substrate causing a fusion bond. This method also describes the Selective Laser Melting (SLM) process in which there is a "powder bed" on the substrate surface [24, 42].

Controlling the heat in these kinds of process is very important in order to prevent high dilution [24].

Figure 7 shows a schema of the two-stage process, representing the laser beam, preplaced material and clad layer.

Figure 7 – Two-stage process, with preplaced powder layer.

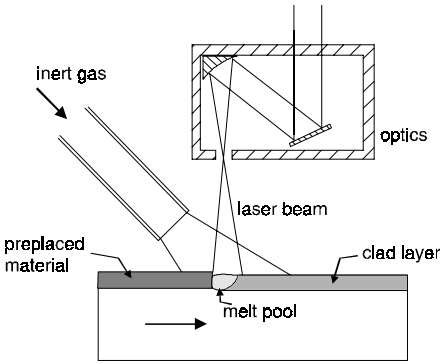

Source: [42].

In SLM, a 3D-CAD model provides the geometrical data necessary to construct the entire part. The model is sliced into layers with specific thickness where the laser will melt the deposited powder material. After cooling down and solidifying, the part in production is lowered by the amount of a layer thickness and a new powder bed is applied, being exposed to the laser radiation again, repeating the process until the entire part is defined [21]. This procedure is represented in Figure 8.

Figure 8 – Example of two-stage LAM procedure - SLM.

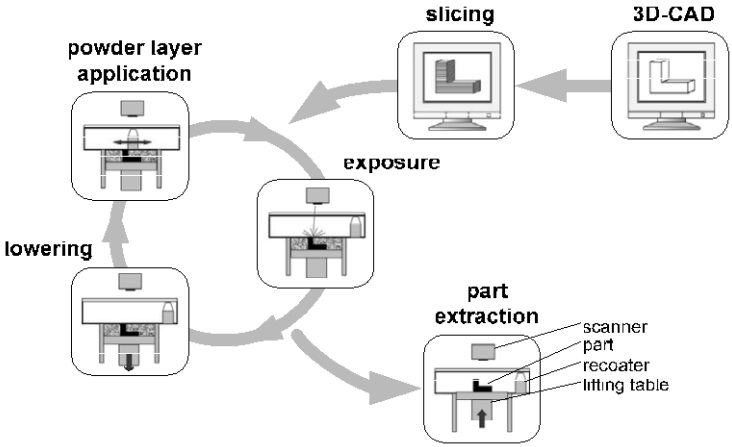

Source: [21].

2.2.2 One-stage process

Laser Metal Deposition process can be characterized as a one-stage process.

Some of the most important physical fundamentals of the LMD are [43]:

- Absorption of the laser beam;
- Heat conduction;
- Melt pool dynamics;
- Powder jet properties;
- Carrier and shielding gas flow and properties;
- Rapid solidification.

In the one-stage process, the feed material is added simultaneously to the laser beam, forming the melt pool and creating a strong fusion bond with the substrate [42]. Feeding materials are available as powder or wire.

Powder feeding can be performed in two methods: coaxial or lateral. Coaxial powder supplying is integrated in the optical system being independent of the process direction while lateral supplying needs to be adapted. Powder particles with a typical size from 5 to 120 µm are carried to the substrate surface and also melting point by the inert gas, which also has the effect of shielding gas, providing oxidation protection to the molten material and to the heat-affected zone (HAZ) [27, 42, 44].

Coaxial powder injection is also classified in continuous (a powder jet cone is produced that encloses the laser beam) and discontinuous (three or more powder jets are fed coaxially to the laser beam) (see more in section 2.4 POWDER FEED NOZZLES) [27].

Assuming the laser can provide enough energy, all particles that reach the molten pool are melted and fused to the substrate; whereas, the others ricochet and are lost. The laser beam melts a thin layer of the substrate's surface thanks to the very local heat-affected zone. Typical HAZ are about one-tenth of millimeter to one millimeter [20, 27].

Figure 9 shows coaxial and lateral methods of powder feeding. When the process is performed using wire as additive material, the same scheme of lateral powder feeding can be used, applying the wire instead of the powder.

CO_2, solid state lasers (SSL - either lamp-pumped Nd:YAG, fiber, or disc lasers) and high-power diode lasers (HPDL) are used for laser metal deposition. Due to the higher absorptivity and the higher process efficiency of the shorter wavelengths of the SSL and HPDL, these lasers are entering more and more into the LMD market [20].

More detailed information about the powder jet and the way powder particles are carried to the melt pool are available at section 2.3 POWDER JET, in this work.

Figure 9 – Powder feeding methods – coaxial (left) and lateral (right).

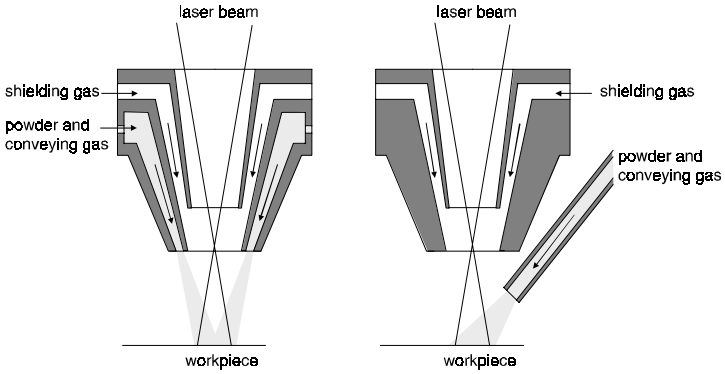

Source: [42].

Wire feeding is mostly applied in situations where the geometry favors one single clad, such as rotationally symmetric components. The nozzle must be close to the working area to permit an exact wire supply into the laser spot. It is also possible to apply preheating into the wire to enhance the process efficiency [45, 46].

A comparison between the one and two-stage methods shows that the one-stage offers more flexibility regarding the surface geometry being not just limited to flat surfaces. Furthermore, the one-stage method allows larger areas, which require the application of several adjacent tracks, to be produced with less dilution and coating thickness can be varied on-line by controlling the material feed rate [42].

2.2.3 Applications

The LMD utilizes a laser heat source to deposit a layer of a desired metal on a substrate [24]. As mentioned, depending on the application, several layers can be deposited constructing complex geometries.

This technology has been widely adopted to provide wear and corrosion resistant layers on machine parts, to repair and modify costly worn parts like injection molds and turbine components and to process distortion vulnerable components [23].

Large area surface cladding and coating is applied in the industry using welding or thermal spraying techniques. In this field, despite de noticeable technological advantages of the laser process, it suffers the

disadvantage of being comparatively slow and cost intensive. When the cladding is only required locally, the laser process may be economically competitive [47].

In exhaust gas turbochargers, sufficient material is welded onto the curved surface of the turbine blade using the laser, and the original geometry is then restored by grinding or milling. The welding tracks are generated on the basis of the CAD model available in the CAD system [48]. Some strategies for developing near-net shape LMD of blade root and blade wing are described in [35]. Figure 10 shows an example of blade repair (left) and blade root and wing construction.

Figure 10 – Turbine blades tip repair and construction by LMD.

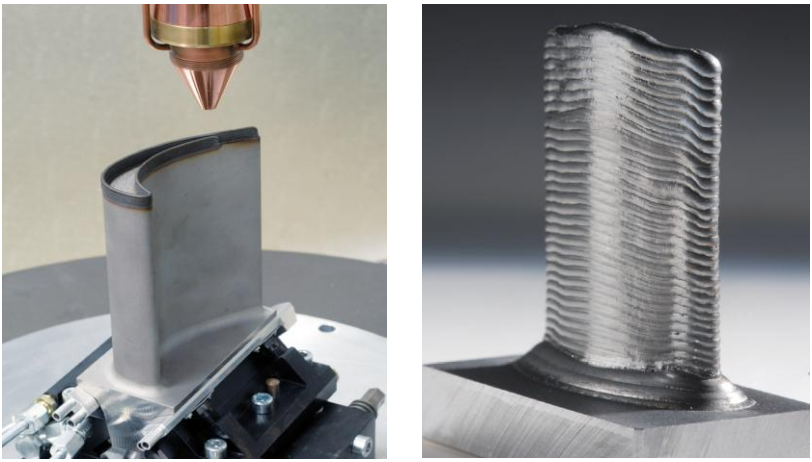

Source: [49].

The manufacturing of BLISKS (Blade Integrated Disks – see Figure 11) is also a strong application of LMD. Due to the integrated lightweight structure of them, they are increasingly being used in compressors of advanced gas turbine engines for improved performance and efficiency. Advantages are the larger airfoil size, increased number of airfoils on a diameter and reduced weight (up to 30% according to Rolls-Royce), all in comparison to conventional rotating disks [35].

On conventional processes, during the manufacturing of an entire BLISK, approx. 70% of the input material is removed in various time-consuming process steps [49]. This is extremely costly in terms of raw material and labor expense.

Figure 11 – Low-pressure compressor totally made of BLISKS (left) and detail of a BLISK (right).

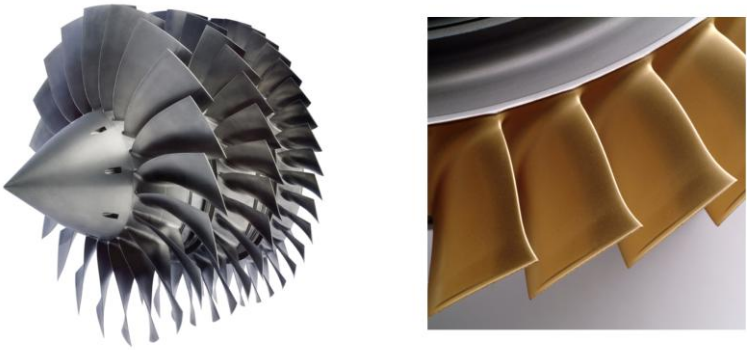

Source: [50].

As one of the well stablished applications mentioned above on the text, Figure 12 shows an example image of laser coating.

Figure 12 – Coating application.

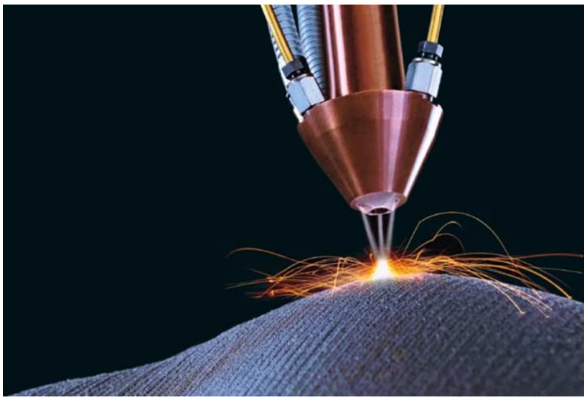

Source: [51].

2.2.4 Comparison with other techniques

Among general conventional coating and material additive processes, the LMD shows considerable advantages regarding material properties and final part quality [20, 52]:

- Low dilution;
- Minimal distortion;
- Smaller heat-affected zone (HAZ) with possibility of very local treatment;
- High heating and cooling rates, which delivers high hardness of the clad layer;
- No oxidation, even for oxidation-sensitive materials;
- Good fusion bond - Very low porosity and no bonding defects and undercuts;
- Wide variety of available powders;
- Process is highly repeatable;
- Adaptable to automated processing.

[24] also compares the LMD with some major coating techniques such as thermal spray, welding, chemical vapor deposition (CVD) and physical vapor deposition (PVD). This comparison is shown in Table 3, within several major features of these coating techniques to provide the advantages and disadvantages of these processes for metallic and non-metallic coating applications.

Table 3 – Comparison between LMD and other technologies.

Feature	LMD	Welding	Thermal spray	CVD	PVD
Bonding strength	High	High	Moderate	Low	Low
Coating thickness	50 µm to 2 mm	1 to several mm	50 µm to several mm	0,05 to 20 µm	0,05 to 10 µm
Repeatability	High	Moderate	Moderate	High	High
Heat-affected zone (HAZ)	Low	High	High	Very low	Very low
Controllability	High	Low	Moderate	Moderate to high	Moderate to high
Costs	High	Moderate	Moderate	High	High

Source: [24].

The LMD creates a very strong bond with low dilution, where a very low heat-affected zone (HAZ) is produced in the substrate. However, the costs with machine maintenance are higher than in other conventional processes. The current level of development of new laser technologies tends to create a better scenario regarding costs and machine maintenance. It is also required experienced specialized staff when working with the LMD (due to laser safety and equipment) [24, 52].

2.3 POWDER JET

The one stage LMD process requires injection of material to the molten pool. This material can be a powder alloy or wire. By the time powder is used, it is necessary to feed it to the working zone as a powder jet, by a powder feed nozzle in a continuous or discontinuous way. The model and adjustment of the nozzle define the geometry and some properties of the powder jet.

The delivery of powder to the melt pool involves various parameters that should be considered when process variables are being defined [3].

Modeling can be a good tool for predicting the process behavior and hence selecting better processing parameters. A rather wide number of researchers have developed different models capable of analyzing different aspects of the deposition process. In order to analyze just the powder jet without its interactions, it necessary to detach the powder jet analysis from the melt pool analysis [36].

In LMD, a powder jet consists of a powder flow, shaped through a powder feed nozzle to produce a converging annular jet of powder particles, which are focused towards the substrate [36]. Nozzle, powder jet and laser beam are shown in Figure 13. This way of powder injection provides a powder jet external geometry similar to the laser beam, with typical sections as the focus, where the powder jet and the laser beam present their smaller diameter (powder stream waist and beam waist, in Figure 13), and where most collisions of particles occur, as they converge to the same point. In this location there is a higher powder particle density as well as a higher energy density in the laser beam (see section 4.1.4 Powder jet focus position and geometry).

Figure 13 – Schematic of powder jet, nozzle and laser beam for the LMD process.

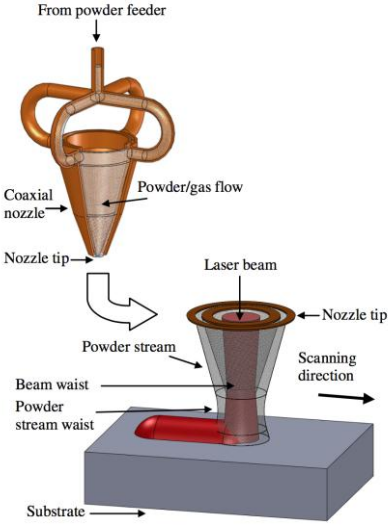

Source: [36].

Traveling along the nozzles, particles collide with the nozzle walls. These collisions determine the concentration distribution and dispersion of the particles. After exiting the nozzles, the powder particles are drawn downward by the action of three factors: gravity, momentum from the transport gas, and momentum from the secondary gas flow (shielding gas). They form one gas powder jet directed to the molten pool [27].

The shape of the powder jet is tailored by the nozzle geometry, which means by the angle with respect to the vertical axis (ß), by the vertical distance from the work piece (standoff distance – l) or the distance from nozzle tip to focus point (f_p), by the gas velocity and flow from carrier and shielding gas, by the powder feed rate and powder particle size. With increasing value of f_p, the core diameter d_p increases due to divergence of the powder jet. An increase of the powder feed rate also increases d_p significantly. Reducing the particle size leads to a smaller focus diameter [27, 43]. Figure 14 represents these measurements and Figure 15 the influence of the slit size on core diameter, both for coaxial powder feed nozzles.

Bigger sizes produce larger focus diameters on coaxial nozzles. The slit size corresponds to the size of the powder jet at the nozzle output. From output to focus position the powder jet diverges, what makes the focus diameter larger than the slit size.

Figure 14 – Powder jet measurement scheme of a coaxial nozzle.

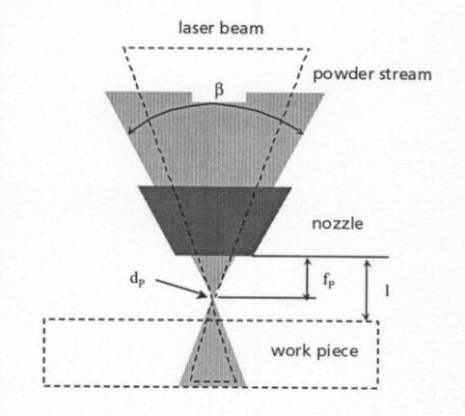

Source: [43].

Figure 15 – Influence of slit size on core diameter for coaxial powder feed nozzle.

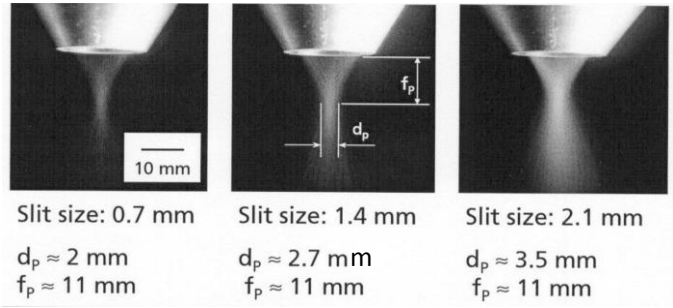

Source: [43].

As many operational parameters depend on the gas–powder jet characteristics between nozzle and deposition point, an extensive understanding of the powder jet properties, such as the concentration of powder and gas/powder particles velocities would be helpful in determining the optimal operational parameters. Given the complexity of the multiphase flow from any kind of nozzle, it is difficult to model

analytically, so a precise simulation of the flow structure is generally regarded as requiring numerical modeling techniques [53] apud [27].

This work will allow a better understanding of the powder jet and its properties, as well as the parameters and its influence to the powder jet geometry. For the first time it is going to be possible to identify and measure changes on the powder jet due to parameter and nozzle selection with a specific measurement system.

2.3.1 Powder feeders

Powder particles are delivered to the working point with the use of a powder feeder.

Powder feeders can be based on various working principles. The literature describes different principles based on specific applications while there are several other models available in the market [42].

The principle to be adopted in this work is based in a commercial powder feeder from GTV GmbH, which consists of a feeder unit (hopper), a base unit that carries the hopper and a pneumatic powder delivery subsystem. A controller and a drive unit for the hopper (DC stepper motor) are located inside the base unit [39, 54].

The hopper itself is an independent module that can be adapted using various kinds of base units. Some commercial feeder options include hopper heater jackets for pre-heated powder and gas mass flow controllers for the precise closed loop control of carrier gases with high reproducibility [54].

The hopper can be roughly divided into two sections: the container and the feed disc with a rectangular ring groove. The container itself consists of a double cone structure in which the upper half of the first cone ensures the downward flow of the powder while the lower half prevents the powder from compacting due to its own weight (see Figure 16). This structure also prevents a segregation of the powder due to the separation of fine and coarse powder particles or blended powders with different densities [54].

Under the force of gravity, the powder from the hopper flows through the second cone and then falls onto the rotating horizontal dosing disk. The second cone is positioned directly under the lower half of the first cone. This second cone ensures the regular filling of the rectangular ring groove within the feed disc using the so called spreader, which distributes the powder at a consistent level within the rotating groove. The rotation of the feed disc enables the powder-filled groove to be transported to the opposite side of the container, where the carrier gas

uses a nozzle-shaped suction mechanism, the so called suction unit, to pick up the powder by sucking it out of the groove. The carrier gas, normally Argon, carries the powder into the outlet tube (anti-static hose) and transports it to the laser head [39, 54].

An accurate parameter setting ensures that the groove is completely empty after it has rotated through the suction unit. The powder feed is linearly proportional to the closed-loop controlled RPM of the feed disc (controls the feeding rate) [54].

Figure 16 shows a powder feeder (left) and the hopper unit (right). At the hopper unit it is possible to identify the two mentioned sections: the container (upper part) and the rotating feed disc (connected under the container).

Figure 16 – Powder feeder (left) and hopper unit (right).

Powder feeder Hopper

Source: [54].

The powder mass flow rate depends on the diameter of the cone hole, the rotating rectangular ring groove and the rotating speed of the feed disc. Changing the feed disc and consequently the groove, gives different operating ranges of the powder feed rate.

2.3.2 Powder materials

There are several different material alloys, which are suitable for Laser Material Deposition. Each alloy provides different size ranges, varying from 5 to 120 µm.

Common manufacturers like Oerlikon Metco (Sulzer Metco) and GTV GmbH use commercial names to describe different alloys, which are mainly nickel-, cobalt- and tungsten-based alloys, as well as cobalt and carbide blends [55].

Most used powder materials in this work were the following:

- Diammalloy 1005
- Amdry 625
- MetcoClad 625F
- INCONEL® 718

Superalloy powders, like the Amdry 625, are produced by a dry gas atomization process to assure consistency, purity and conformity to rigid industrial, aerospace and military specifications. They are designed not to melt during the braze process, but to form a matrix within the braze joint that is metallurgically compatible with the substrate material.

Figure 17 shows an image produced by SEM of gas atomized superalloy powder particles (Diamalloy 1005). Each manufacturer provides a diameter report with particle size distribution of the produced batch.

Figure 17 – SEM image of typical gas atomized superalloy powder – Diamalloy 1005.

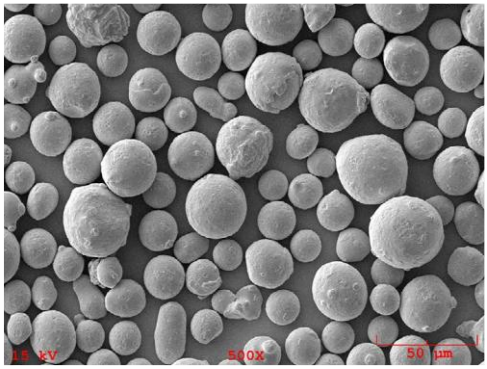

Source: [55].

The next sub-sections describe specific properties, composition and applications of these powder materials.

2.3.2.1 Diamalloy 1005 and Amdry 625

These alloys produce dense, self-bonding, single-step coatings that are oxidation and corrosion resistant at elevated temperatures. Their compositions are similar to INCONELs®, thus the coatings have excellent high temperature oxidation and corrosion resistance for restoration and repair of superalloy components. They are also recommended as overlay coatings to protect less noble materials from oxidation [55].

Chemical composition and particle size distribution are described in Table 4 and Table 5.

Table 4 – Chemical composition of Diamalloy 1005 and Amdry 625.

Product	**Chemical composition – Weight percent (nominal)**							
	Ni	**Cr**	**Fe**	**Mo**	**Al**	**Nb+Ta**	**Ti**	**C**
Diamalloy 1005	Bal.	21,5	2,5	9,0	-	3,7	-	-
Amdry 625	Bal.	21,5	2,5	9,0	-	3,7	-	-

Source: [55].

Table 5 – Particle size distribution and other characteristics.

Product	**Nominal particle size distribution (µm)**		**Similar to**	**Morphology**	**Manufacturing method**
Diamalloy 1005	-45	+11	INCONEL® 625	Spheroidal	Gas atomized
Amdry 625	-90	+45	INCONEL® 625	Spheroidal	Gas atomized

Source: [55].

2.3.2.2 MetcoClad 625F

The MetcoClad 625F is a nickel-based superalloy powder, specifically designed for LMD applications. As welded, it produces nonmagnetic surfaces with outstanding strength and toughness, resistant to a wide range of corrosive media and guard against crevice corrosion and pitting, as well as other generalized and localized corrosion. It is manufactured through gas atomization, which ensures that the powder particles are chemically homogeneous, yielding excellent results during processing. When used for LMD, dilution rates are low and surfaces are nearly 100 % dense [55].

Typical uses and applications for this powder material are:

- Components exposed to seawater and high mechanical stresses;
- Oil and gas production where hydrogen sulfide and elementary sulfur exist at temperatures in excess of 150 °C;
- Components exposed to flue gas and flue gas desulfurization equipment;
- Flare stacks on offshore oil platforms;
- Hydrocarbon processing from tar-sand and oil-shale recovery equipment.
- Thin deposit layers, as low as 0,2 mm and high speed laser LMD.

Table 6 shows the chemical composition of the MetcoClad 625F.

Table 6 – Chemical composition of the MetcoClad 625F.

Product	**Chemical composition – Weight percent (nominal)**					
	Ni	**Cr**	**Mo**	**W**	**Nb**	**Fe**
MetcoClad 625F	58,0 – 63,0	20,0 – 23,0	8,0 – 10,0	-	3,0 – 5,0	≤ 5,0
	Ti	**Si**	**Mn**	**C**	**B**	**Other**
	-	-	-	-	-	< 2,0

Source: [55].

2.3.2.3 INCONEL® 718

INCONEL® alloy 718 is a high-strength, corrosion-resistant nickel chromium material. Its welding characteristics, especially its resistance to post weld cracking, are outstanding.

The ease and economy with which this alloy can be fabricated, combined with good tensile, fatigue, creep, and rupture strength, have resulted in its use in a wide range of applications, e.g. components for liquid fueled rockets, rings, casings and various formed sheet metal parts for aircraft and land-based gas turbine engines, and cryogenic tankage [56].

Table 7 shows the chemical composition of the INCONEL® 718.

Table 7 – Chemical composition of the INCONEL® 718.

Product	**Chemical composition – Weight percent (nominal)**					
	Ni+Co	**Cr**	**Fe**	**Nb+Ta**	**Mo**	**Others**
INCONEL® 718	50,0–55,0	17,0 – 21,0	Bal.	4,7 – 5,5	2,8 – 3,3	< 5,0

Source: [56].

2.4 POWDER FEED NOZZLES

Different models of powder feed nozzles are available for the LMD. Process parameters, desired results and properties will define the most suitable nozzle type. Its design and capabilities vary from one manufacturer to another.

Within this work, the studies of the powder feed nozzles are based on the ones produced by the Fraunhofer ILT.

There are coaxial and lateral nozzles. Coaxial powder feeding involves feeding the powder along the axis of the laser beam. These nozzles can be classified in “ring-shaped” and “3-jet” or “3-way” nozzles.

A distinction is drawn between continuous and discreet (discontinuous) powder feed, where continuous feed is related to ring-shaped nozzles and discreet to 3-jet nozzles [43].

Figure 18 shows the ring-shaped nozzle.

Figure 18 – Coaxial ring-shaped nozzle.

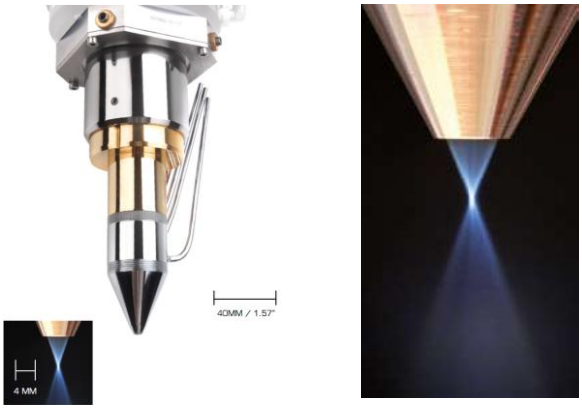

Source: [57].

Within these types of nozzles, the powder is distributed in a conical ring-shaped cavity, forming a hollow powder cone, which encloses the laser beam. The cone is produced as follows: the powder stream of the powder feed unit is split into three identical streams, which are fed into a ring-shaped expansion chamber inside the nozzle. In this chamber a homogenous “powder cloud” forms being fed into a cone-shaped slit. The powder leaves the nozzle in the form of a hollow cone. The diameter of the powder stream focus can be adapted to the laser beam area on the work piece. Depending on process parameters such as particle size, gas flow rate, and powder mass flow, powder stream diameters below 500 µm can be achieved, thus enabling cladding to be applied with optimum precision and efficiency even with a small laser beam diameter. The thickness of the cone wall, which corresponds to the powder jet itself, is produced by the gap existing between an inner and outer part of the nozzle (correspond to the ring-shaped expansion chamber inside the nozzle).

Some advantages and disadvantages of ring-shaped nozzles are [43, 57]:

- Advantages:
  - Good focusability of the powder stream;

- Powder efficiency: > 80 %;
- Good shielding of the molten pool.

- Disadvantages:
  - Limited 3D capability – Maximum tilt angle of approximately 20˚.

With 3-Jet nozzles, three powder jets running coaxially to the laser beam generate a unique powder jet focus, which has a core diameter of 1-3 mm. This diameter depends on the angle between the individual powder streams, the diameter of the nozzle holes, the distance between nozzle tip and powder stream focus, the powder feed rate, and the particle size [43, 58].

3-Jet nozzles are particularly suited for depositing thicker layers with high laser outputs (> 2 kW) and also depositing 3-D contours even in overhead conditions [58].

Advantages and disadvantages related to 3-Jet nozzles are [43, 57]:

- Advantages:
  - Complete 3D capability – Tilt angle up to 180˚ - as each powder stream is produced separately;
  - High robustness.
- Disadvantages:
  - Lower powder efficiency.

The “3-jet” coaxial nozzle is shown in Figure 19.

Figure 19 – Coaxial 3-jet nozzle.

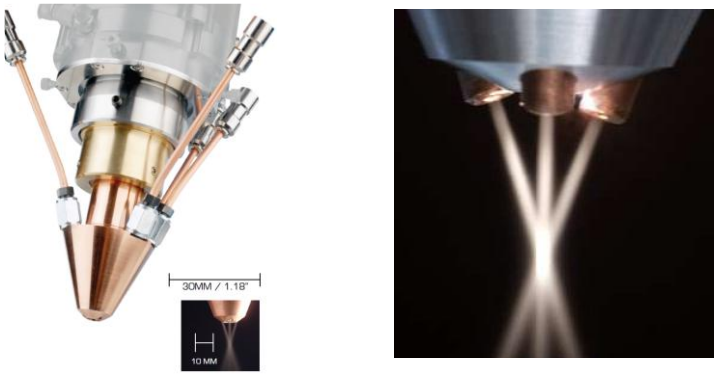

Source: [57].

Among the many parameters of the LMD, the quality of the produced parts is strongly dependent on the alignment and adjustment of the powder feed nozzle. Such adjustment is handmade at the Fraunhofer ILT and can determine the powder focus diameter and position as well as modify the entire powder jet geometry, also influencing the particle density distribution and symmetry.

One of the most important factors to be considered when evaluating a powder feed nozzle, is its internal adjustment. Crucial properties of the powder jet to be produced by the nozzle are defined during the adjustment and connection of the parts inside it.

Powder particles can interact with different surfaces in the working zone (molten pool), what results in different impact phenomena. For example, solid particles to solid surface impact cause ricochet; solid or liquid particles to liquid surface of the melt pool cause catchment and liquid particles to liquid surface also causes catchment [59]. A good nozzle provides the minimum of solid particles to solid surfaces, reducing the ricochet and loss of particles and increasing the catchment efficiency [24].

Not only the nozzle but also the entire cladding head must be prepared and robust enough to guarantee an accurately defined process, so that high product quality and reproducibility can be ensured. In coaxial powder feeding, for example, nozzle and cladding head guide and focus both the laser beam and the powder jet simultaneously on the surface of the work piece. Normally, several optical components, such as a dichroitic beam splitter, focus lens and protective glass are integrated in the processing head [41].

Figure 20 shows two examples of cladding heads assembled with the powder feed nozzles. The image in the left represents a common cladding head, from the Precitec Group, for fiber-guided laser in the medium to high powered range, to be applied in areas like repair welding of tools, turbine blades or casting molds, tempering of surfaces as well as generation of structures in tool, automotive and airplane manufacturing [60]. The image in the right shows a special cladding head developed by the Fraunhofer ILT together with Reis Lasertec GmbH, equipped with zoom optics, which enables a variation of the laser beam diameter for producing different track widths during the process of machining. The final goal of this head is to increase the overall productivity and to save process time by maintaining the accuracy of the cladded shape [34].

Figure 20 – Cladding head configurations.

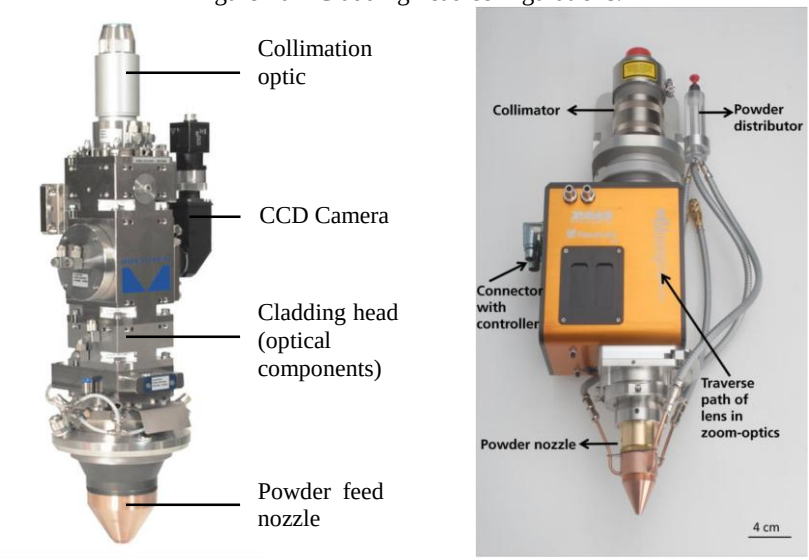

Source: [60] (left) and [34] (right).

Fraunhofer has also pioneered the development of state of the art innovative processing heads, which enable LMD to be carried out inside tubes, pipes and other hard to reach places. Internal diameter LMD can be performed with heads that operate reliably in hostile environments, travelling up to 1000 mm deep inside tubes that are smaller than 100 mm internal diameter. A monitoring system is installed in the head in order to ensure consistent coating quality [61]. Figure 21 shows an example of internal diameter LMD application.

Figure 21 – Laser material deposition with a telescopical optical system.

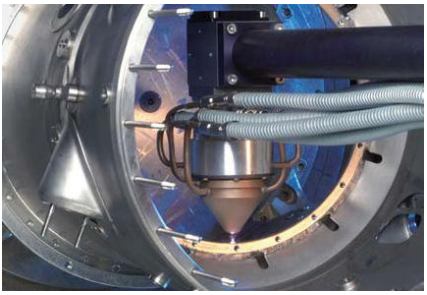

Source: [58].

Lateral feed nozzles are suited for rotationally symmetric components or for difficult to access processing areas (e.g. grooves). With a rectangular nozzle high deposition rates of up to 6 kg/h can be achieved [58].

Figure 22 shows an example of lateral nozzle.

Figure 22 – Lateral nozzle.

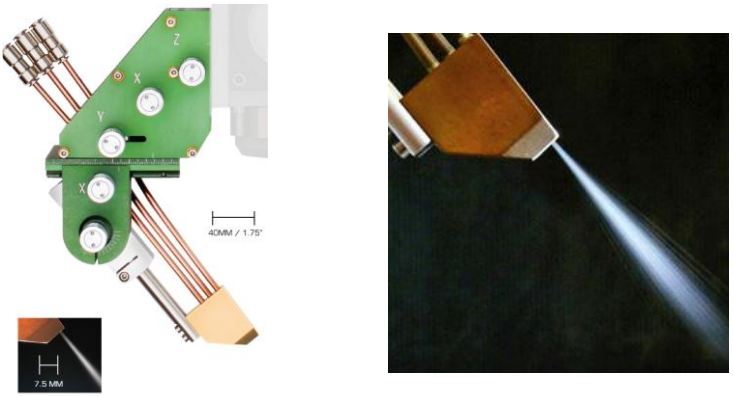

Source: [57].

An advantage of these nozzles when compared to the other models is that they have good accessibility to the work piece while a disadvantage is its low powder efficiency (50 to 70%) [57].

The powder efficiency (P.E.), or the catchment efficiency of the nozzle can be calculated by the following equation [62]:

$$\frac{Mass\ of\ clad\ layer(s)}{Mass\ of\ powder\ ejected\ from\ the\ nozzle}\ x\ 100 = \text{P. E.} \qquad (1)$$

Depending on the kind of nozzle (coaxial, ring shaped, 3-Jet or lateral) as well as on its manufacturing and adjustment, its efficiency can vary drastically. Typical values are in the range of 80 to 95% [63].

2.5 PROCESS MONITORING

High demands of quality required in most of the modern processes as well as the necessity of low costs, allow the development of different techniques of quality control. In laser material processing, its quality standards are guaranteed by continuous supervision of the manufacturing process as well as by the control of specific properties of the manufactured parts. Therefore, process monitoring plays a vital role to the quality assurance in laser processes [64].

Many of current new manufacturing technologies bring more variables to processes and also more sensitivity to process results against changes in machine parameters. More variables mean also more error sources, increasing the necessity to apply monitoring systems to industrial processes [44].

Applying process control techniques offers many benefits to the understanding and optimizing of laser processes. Efficient and stable usage of process diagnostics in the industrial environment calls for an extensive understanding of the process as well as precise knowledge of the systems and machines in use. In the following list, some key benefits are described [65]:

- Generation of new process knowledge by process visualization and process diagnostics;
- Closed loop-control for online failure detection;
- Quality assurance and process optimization;
- Documentation of laser processes by monitoring setting parameters and product quality;
- Detection and reduction of the occurrence of insufficient product quality;
- Robust process operation at the limits of stable process windows;
- Efficient usage of laser manufacturing processes, leading to cost and material loss reduction;
- Facilitating highly dynamic laser processes with stringent requirements on mechanical precision;

A wide variety of tests and measurement methods to analyze results and parameters of the laser processes permit detection of defects and modifications to different qualitative and quantitative criteria in three points of the process: pre-process, in-process and post-process.

In this work, the quality control system analyzes the powder gas jet properties extracting quality relevant information at the pre-process stage, where no working laser is used.

At the in-process stage, closed-loop control systems can be used giving online information to compensate unwanted effects of any irregularly that could change process parameters on the process result [15].

The post-process monitoring allows the inspection of the processing results.

These evaluations are achieved through the use of sensors (cameras, spectrographs and photodiodes), optical setups, coaxial process control modules (CPC) and computer algorithms.

CPC modules allow different assembling options for the system's structure. They are customizable modular optical systems, in various sizes and specific formats (for attaching lenses, filters or other optical components), for the integration of sensors into laser based manufacturing systems [66]. This system was developed at the Fraunhofer ILT. An example of CPC-system is represented in Figure 23, where each module is shown separated.

Figure 23 – CPC System examples.

Source: [65].

Processes can be monitored with coaxial or lateral (off-axial) mounted sensors.

The lateral systems represent more flexibility since they provide quick and simple ways of optimizing existing installations with sensors,

just mounting them aside, where the optical axis of the sensor is not parallel to the working laser beam.

In coaxial systems the sensor is integrated in the same optical axis of the working laser, so the capture of data in the interaction zone between laser and work piece and also in surrounding areas is possible. This setup also protects the sensor against external pollution, especially in harsh industrial production environments.

A setup of coaxial and lateral process monitoring system is shown in Figure 24, where the sensor is a CMOS camera.

Figure 24 – Coaxial (left) and lateral (right) monitoring concepts.

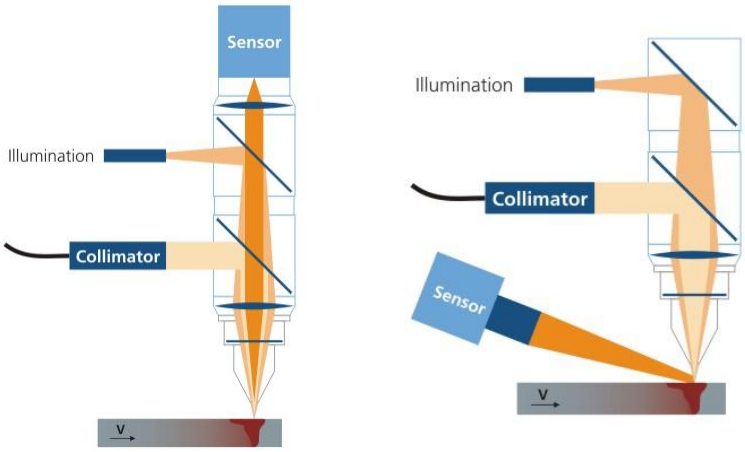

Source: Author.

Generally, a high-speed camera is needed to perform the monitoring of laser processes, whether it is a coaxial or lateral system setup. For instance, high-speed cameras with CameraLink® interface, also used in this work, can achieve speeds of up to 600 frames per second and data rates of up to 850 MB/s. Depending on camera model and image size, higher speeds can be achieved [67].

Defining the best monitoring strategy (kind of camera, coaxial or lateral sensors etc.) depends on the process to analyzed, the working conditions, variables involved and mainly, on what must be monitored.

2.5.1 Application examples

Even in the most modern laser based manufacturing systems in operation some of the key process input parameters are monitored or recorded in any way. Process monitoring techniques are applied in several laser applications, investigating and controlling crucial parameters [68]. It is an important factor to develop more efficient processes and produce better results.

According to [41] it is essential to monitor the operating status of the components online, in order to access their condition and avoid the deterioration in time, also meeting increasing demands on product quality. The economic efficiency of the process can be significantly increased through the decreased scrap rate.

The combination of process knowledge from experiments, simulations and physical descriptions can be used as a basis for self-optimizing systems. In process control the use of optimization results requires a modular system structure consisting of reconfigurable, information-processing sensor/actuator systems. They enable the production system to be adapted to the process status and production task in real time [69].

Process technology, set up and parameters help defining the most suitable monitoring system to be developed. Regarding the variety of sensors (cameras, pyrometers, photodiodes etc.) and illuminations (lasers, LEDs, halogen lamps) that can be applied, the investigated process must be well characterized so that the system can work properly.

This section shows some application examples of monitoring techniques in laser welding, brazing and morphology recognition processes.

[68] explains that in laser welding, one of the key aspects of maintaining the quality of a weld seam is the online assessment of it, during the process, in applications with high penetration depths, as well as those used for the joining of flexible sheets (both metal and non-metals).

A coaxial monitoring system is able to monitor welding process speed, position, perform seam tracking and also measure the molten pool size online. Figure 25 shows an application of image processing technique to control melt pool size and contour.

Figure 25 – Melt pool control analysis through image processing.

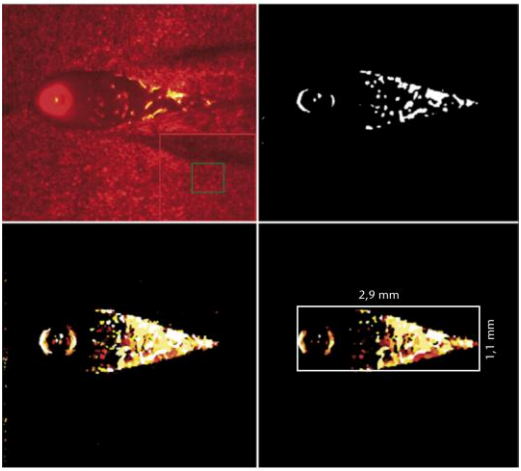

Source: [68].

[70] developed a system for monitoring laser brazing process, mainly used in the automotive industry, for car body manufacturing, requiring high demands brazed seam quality, in terms of the absence of pores and connection of the braze to the joint members. Process monitoring systems can record all the requisite process parameters and provide all data on the joint quality.

An example of it is the development of a CPC system with two cameras and an illumination source to monitor the quality of the brazed seam in both, the visible and the infrared spectral range. The camera images, combined, enable the feed rate as well as process imperfections (e.g. pores) to be identified and documented during de joining process [70].

Figure 26 shows the set up and some image results of this application.

Figure 26 – Monitoring system for laser brazing.

Monitoring system set up

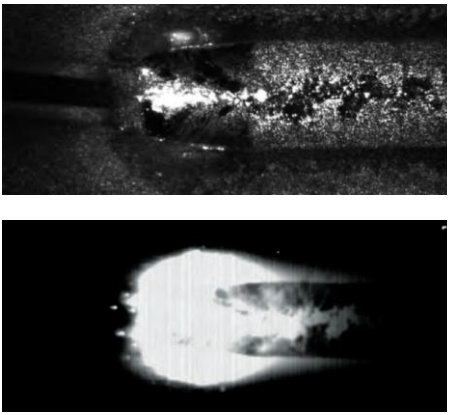

Images of the melting pool

Source: [70].

3 METHODOLOGY

The qualification and characterization of the powder jet and the powder feed nozzle for the LMD process were accomplished throughout the employment of multidisciplinary knowledge. Process control and system monitoring techniques as well as theoretical and practical expertise in laser material processing, powder materials, powder jet dynamics, simulation and programming were applied in this work.

Five technology clusters sub-divided the project in which this work was developed, as process chains for manufacturing and repair. Process control and Laser Metal Deposition were involved in this thesis. Process Control addresses the measurement and extraction of quality-relevant process information in-situ whilst laser processing. This information can be used to interrupt defective processes in time to initiate corrective processing strategies, and fulfill relevant quality assurance documentation requirements [23].

Figure 27 shows the clusters involved in the project and their relationship.

Figure 27 – Project's technology clusters.

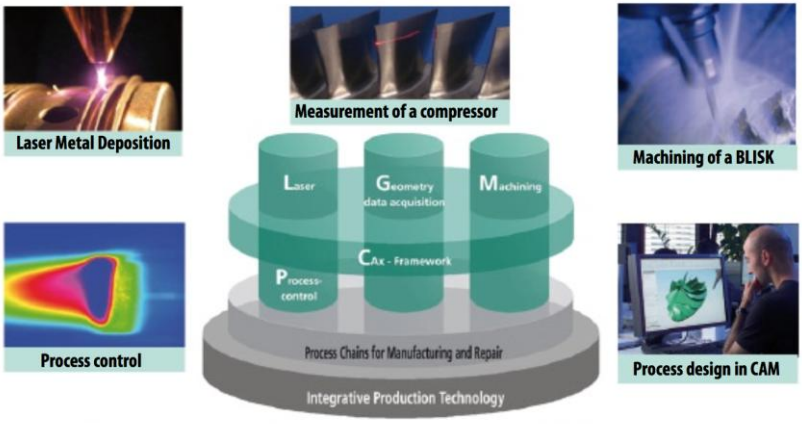

Source: [23].

It is difficult to find practical cases where a general quality factor for qualifying the powder jet is used. Normally this qualification is based on operator and nozzle manufacturer experience. Defining a

factor, the same way it was done for the laser beam is a great breakthrough for the powder jet and nozzle manufacturing technology.

A comparison of the laser beam and the powder jet shows some similarity between them, due to their geometry. The laser beam is well characterized and qualified by various factors and parameters, different from the powder jet. Figure 28 shows the alignment of powder jet and laser beam and their geometry, very similar to each other. The position of laser focus and powder jet focus can define some of the interaction between beam energy and powder particles.

Figure 28 – Overview of powder jet, nozzle and laser beam.

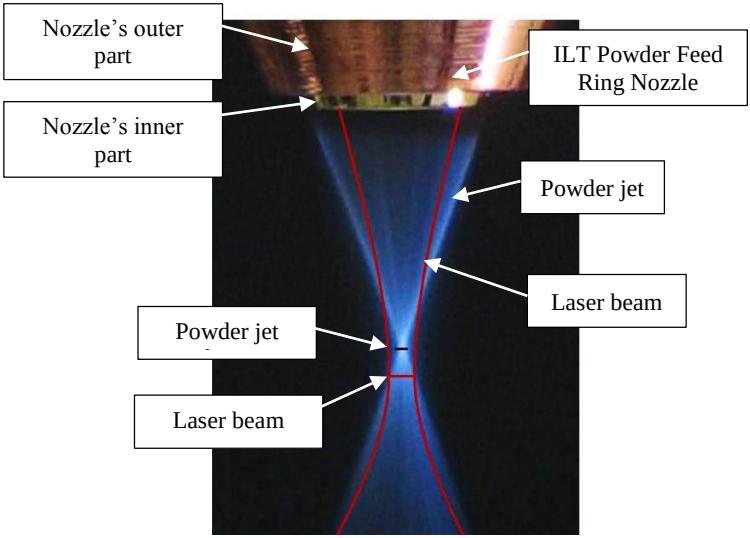

Source: [71].

Defining the right properties of the powder jet, their correlation to the laser beam parameters and knowing the influences each one of these properties will cause on the final result and produced parts, requires practical experience in the area. The Fraunhofer ILT has the necessary expertise and experience in this process to present the right set of parameters in order to achieve the desired results.

A large variety of operating parameters and physical phenomena determine the quality of the LMD. Figure 29 summarizes these parameters in inputs, processes and outputs. Generally, the inputs or operating parameters are the laser (power, type, pulsed or continuous wave, focus etc.), motion device, powder feeder set points, and also the

material and ambient properties (gas properties). The outputs of the process, which represent the clad quality, are the geometry, microstructure, cracks, porosity, surface roughness, residual stresses and dilution [24, 72, 73, 74, 75].

The right set up of powder jet and laser means the achievement of a good clad quality within all those outputs shown in Figure 29.

Figure 29 – Inputs, outputs and process parameters of the LMD.

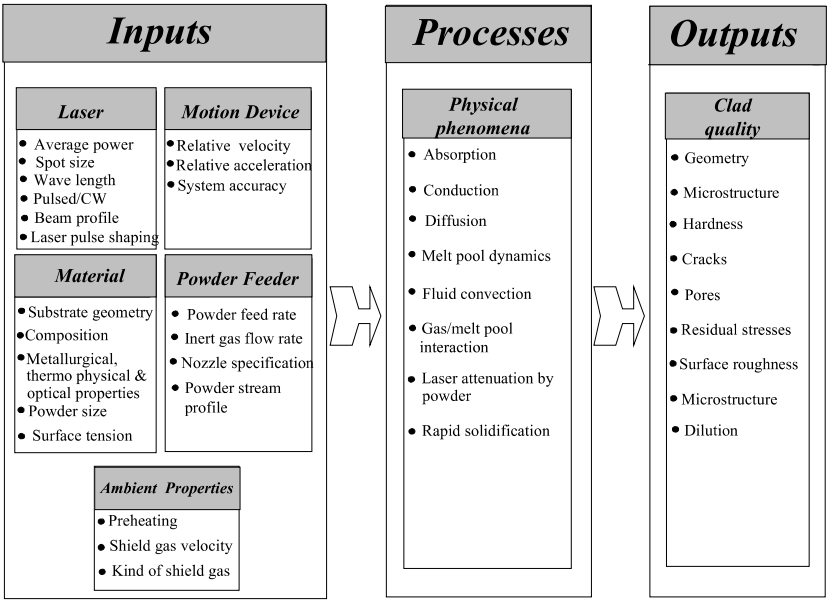

Source: [24].

A work's methodology overview is shown in Figure 30. Three main areas are necessary to the executing of the experiments, powder material, equipment and expertise in laser technology, process monitoring and image processing. These areas must be well integrated in order to have the best results and a good workflow.

Image processing and process monitoring are crucial in this work, since they need to be developed and studied to identify the best equipment and allow the construction of the experimental setup.

Figure 30 – Work's methodology overview.

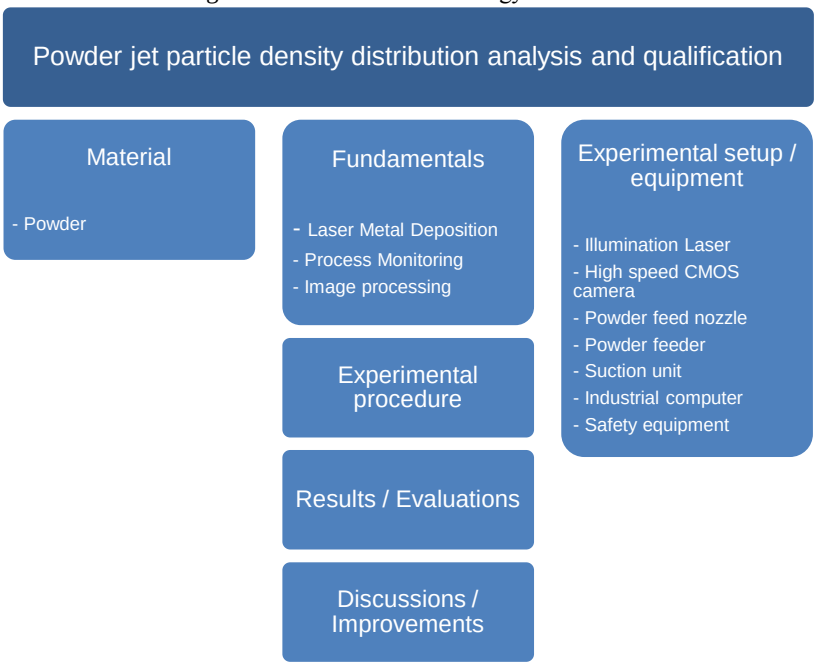

Source: Author.

The experiments consist of recording the powder jet coaxially with lateral illumination. All the experimentation occurs in a pre-process stage, as described in the section of 2.5 PROCESS MONITORING. There is no use of working laser during the experimentations.

The results can be compared with models and simulations of the powder jet, as well as with practical results, expected from the parameters used at each experiment.

3.1 EXPERIMENTAL SETUP

A scheme of the main part of the system is represented in Figure 31. Crucial parts for the system functioning are: industrial computer (to control the camera and linear automated axis), high speed CMOS camera, powder feed nozzle and illumination laser.

Figure 31 – System main components.

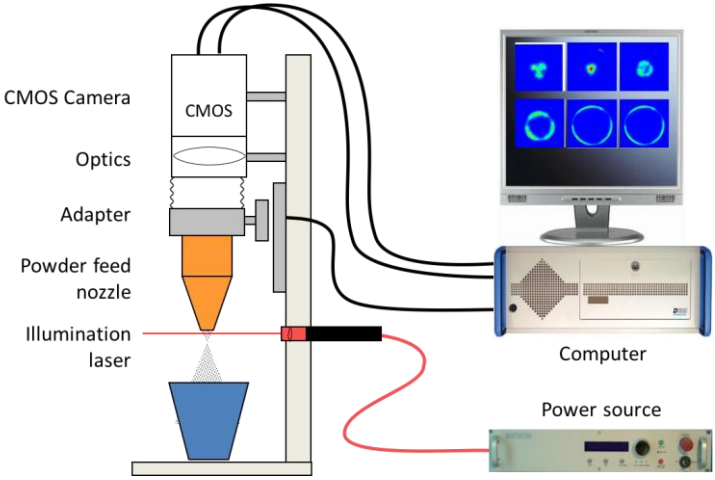

Source: Author.

The system setup and components is represented in different versions, in Figure 32 and Figure 33. To achieve the current configuration and automation level, several structure and equipment upgrading were performed.

The first system versions were fully manual and needed to be placed in specific places where the experiments could be carried on.

Setup variations and different strategies of illumination and positioning of the camera were mounted during the first experiments in order to optimize quality and reliability of the produced images and results.

Lenses and filters were also tested to generate sharp images with enough resolution (320x320 to 512x512 pixels) for the later image processing.

Figure 32 shows two different versions of the system. Lateral illumination was used on the left figure and coaxial illumination on the right. The current version uses the strategy shown on the left, where a laser line illuminates the powder jet.

Coaxial illumination, as shown in Figure 32 (right) was tested in the beginning of the prototype development. After several experimentation and tests, this strategy was changed by lateral illumination. When coaxial, the laser light illuminates the sharp level of particles as well as the other levels (upper and down), so that sharp and

blurred particles were recorded. This way, it would be difficult for the algorithm to identify which particles should be analyzed or not. It produces too much information in each video frame recorded.

Figure 32 – Previous versions of the system setup – Similar to current version (left) and one of the first set ups (right).

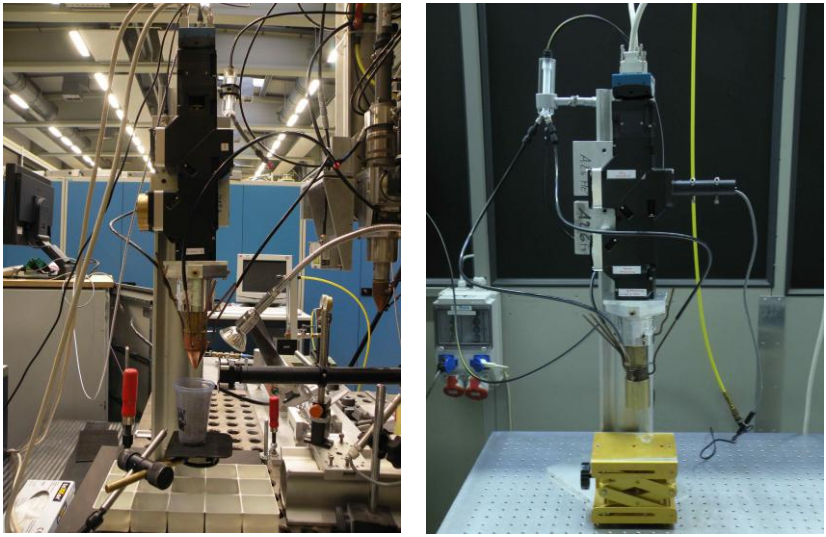

Source: Author.

The current version is partially automated and designed within safety reasons, regarding laser beam and powder material. It is involved in a case, sealed on its sides and opened in the front with a protective window, specific for the illumination laser wavelength. The operator does not need to open the case during the process since it is automated and can be controlled through an external computer.

A suction system gets the powder particles after they come out from the powder nozzle, keeping the experiment's environment clean.

It is fully mobile so that it can be transported to different places where the experiment should be performed. This way the same equipment (powder feeder, powder and gas supply) which is going to be used later on the LMD process can be used also on the measurement. The reliability of the results as well as the reproducibility of the powder jet later on the LMD process increases in these cases.

Several presentations were performed in different workshops and fairs, taking advantage of the fact that the system was mobile and could

be mounted anywhere. Some of the fairs and congresses were the "International Conference on Turbomachinery Manufacturing - ICTM", the "International Laser Technology Congress – AKL", both of them located in Aachen, Germany, and the "Laser World of Photonics", in Munich, Germany.

Figure 33 – Current system setup and components.

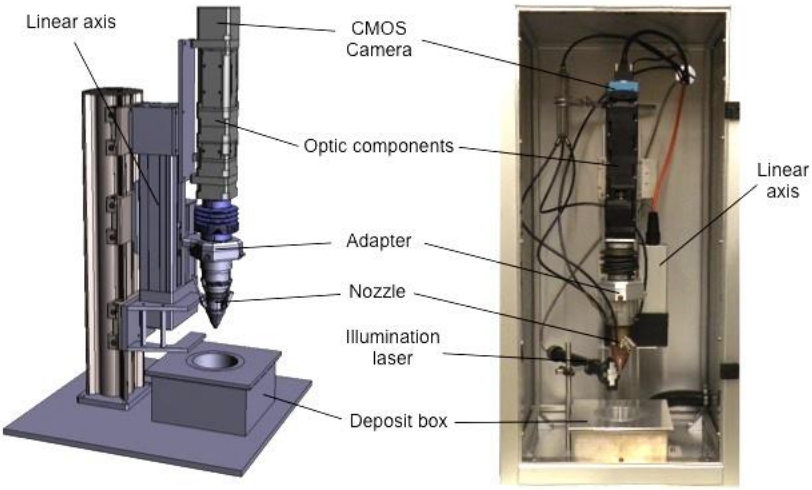

Source: Author.

As shown in Figure 33, various equipment and components were assembled setting up the monitoring system. A list of the experimental setup is presented below:

i. Powder feed nozzle
Different models of powder feed nozzle manufactured at the Fraunhofer ILT, and therefore different configurations of powder jet, were evaluated

ii. Powder feeder;
Model: GTV PF2/2.

iii. Gas supply system (cylinders, flow control, cables and hoses);

iv. Powder suction system;
Temporary vacuum cleaner specific for powder materials was connected to the system.

v. Illumination laser;
Model: LIMO Laser LDD550.

vi. High-speed camera;
Model: Mikrotron EOSENS CMOS High-speed camera.

vii. Optical fiber cable for guiding the laser beam;

viii. Laser line generator;

ix. Optical components (lenses, filters, adapters);

x. CPC Modules and adapters for assembling nozzle or external parts;

xi. Automated axis;

xii. Industrial rugged computer and specific software for executing experiments and controlling the camera and axis;

xiii. Computer and developed software for evaluating experiments;

xiv. Personal protective equipment for working with laser beam and micro powder materials (appropriate dust mask and safety glasses).

Technical specifications of each item cannot be describe due to classified information of this work.

3.2 EXPERIMENTAL PROCEDURE

In considering a powder jet, some important variables that need to be monitored include the constancy of the powder mass flow, the symmetry of the powder jet, and the position and size of the powder

focus. Every powder feed nozzle produced or repaired has a set of adjustments for the alignment of its internal parts, which have a strong influence on the above-mentioned variables [76].

These characteristics are first assured by means of visual testing, counting on the high level of experience of its manufacturer. The system, subject of this work, is able to quantify and also confirm if the alignment of the powder feed nozzle is correct, qualifying its production. It is also able to reproduce the measuring process several times with the same parameters used, allowing the operator of the nozzle to frequently check its conditions, due to use and wear of the equipment.

A structure for the experimental procedure and its related items is described in Figure 34, dividing the whole process into three main areas:

- Data source and experimental setup;
- Data acquisition;
- Data processing.

Figure 34 – Overview structure of experimental procedure.

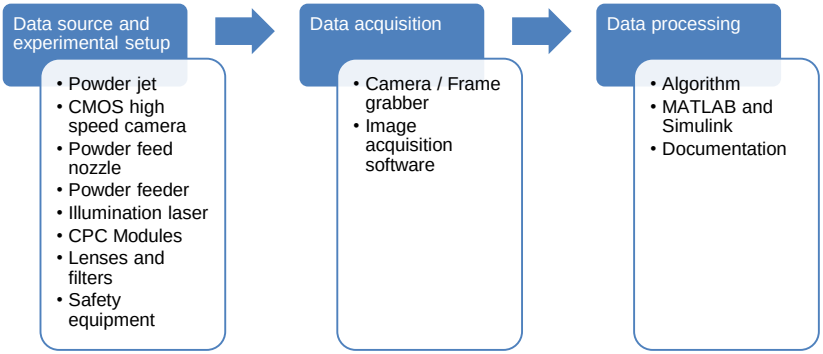

Source: Author.

Following the above-mentioned structure (Figure 34), an experimental procedure is illustrated on Figure 35. Sensors, allied to software, acquire the data as video recordings and store it in a computer to be later analyzed and generate the outputs.

Figure 35 – General procedure of the experiments.

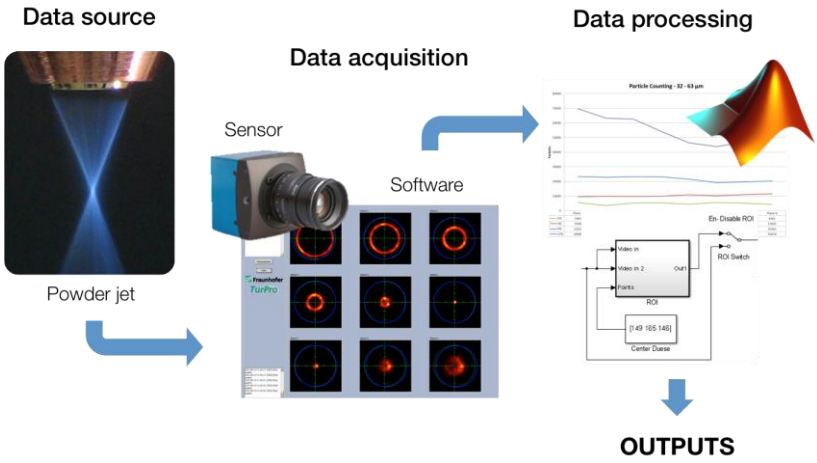

Source: Author.

The following sections describe the inputs and outputs of the process, from data source to acquisition and processing of the data.

3.2.1 Data source

The main data source of the whole experimentation is the powder jet, allied to the powder feed nozzle, powder material and gas flow. It corresponds to the delivery of powder to the melt pool via the nozzle, being a crucial element at laser material deposition. It has a major influence on the consumption of powder material and the quality of the coating layer [3].

All the sources are adjusted with the same properties and parameters that are going to be set for the laser cladding process.

At first, the department of Laser Cladding, at the ILT, provides a powder feed nozzle. This nozzle is adjusted and aligned to produce specific results, with its properties assured by experienced manufacturers. Some properties are:

- Powder jet geometry;
- Powder jet symmetry;
- Focus position;
- Focus diameter.

Once these properties are defined by the manufacturer, the monitoring system will then assure and proof if they are consistent or not, qualifying, therefore, the powder feed nozzle and de powder jet. Details of each mentioned property can be checked in the subsections of section 4 Results.

The powder feed nozzle is then mounted on the system's structure. Camera focus is adjusted by moving the lens position. Its sharp level is aligned to the position of the laser line. The nozzle will be moved upwards by the automated axis, step by step, relatively to the camera and laser line. This way, the powder jet can be recorded entirely, from nozzle exit, to powder jet focus and further.

3.2.2 Data acquisition

Relevant data for the measurement is acquired through the illumination and recording of the powder particles.

The laser line is positioned laterally, aligned at the sharper level of the camera (lens focus). The camera monitors reflections of the illumination laser at the particles, coaxially through the nozzle.

By the time the measurement is initiated, the nozzle moves to a reference point, pre-defined by the operator. Standard measurements have the reference point where the nozzle exit meets the laser line, defining the first level. Powder feeder, gas supply and suction system are initiated and the CMOS camera starts recording. The video is stored, the nozzle moves up and another level is recorded. This procedure repeats until all the defined levels are done.

Properties for the overlapping of levels are defined in the recording software. Level height corresponds to the height of the illumination line. Depending on the step of the nozzle movement, overlapping can occur.

More details of the powder jet can be acquired when more levels are recorded.

In Figure 36 a scheme of the measuring concept is illustrated. As described above, the linear axis moves the nozzle in pre-defined steps, while the illumination line provides sufficient light to the high-speed camera to record the powder particles.

Figure 36 – Measuring concept.

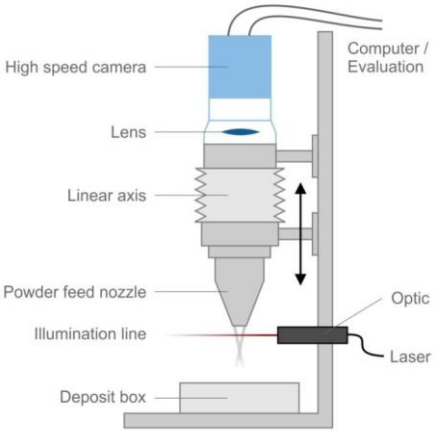

Source: Author.

Detailed recording layers' scheme is represented in Figure 37. Each recorded layer is described as "Level", numbered from 0 to 9 in this case. Depending on the focus position (f_p distance, as described in 2.3 POWDER JET, Figure 14) and layer thickness, more levels can be recorded. The layer thickness (represented as a green stripe and named as "Level") corresponds to the illumination line thickness, which can be adjusted at the illumination laser optics.

Figure 37 – Recording layers' scheme of the powder jet.

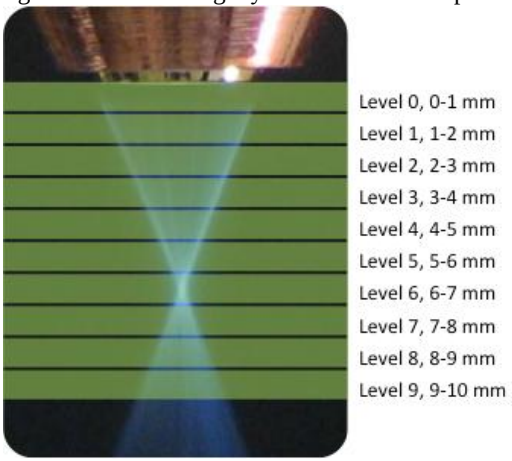

Source: Author.

Summarizing the acquisition process described above using Figure 37: from the reference point, the nozzle moves to the position it appears in the figure, meeting the first recording layer (Level 0), also the level of the illumination line. The recordings initialize at this point. The nozzle moves upwards, (move in adjustable steps, normally 1 or 0,5 mm) camera and optics stay in the same position, always aligned with laser illumination line, and the powder jet area recorded corresponds to the area covered by Level 1. This procedure repeats to the next levels, until Level 9 is recorded. Videos and images are stored to be later analyzed.

During the acquisition process, some image processing occurs in the acquisition software. The software shows a quick overview of each recorded level, where the operator can detect errors and stop the process to correct them before spending more powder material. This overview is images of each level formed when single frames of the videos are superimposed.

Since they represent each level recorded, superimposed images are also a result of the system. More details on how these images are created are available in the next sections of data processing (3.2.3.3 Superimposed images).

A quick overview, for a better understanding of what is “seen” and recorded by the camera is available in Figure 38.

Figure 38 – Overview of lateral and coaxial views in different powder jet levels.

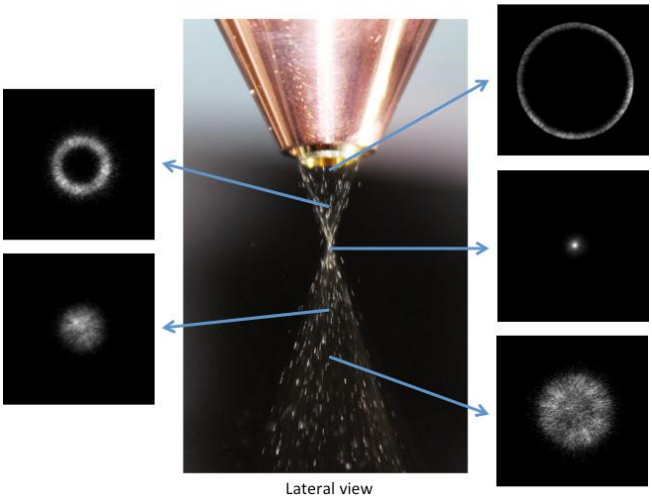

Source: Author.

The central image represents a lateral view of the powder jet and nozzle. The camera, positioned above the nozzle, sees the powder jet coaxially from an upper view as shown in the images at the sides, in different levels of the powder jet.

3.2.3 Data processing

In order to extract the necessary information to the qualification and characterization of the powder jet and powder nozzle, once the videos are recorded, single frames are going to be processed by specific algorithms.

The processing algorithm is responsible for generating necessary data for this work's results.

3.2.3.1 Processing algorithm

The main function of the algorithm is to analyze the recorded videos in order to extract relevant information to qualify and characterize the powder jet and its nozzle.

The development of the algorithm was done through intensive testing and experimentation, where theoretical and practical knowledge was applied. It was written mainly in MATLAB® and Simulink®, what made its use simpler to other project members.

MATLAB® is a high-level language and interactive environment for numerical computation, visualization, and programming [77].

Simulink® is a block diagram environment for multidomain simulation and Model-Based Design, where system models are used through the design of blocks and shapes which represent some programming. It supports simulation, automatic code generation, and continuous test and verification of embedded systems [78].

The Simulink® model of the developed algorithm can be divided in three main sections: Inputs, Data processing and Outputs, as shown in Figure 39.

Figure 39 – Algorithm sections and basic structure.

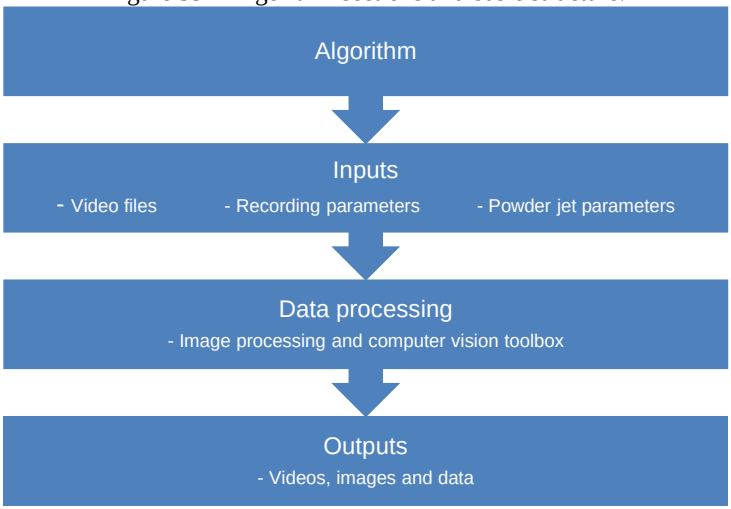

Source: Author.

The “Inputs” section corresponds to the parameters that need to be declared prior to the compilation of the algorithm. They are parameters of the camera and the powder jet.

Camera input parameters are:

- Image resolution;
- Exposure time;
- Frame rate;
- Pixel per millimeter of the recorded images.

Powder jet input parameters are:

- Powder mass flow;
- Carrier and shield gas flow.

Inside the Simulink® model, the image processing and computer vision toolbox from MATLAB® are used.

The Image Processing Toolbox provides a comprehensive set of reference-standard algorithms, functions, and apps for image processing, analysis, visualization, and algorithm development, like image analysis, segmentation, enhancement, noise reduction, geometric transformations, and image registration [79].

The Computer Vision System Toolbox provides algorithms, functions, and apps for the design and simulation of computer vision and

video processing systems, like object detection and tracking, feature detection and extraction, feature matching, stereovision, camera calibration, and motion detection tasks. The system toolbox also provides tools for video processing, including video file I/O, video display, object annotation, drawing graphics, and compositing [80].

One of the core processes for this algorithm is the image binarization process. It allows the recognition of single particles in each frame providing crucial information for the processing. The next section describes this process more detailed.

After the binarization and some other Simulink® processes are completed, the algorithm has sufficient data to generate the so-called "Outputs". At the "Outputs" section, the algorithm shows processed videos, generated images (superimposed images) to further evaluations, and also relevant data from the powder jet, as text files.

All the information regarding some applied processes, aspects and codes of the algorithm itself, developed to the purposes of this work are classified information and should not be distributed or reproduced.

3.2.3.2 Image binarization process

Videos recorded by the camera in the monitoring system are composed by single frames, which are grayscale images.

Grayscale images are characterized as images in which the value of each pixel is a single sample that carries only intensity information. These images are composed exclusively of shades of gray varying from black at the weakest intensity, to white at the strongest [81]. They are generally stored as an 8-bit integer giving 256 (2^8) possible different shades of gray from black to white, where 0 corresponds to the intensity level of black and 255 to the intensity level of white. If the levels are evenly spaced, then the difference between successive gray (intensity) levels is significantly better than the gray level resolving power of the human eye [82].

The image binarization process converts an image of up to 256 gray levels to a binary image (black and white) [83].

Binary images are images whose pixels have only two possible intensity values. They are normally displayed as black and white. Numerically, the two values are often 0 for black, and either 1 or 255 for white [82].

The simplest way to use image binarization is to choose a threshold value and classify all pixels with values above this threshold as white, and all other pixels as black. The thresholding process can

separate out the regions of the image corresponding to objects in which we are interested, from the regions of the image that correspond to background. It is a convenient way to perform this segmentation on the basis of the different intensities or colors in the foreground and background regions of an image [82, 83]. It means that thresholding allows the system's algorithm to separate the powder particles from the background. Therefore, the algorithm is able to perform calculations with the amount of particles in each frame.

Image thresholding is one of the most formidable tasks in image processing. One of the big challenges within the algorithm that demands experience and expertise from the system operator is setting the correct threshold value. Wrong values bring wrong calculations from the processing algorithm, which lead to errors on focus diameter and particle counting [84].

Figure 40 shows an example of thresholding, where the value is set to 155. Pixels with intensity values under 155 are transformed to black and the other ones above to white. Image details are lost depending on the threshold value. This is also an example of the above-mentioned challenge when setting the threshold. Some details should not be lost from image parts.

Figure 40 – Image thresholding – From grayscale to binary image.

Source: Author.

Choosing an optimal threshold value in each image depends upon many factors such as the image itself, the desired region, definition of the object, and applications. For example, in one image the area of interest or the object for one specific application could be completely different from that of another application [84].

3.2.3.3 Superimposed images

Single frames of the recorded videos are superimposed to generate images of every powder jet level. These images give the operator an overview of the powder jet.

Each frame has a specific size, for example, 256x256 pixels. Each pixel has an intensity value, since the frames are grayscale images. When superimposing several frames from a video, the intensity value of each image pixel is summed. These values are then normalized to be in the range of 1 to 255, as normal grayscale images. Therefore, the generated image has all the frames summed into one single frame, having powder jet particles represented where they mostly appear.

An example of single frames from a video and the corresponding superimposed image, of the same powder jet and level is shown in Figure 41. The images were created from a video of 3000 frames.

Figure 41 – Example of single frames and superimposed images.

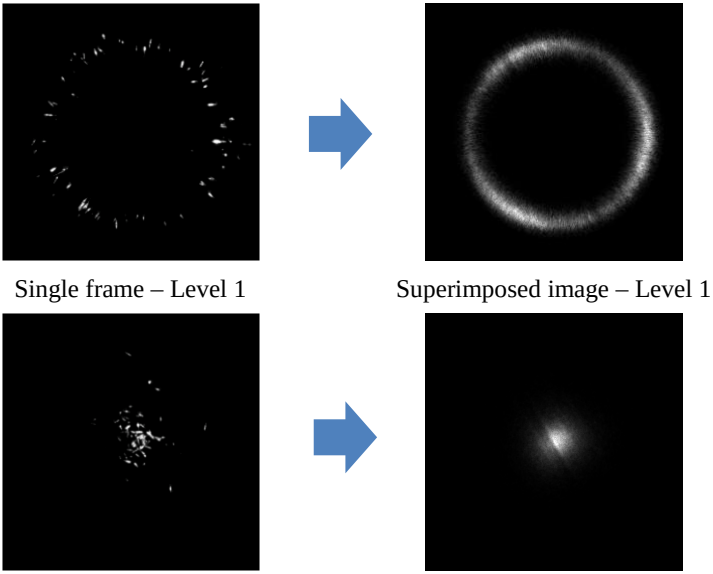

Source: Author.

4 RESULTS

The results allow a better understanding of the LMD process, the powder jet itself and of the related equipment. It makes it easier to the operator to set up the system and produce the desired parts with the necessary quality standards.

There is also a contribution to the powder feed nozzle-manufacturing knowhow, since it is now possible to assure nozzle properties by measuring its powder jet by the monitoring system.

Nozzles that are already in use can be measured anytime to proof whether it is still reliable or not.

This work's results were also reference in some master and bachelor thesis of LMD applications. [71] and [85] used the measurement system to qualify the nozzles used in the experiments and to understand process variables that were dependent of powder jet properties.

The expected primary results to be delivered by the system after each measurement and for each recorded level are the following:

- Superimposed image from intensity values;
- Superimposed image from centroids (see section 4.1.2 Particle counting for more information);
- 3D Superimposed from centroids;
- False color superimposed image from intensity values;
- Diagram "Intensity x pixels";
- Diagram "Number of particles x pixels";
- 5 matrixes with information, intensity values and particles for each level.

Some of the above-mentioned images can be checked in APPENDIX A.

These results can be further analyzed allowing the user to get the final results, which are powder jet qualification, and powder feed nozzle qualification.

4.1 POWDER JET QUALIFICATION

There are mainly two properties that could qualify the powder jet as suitable for the LMD process: particle density distribution and powder jet geometry.

These two properties can be almost directly recognized after executing a measurement. The system shows as a first result superimposed images, which allow the operator to identify particle density concentrations as well as to see the powder jet geometry at specific levels.

The measurement software shows as a first and prompt result images from each recorded level. Figure 42 shows these images and the software interface. Recording time varies, depending on program properties. Due to a color filter, images appear in red. The green cross shows the center of the nozzle while the circle represents nozzle exit. Marks on the green cross correspond to a millimeter scale. The blue circle represents the centroid of the powder jet geometry, considering the point where more particles are concentrated.

Figure 42 – Software interface and first measurement results.

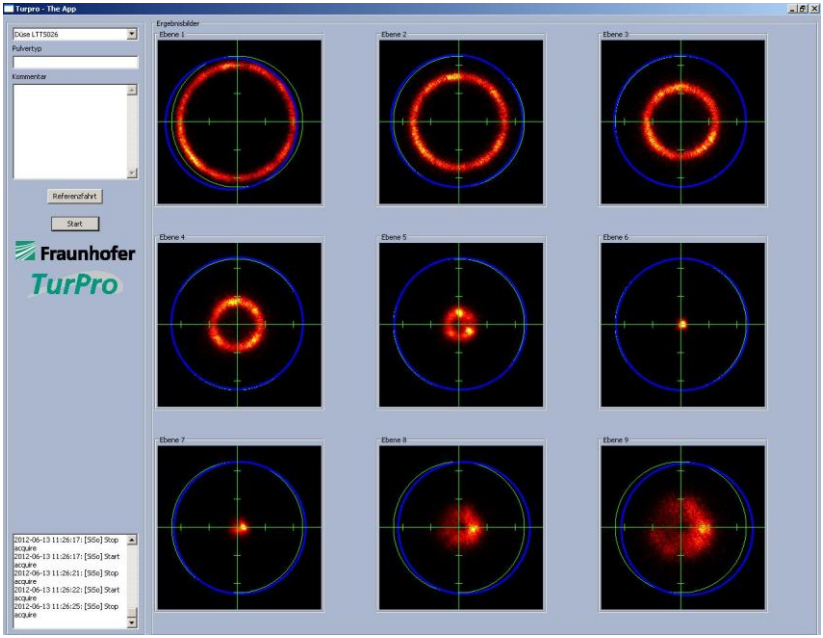

Source: Author.

These images and its corresponding videos are stored in the computer to be analyzed by relevant algorithms, which generate the results of this work.

The final results of some measures, considering their important factors are shown from APPENDIX D to APPENDIX H of this work. The images are presented in an organized way to the project stakeholders, so that nozzle manufacturers and LMD operators can give their feedback on how the powder jet is working correlated to its measured characteristics.

4.1.1 Particle density distribution

The delivery of powder to the melt pool needs to be mostly uniform from nozzle exit to powder jet focus. Nozzles are designed to deliver the powder particles equally at its exit. By the time the particles start to travel in the powder jet, they converge to a point (focus) where particle collision is inevitable. In the center of the jet, there are more particles per volume and therefore more particle density then in the boundaries.

Figure 43 shows images, which represent the particle density distribution of different levels from a ring nozzle. It is noticeable in level 11 (focus) that the powder density is higher in the center, as mentioned above.

The powder and gas properties of this measurement are described in Table 8.

Table 8 – Powder and gas properties for ring nozzle particle density distribution.

Powder material	Ni-Basis Diamalloy 1005
Powder grain size	25 – 45 µm
Powder mass flow	1,10 g/min
Gas	Argon
Pressure	1 Bar
Carrier gas flow	2,7 L/min
Shielding gas flow	0 L/min

Source: Author.

Figure 43 – Particle density distribution of a ring nozzle.

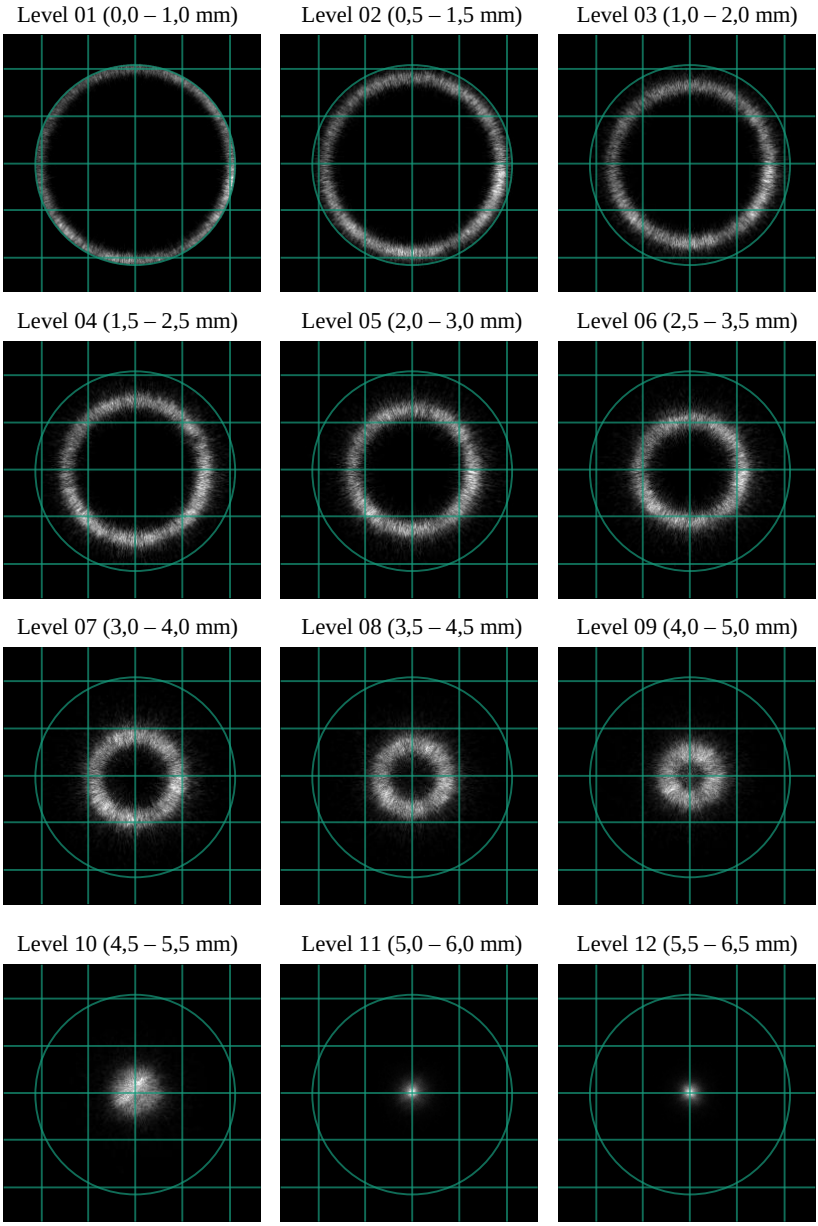

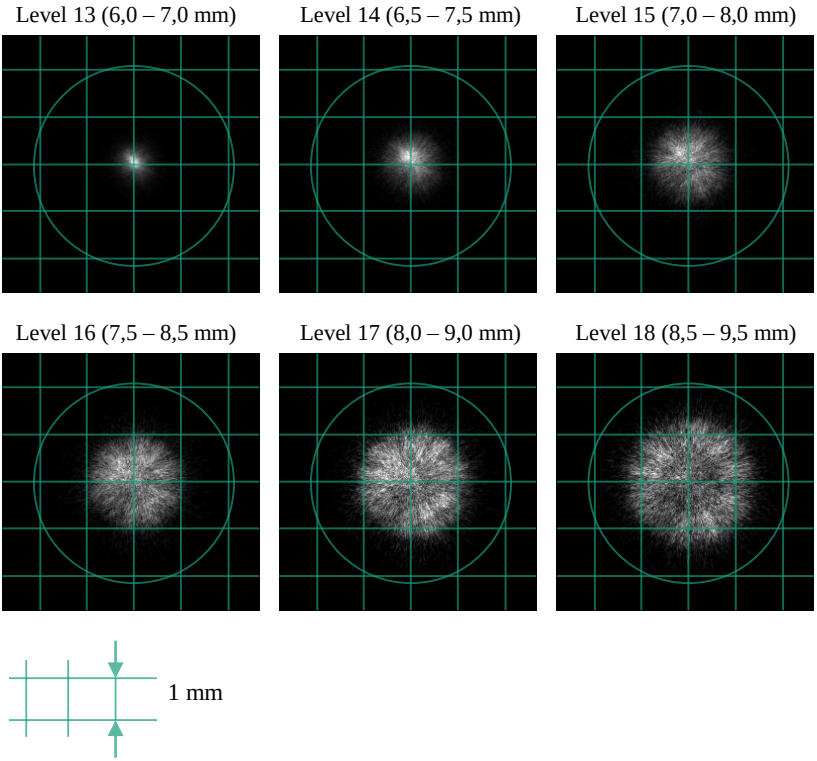

Source: Author.

3-Jet nozzles were also measured. The results are registered in Figure 44. The first images show clearly each jet from the nozzle output, allowing the measurement of its size. Practical results show that the size of the powder jet focus should be similar to the size of the jet at the nozzle output (slit size). In this case, the focus diameter is 1810 µm, located at level 12, about 15 mm from nozzle exit.

The particle density distribution follows the same rule of the focus position to almost all levels in this kind of nozzle, where the density of particles is higher in the jet center.

The powder and gas properties of this measurement are described in Table 9.

Table 9 – Powder and gas properties for 3-Jet nozzle particle density distribution.

Powder material	Titan alloy
Powder grain size	45 – 75 µm
Powder mass flow	5 g/min
Gas	Argon
Pressure	4 Bar
Carrier gas flow	3 L/min
Shielding gas flow	18 L/min

Source: Author.

Figure 44 – Particle density distribution of 3-Jet nozzle.

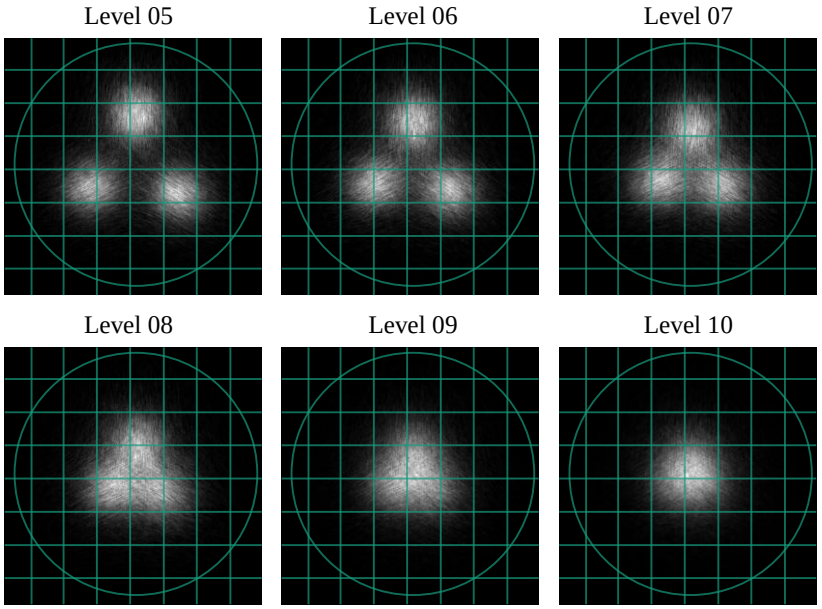

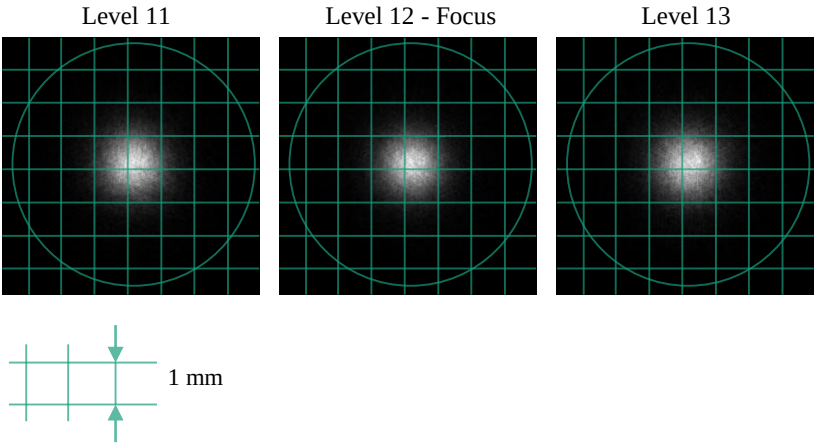

Source: Author.

Malfunction, misuse or unadjusted gas or powder feeding system can be detected through these images. Experienced operators and nozzle manufactures check the measurement results in order to evaluate the nozzle quality. Corrections and repairs are performed prior to LMD process.

Other authors as in [86] and [87] use a different experimental setup and to record images and process the particle concentration. Instead of using a coaxial image, a lateral image is generated also applying a laser line as illumination.

Diagrams can be created to each level recorded, representing the intensity values (0 to 255) of each pixel in the horizontal axis (X). Such diagrams are shown in APPENDIX B, gathered in one single figure, where outer lines represent the first levels while the middle diagram represent the focus (with white filling color and no vertical lines inside). Since the images are 256x256 pixels, the intensity levels of the 256 pixels in Y-axis where summed and normalized from 0 to 255. Corresponding superimposed images for each level shown on the diagram are represented in APPENDIX C.

4.1.2 Particle counting

Counting particles per frame in a recorded video is one of the possibilities of algorithm's application. Not only particle counting but also particle travel direction can be identified through several frames.

Despite the fact that it is still not possible to count exactly the number of delivered particles to the molten poll, since particles are in the micrometer scale and they travel in considerably high speed, calculations can be done to approximate this number. Particle speed depends on gas flow and particle size, but it can speed up to 30 m/s.

The results of particle counting still need to be improved in order to really validate the obtained data, since too many variables are involved in this process. Hardware updates such as illumination power and optics as well as a better CMOS camera in the system can also help on future measurements, allowing sharper recordings of faster particles. A negative point of these updates is a higher cost of the entire system.

Some tests on counting particles manually were performed. Measuring the weight of the delivered particles in a determined time and knowing the size, material (density) and approximated weigh of each particle, it is possible to estimate the number of particles.

Image binarization process, as described in section 3.2.3.2 Image binarization process, is necessary for applying a function to count particles in the algorithm. Each frame, as shown in Figure 45, provides a number of particles and its position. The algorithm calculates the centroid of each particle applying a threshold to the original image. Then, it counts the total number of centroids, which corresponds to number of particles.

As already mentioned on previous sections (3.2.3.2 Image binarization process), defining the right threshold value is crucial at this point of the algorithm calculation, since a wrong value could lead to less or more particles counted.

Applying this algorithm function at the focus level is a difficult task, since it can bring some errors on counting. High density powder jet levels, as it is in focus, show too much particles together, making it harder to the algorithm to perform the threshold and to identify centroids of two different particles when they are too close to each other. Therefore, two or more particles are represented as just one centroid and also as just one particle. As already mentioned above, future improvements on hardware and also software will allow the system to overcome such errors.

Figure 45 – Illustration of processing for counting single particles.

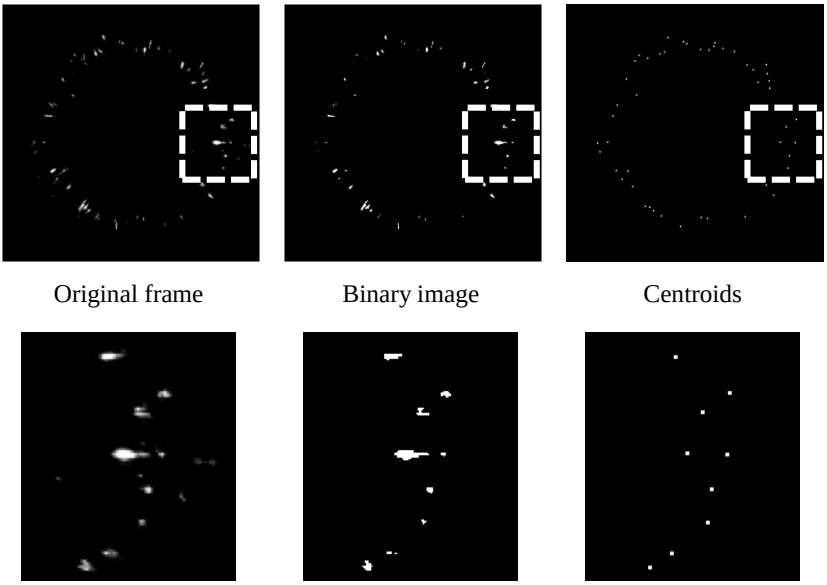

Cropped region of each image for zoom view

Source: Author.

Further developments on particle counting could also help defining the catchment efficiency of powder feed nozzles.

4.1.3 Powder jet focus diameter

One of the big challenges of this work was defining a calculation method for the powder jet focus diameter. There is no specific method to do it in the literature or praxis.

Considering the similarity of powder jet and laser beam in their geometry, the powder jet focus diameter was defined analogous to the laser beam focus as the minimum diameter that contains 86% of all particles counted on that specific level.

This calculus is done to the laser beam as 86% of the beam energy, also called “D86” method. It is actually defined as the diameter of the circle that is centered at the centroid of the beam profile and contains 86% of the beam power [88].

Regarding the algorithm limitations and the current low reliability of particles counting process, such measurement of powder jet diameter

was performed considering the intensity level of each pixel instead of the number of particles. The powder jet focus diameter corresponds to the minimum diameter, which contains 86% of the image intensity. Considering the “Intensity x Pixel” diagram of a superimposed image in focus, as seen in Figure 46, the 86% means 86% of the area under de diagram, centered in the middle of the image. The amount of pixels in the X-axis, which cover that area, correspond to the diameter. Using the input scale pixel per millimeter, the algorithm is able to calculate the diameter in millimeters. As the intensity level is directly related to the amount of particles, calculations can be correlated.

Several calculations and also comparisons with the nozzle manufacturer’s set up focus diameter were performed to define this method as standard for this work.

Figure 46 – Image intensity diagram – focus level.

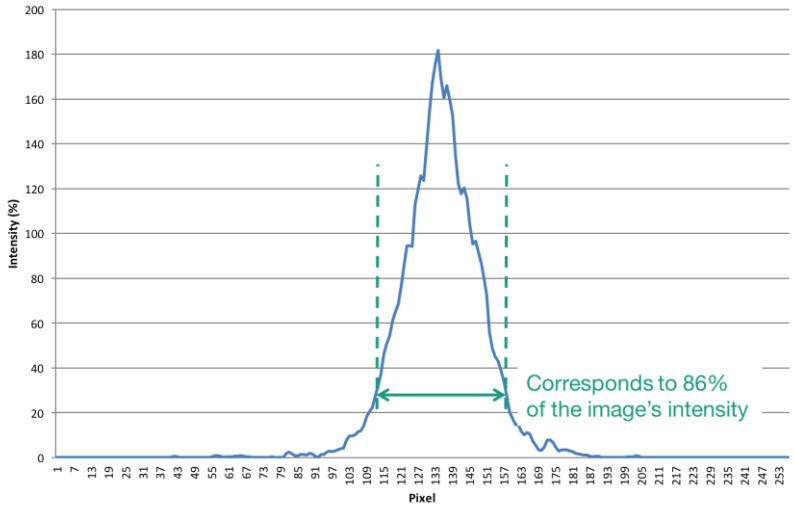

Source: Author.

In order to illustrate the focus diameter calculation, the diagrams for each axis are represented with the superimposed image in Figure 47. The same procedure taken to the X-axis can be applied to the Y-axis, what allows further analysis of the powder jet geometry.

Figure 47 – Illustration of focus diameter calculation.

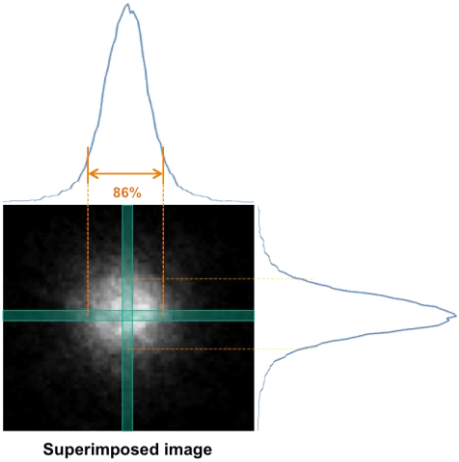

Source: Author.

An example of evaluation done with the results of some measurements is represented in Figure 48. The diagram shows a comparison between focus diameters in different situations: two different carrier gas flow (2 and 3 L/min) and with the use of shielding gas and without it. Powder and gas properties for this measurement are listed in Table 10.

More information about the use of shielding gas, its interference on the powder jet as well as the way the software recognizes it and how do the images look like is available in section 5.3 Use of shielding gas.

Table 10 – Powder and gas properties for powder jet focus diameter comparison.

Powder material	TLS Ti6A14V
Powder grain size	45 – 75 µm
Powder mass flow	5 g/min
Gas	Argon
Pressure	4 Bar
Carrier gas (CG) flow	2 and 3 L/min
Shielding gas flow	0 and 18 L/min

Source: Author.

Figure 48 – Powder jet focus diameter comparison – with and without the shielding gas (SG).

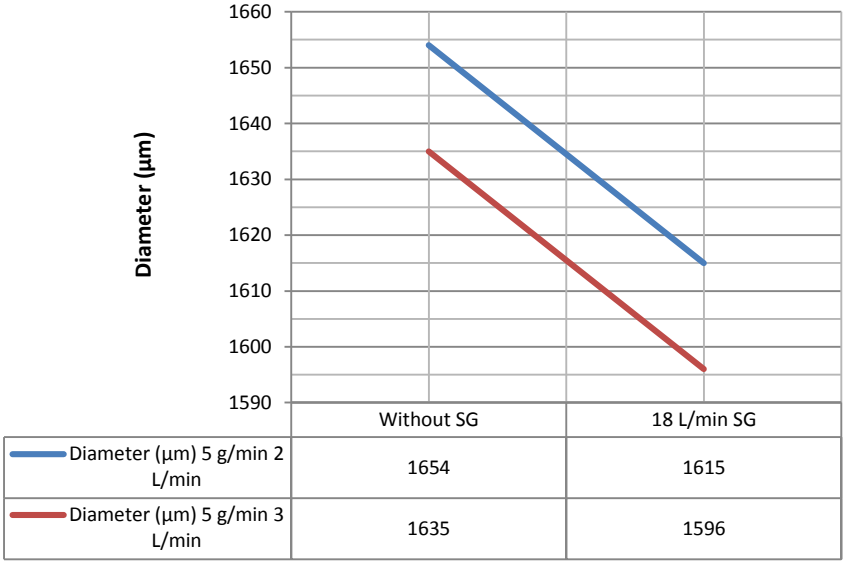

Source: Author.

The corresponding superimposed images for each result of the diagram, delivered by the software, are shown in APPENDIX D (CG 2 L/min – SG 0 L/min), APPENDIX E (CG 2 L/min – SG 18 L/min), APPENDIX F (CG 3 L/min – SG 0 L/min) and APPENDIX G (CG 3 L/min – SG 18 L/min) at level 09.

4.1.4 Powder jet focus position and geometry

Correlations between powder jet and laser focus position determine crucial properties of deposited tracks.

The focus position can be easily identified within the produced images where the powder jet has its smaller diameter. It is possible to identify this image through simple visual inspection in most of the cases, with no need of measurement. Once the image is identified, its level position determines the focus position from nozzle exit, in the Z-axis.

Figure 49 shows an example of diameter measurement for various levels of the powder jet. Within the diagram, the lowest point of the curve represents the smallest diameter and hence the focus level – in this

case, level 09 – 10 to 11 mm from nozzle exit. The corresponding images for this measurement of Figure 49 can be analyzed in APPENDIX F.

Nozzles are manufactured and aligned to produce a pre-determined focus position. Hence, measurement result can be compared to the manufacturer's set up. This procedure helps defining the reliability of the manufacturing process as well as the ability and experience of the manufacturer during the alignment process. The non-conformity of results determines a poor quality nozzle.

Figure 49 – Diameter (µm) of powder jet in various levels. Level 09 is the focus position – its position from 10 to 11 mm from nozzle exit.

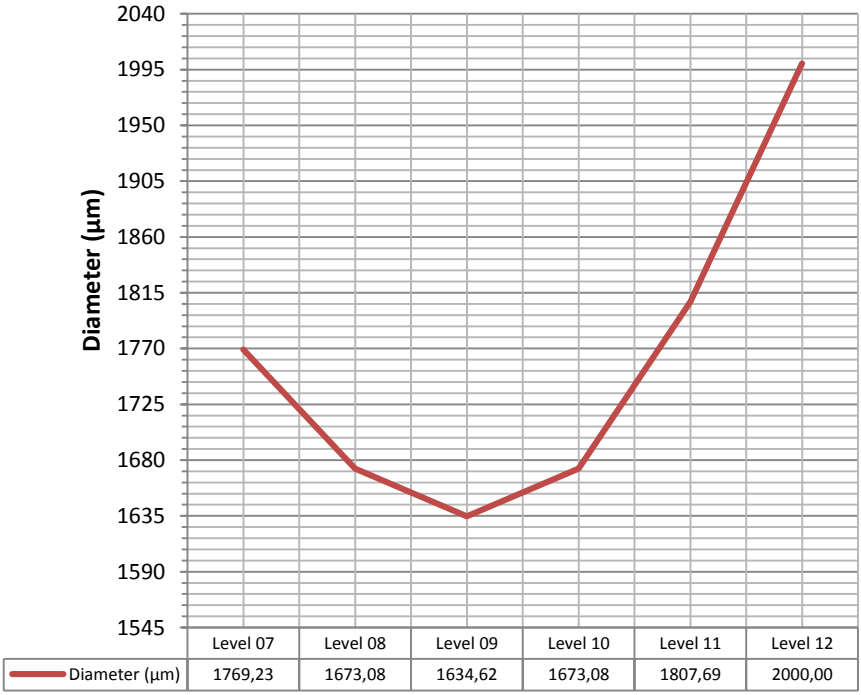

Source: Author.

Powder jet geometry is very similar to the laser beam geometry, where the smaller diameter also represents the focus and the higher energy density. Figure 50 shows a jet produced by a ring nozzle in a lateral image (left), produced by a DSLR Camera and special illumination and the geometry's sketch, represented on the right. The

geometry is easy to be identified and also compared to the laser beam. Such images can also be used to compare measurements of focus diameter and position.

Figure 50 – Ring shaped powder jet (left) and sketch of powder jet geometry (right).

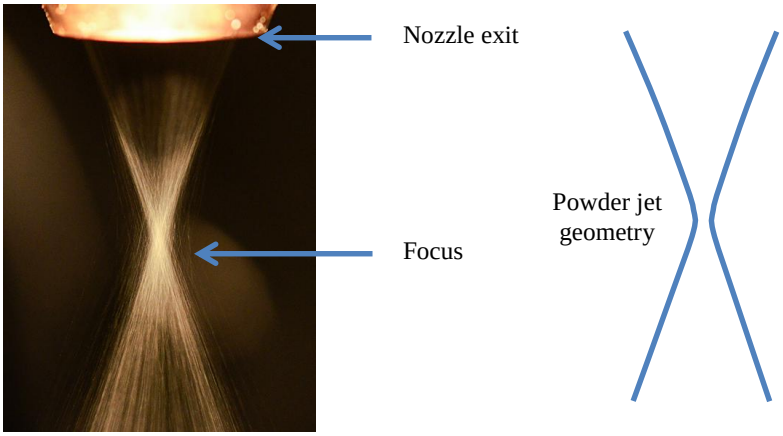

Source: Author, [58].

The geometry of the powder jet in each level, for two main different kinds of nozzles, can be also checked analyzing the superimposed images in APPENDIX G and APPENDIX H.

4.2 POWDER FEED NOZZLE QUALIFICATION

By the time all the properties of the powder jet have been identified and correlated to the LMD process, the operator is able to qualify the powder feed nozzle. Once the powder jet is qualified as good for production, so is also the powder feed nozzle.

Qualifying a powder feed nozzle means assuring that the nozzle properties, set up on manufacturing and alignment, will reproduce the corresponding powder jet. It also means that the nozzle is fully suitable for the LMD process, regarding its pre-defined parameters.

All the results detailed in this work are necessary as well as they are part of the nozzle qualification.

This system also allows the manufacturer to produce certificates of quality for new nozzles or for other ones being repaired or adjusted. Certified nozzles have more value, produce better revenue and are more reliable.

A certificate would bring, within the nozzle model, essential information about it as well as about the qualification procedure and utilized material so that the operator could reproduce the experiment in the industry, for measuring reasons.

Delivered nozzles would also be assured about its properties, since they have been tested and qualified prior to customer delivery.

5 SYSTEM APPLICATION EXAMPLES

5.1 NOZZLE TYPE COMPARISON

Different nozzles can be compared within the same process parameters. Therefore, the operator is able to analyze the best nozzle option.

This application also allows the correlation of variations in parameters of various nozzles. It is also a source of information for the improvement of nozzle manufacturing processes, as well as the investigation of future changes in nozzle design.

Figure 51 shows two superimposed images of two similar 3-Jet nozzles with different aperture for the powder on the nozzle exit. Even small changes could be detected when analyzing these kinds of images. In this particular case, the focus diameter has noticeably changed, from 1280 µm on the left (smaller aperture) to 1660 µm on the right image (larger aperture).

Figure 51 – Nozzle type comparison.

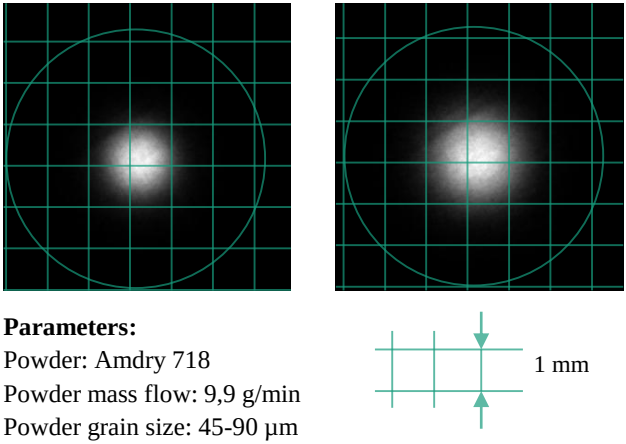

Source: Author.

Not only different nozzles but also the same nozzle in different adjustments can be compared. The same procedure would be adopted.

5.2 NOZZLE ALIGNMENT COMPARISON

One of the important capabilities of the measuring system is checking the proper alignment of the nozzle, as a part of the powder feed nozzle qualification.

Table 11 describes powder and gas properties of the application shown in Figure 52, comparing the alignment of a same nozzle, before (upper row) and after misuse (lower row).

Table 11 – Powder and gas properties for nozzle alignment comparison.

Powder material	Titan alloy
Powder grain size	10 – 40 µm
Powder mass flow	5 g/min
Gas	Argon
Pressure	4 Bar
Carrier gas flow	3 L/min
Shielding gas flow	0 L/min

Source: Author.

Figure 52 – Comparison of nozzle alignments. Upper row: well-aligned nozzle; Lower row: misaligned nozzle.

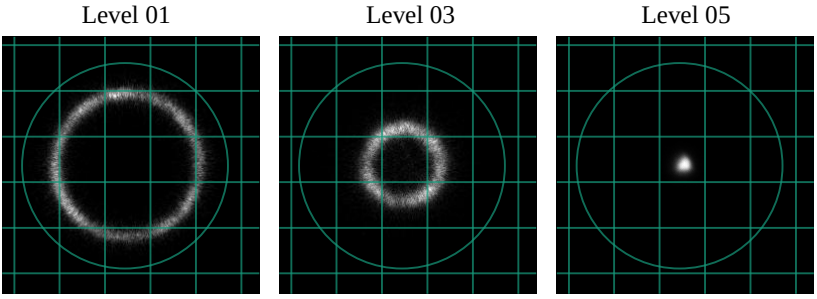

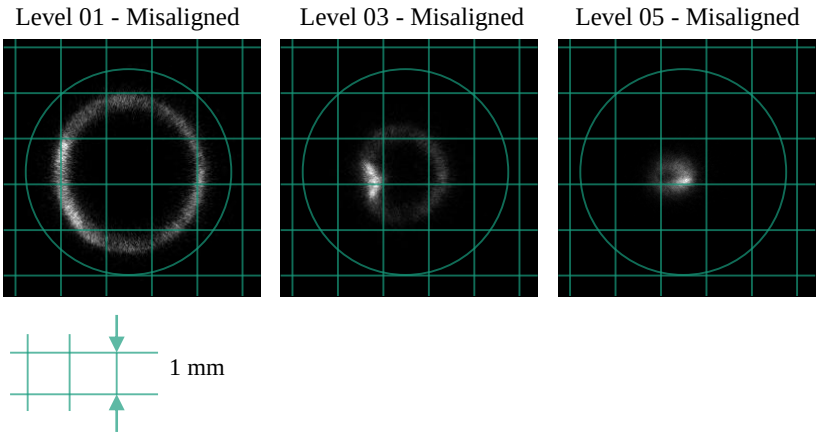

Source: Author.

The irregular distribution and the effect on the focus are clearly visible. It is important to document the adjustment of a nozzle in regular intervals in order to recognize deviations caused e.g. by wear or damages and also misuse of the nozzle. In this particular case, a misuse, due to an impact, drove to a misaligned powder jet. The system is able to identify the problem, avoiding waste of time, material and energy in the LMD process. This nozzle was sent back to the manufacturing at the Fraunhofer ILT, being adjusted again to be suitable for use.

Other possible causes of a misaligned powder jet could be the obstruction of the hoses that take the powder particles to the nozzle. During the change of particle sizes, when this hoses and the equipment are not properly cleaned, obstruction by bigger particles can occur.

ILT's ring-shaped powder feed nozzles have three inputs to connect the hoses from the powder feeder. The particles should be equally distributed between the three hoses, since the pass through a three-way particle distributor.

Using a nozzle with inappropriate particle sizes can also lead to obstruction of the nozzle's inner channels.

Another example of nozzle misalignment detection is shown in Figure 53, where a secondary focus is detected in levels prior to the focus level. Upper row images show 3 levels of a well-aligned powder jet while lower row images show the same 3 levels and nozzle misaligned. This example is a real situation where the nozzle was measured just before for starting production. After testing it, the

misalignment was detected (lower row images were the result) and the nozzle was back to the manufacturing department. By the time the nozzle was back to production, a new measurement was performed and it was then well aligned (upper row images were the result).

Figure 53 - Comparison of nozzle alignments. Upper row: well-aligned nozzle; Lower row: same nozzle but misaligned – Secondary focus was detected.

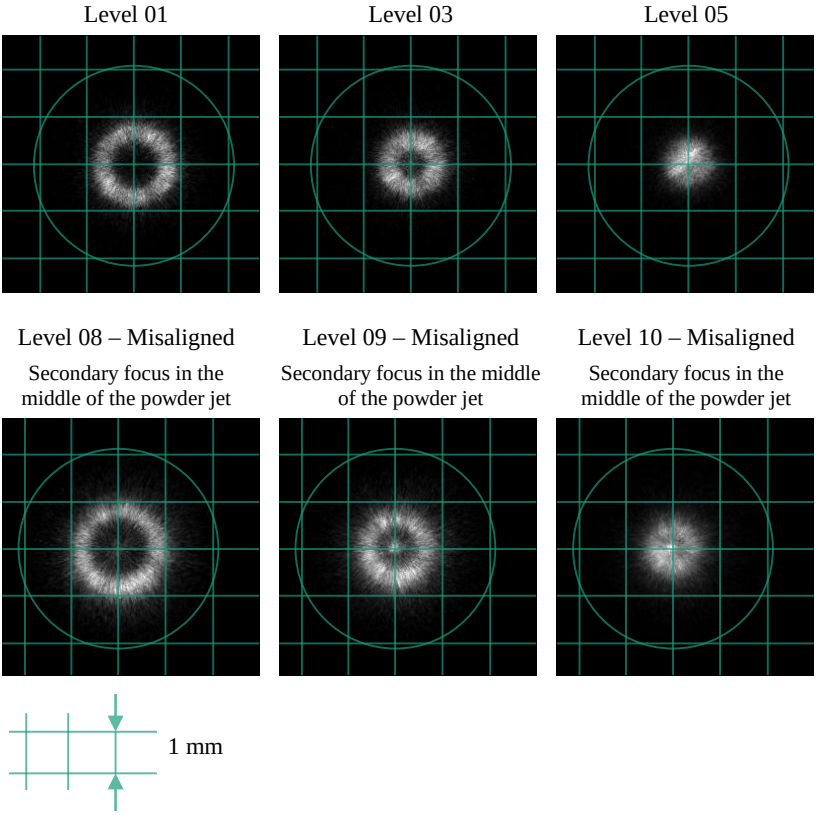

Source: Author.

5.3 USE OF SHIELDING GAS

The carrier gas carries powder particles and shielding gas is used for cladded tracks protection. Both of them have different output points on the powder feed nozzle. When the shielding gas is applied, a change

on the focus diameter is not expected but a change on the focus position. This occurs since the shielding gas is applied through the middle of the powder feed nozzle, pushing the powder jet focus in the direction of its flow.

The differences can be noticeable on the images. Depending on powder material and mass flow, they can be detected easier. These differences must be included on process calculation, especially the ones regarding the variation of focus position.

Figure 54 shows summarized images of the powder jet without the use of shielding gas ("No SG") and using it at 16 L/min. These results were produced under the powder and gas properties described in Table 12.

Table 12 – Powder and gas properties for shielding gas comparison.

Powder material	Titan alloy
Powder grain size	45 – 75 µm
Powder mass flow	5 g/min
Gas	Argon
Pressure	4 Bar
Carrier gas flow	3 L/min
Shielding gas flow	16 L/min

Source: Author.

Figure 54 – Comparison of the use of shielding gas (SG) in the powder jet.

Level 04 – No SG Level 06 – No SG Level 08 – No SG

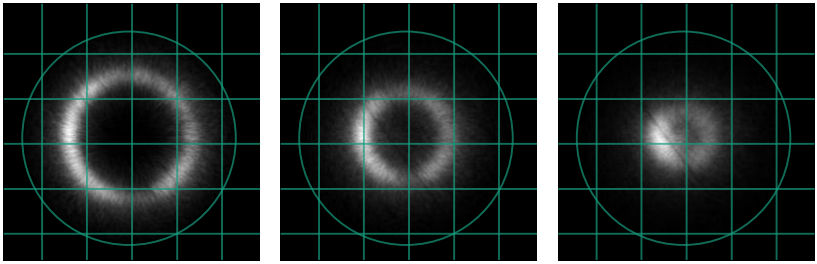

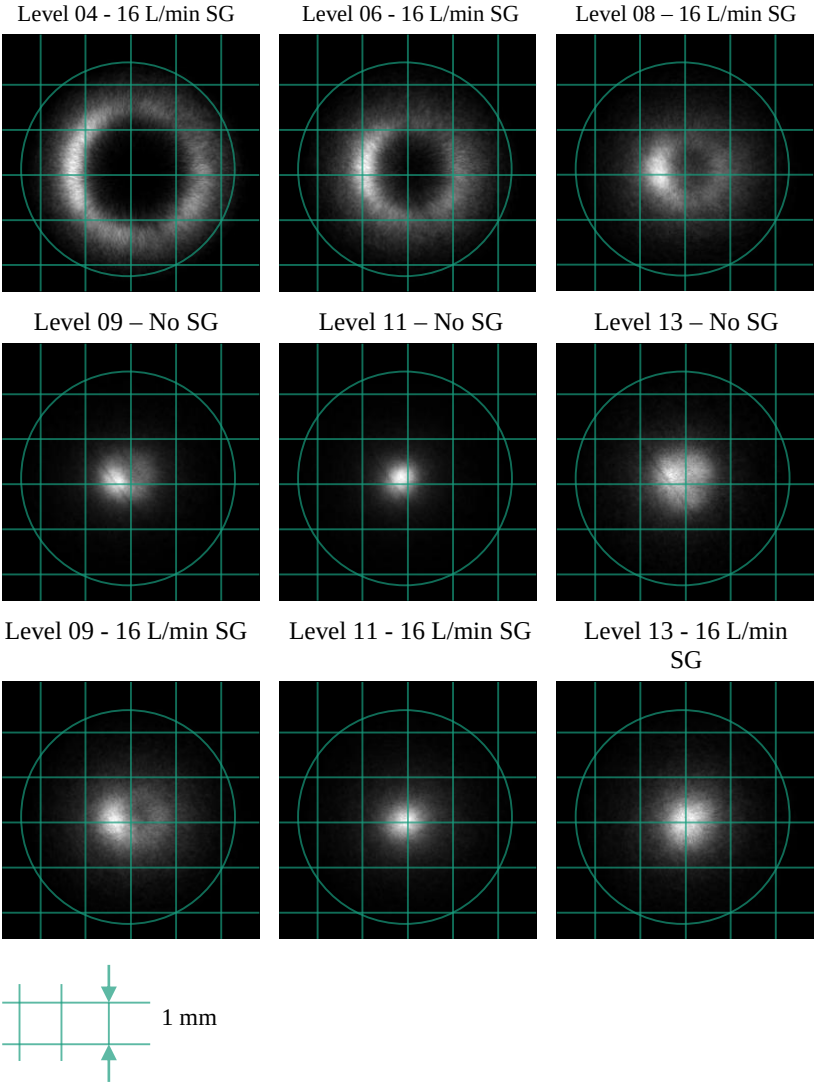

Source: Author.

These images show a more spread jet when shielding gas is used. The focus diameter although slightly varies in its core.

More apparent is the shift on focus position, as illustrated in Figure 55. The use of shielding gas pushes the focus down on the powder jet, due to its application point, centered in the nozzle, coaxial with the laser beam.

Figure 55 – Shift on focus position due to application of shielding gas.

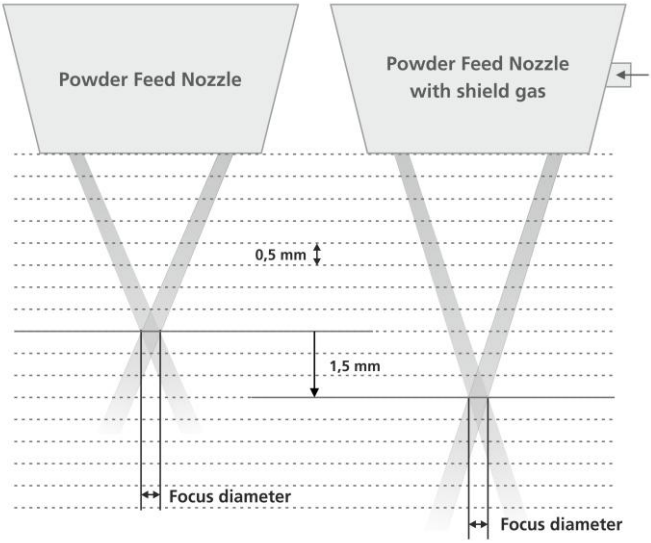

Source: Author.

This application is an example of a great breakthrough of this measurement system. It allows the operator to include small changes, but important ones, in his process calculations, being more efficient and generating results with a better quality.

5.4 VARIATION OF CARRIER GAS AND POWDER MASS FLOWS

The system also allows the investigation of independence of parameters like carrier gas and powder mass flows on the focus diameter. It is important to remember that despite the fact that the powder jet focus has its diameter independent of some parameters, the

density of the jet may change and produce differences in the results of the LMD. Higher density means more particles per volume and thus more energy required from the laser to melt the high amount of particles.

The carrier gas is responsible for carrying the powder particles from the powder feeder to the powder feed nozzle. Two carrier gas flows, commonly employed on LMD processes, were evaluated: 2 L/min and 3 L/min.

The comparisons have been carried out with the same 3-Jet nozzle with the smaller aperture, evaluated in the section 5.1.

The resulting particle density distributions in the focus level are shown in Figure 56. An increase of the carrier gas flow produced just a slight raise of the focus diameter, from 1277 µm at 2 L/min, on the left image to 1319 µm at 3 L/min, on the right.

Figure 56 – Carrier gas flow comparison

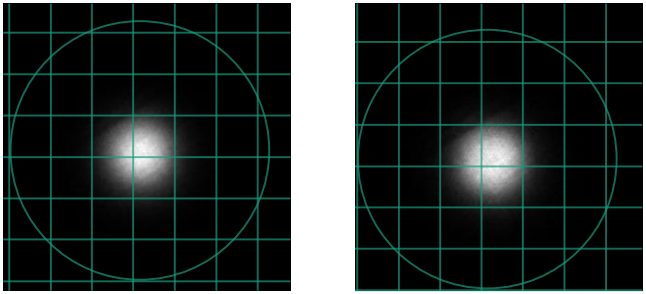

Parameters:
Powder: Amdry 718
Powder mass flow: 9,9 g/min
Powder grain size: 45-90 µm
Shielding gas flow: 18 L/min
Carrier gas flow: 2 L/min (left)
3 L/min (right)

Source: Author.

The powder mass flow influences the cladded geometry and corresponds to the revolutions of the powder feeder. Therefore, the rate has been measured at the powder feeder in advance. Two powder mass

flows were evaluated: 4,8 g/min at 1,2 rev/min and 9,9 g/min at 2,5 rev/min.

The carrier gas flow was set to 2 L/min and no shielding gas was used.

Figure 57 shows the two images of the focus level to each powder mass flow configuration.

Figure 57 – Powder mass flow comparison

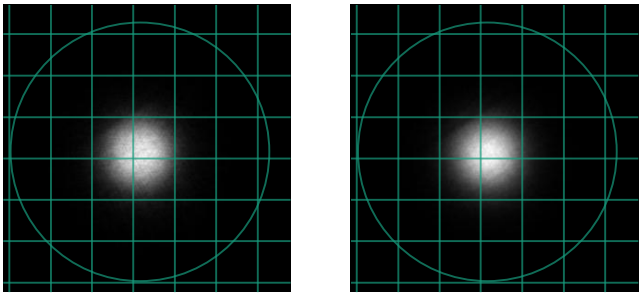

Parameters:
Powder: Amdry 718
Powder mass flow: 4,8 g/min (left)
9,9 g/min (right)
Powder grain size: 45-90 µm
Shielding gas flow: 0 L/min
Carrier gas flow: 2 L/min (left)

Source: Author.

The focus diameter varies just a small amount, from 1280 µm on the left, at 4,8 g/min of powder to 1300 µm on the right, at 9,9 g/min.

Considering that the particle size varies between 45 to 90 µm, this difference in the diameter of 20 µm cannot be considered, since the smaller particle is bigger than it. Differences of +/- 90 µm should be considered. Again, this conclusion shows an independence of the diameter size to the powder mass flow for these kinds of nozzles.

Although the variation of particle density distribution of this images is not expressive, higher powder mass flow rates produce higher density jets, since more particles are carried per volume of gas with more revolutions per minute.

5.5 VARIATION OF POWDER GRAIN SIZE

Differences on varying the particle grain sizes can be identified from particles smaller than 20 µm to others over 90 µm.

Current limitations of the system, regarding the optics and the camera, make the system more reliable to counting particles for grain sizes bigger than 45 µm. This occurs due to the algorithm's thresholding process, where smaller particles that are near each other are processed as just one single particle. It can reduce the number of counted particles drastically, although focus diameter calculations remain stable and reliable.

Particle grain sizes from 10 to 90 µm were tested with the system. Table 13 shows properties of powder and gas for this comparison and Figure 58 shows the results, where the smaller particles (10 – 40 µm) are shown in the upper row and bigger particles are shown in the lower row (63 – 90 µm), all shown in three levels, being the last image of each row, on the right, the focus level.

For each size, a corresponding nozzle was used, due to its adjustment and alignment for each grain size.

Table 13 – Powder and gas properties for powder grain size comparison.

Powder material	Titan alloy
Powder grain size	10 – 40 µm (1st row) 32 – 63 µm (2nd row) 63 – 90 µm (3rd row)
Powder mass flow	5 g/min
Gas	Argon
Pressure	4 Bar
Carrier gas flow	3 L/min
Shielding gas flow	0 L/min

Source: Author.

Figure 58 – Powder grain size comparison. From smaller (upper row) to bigger particle grain sizes (lower row).

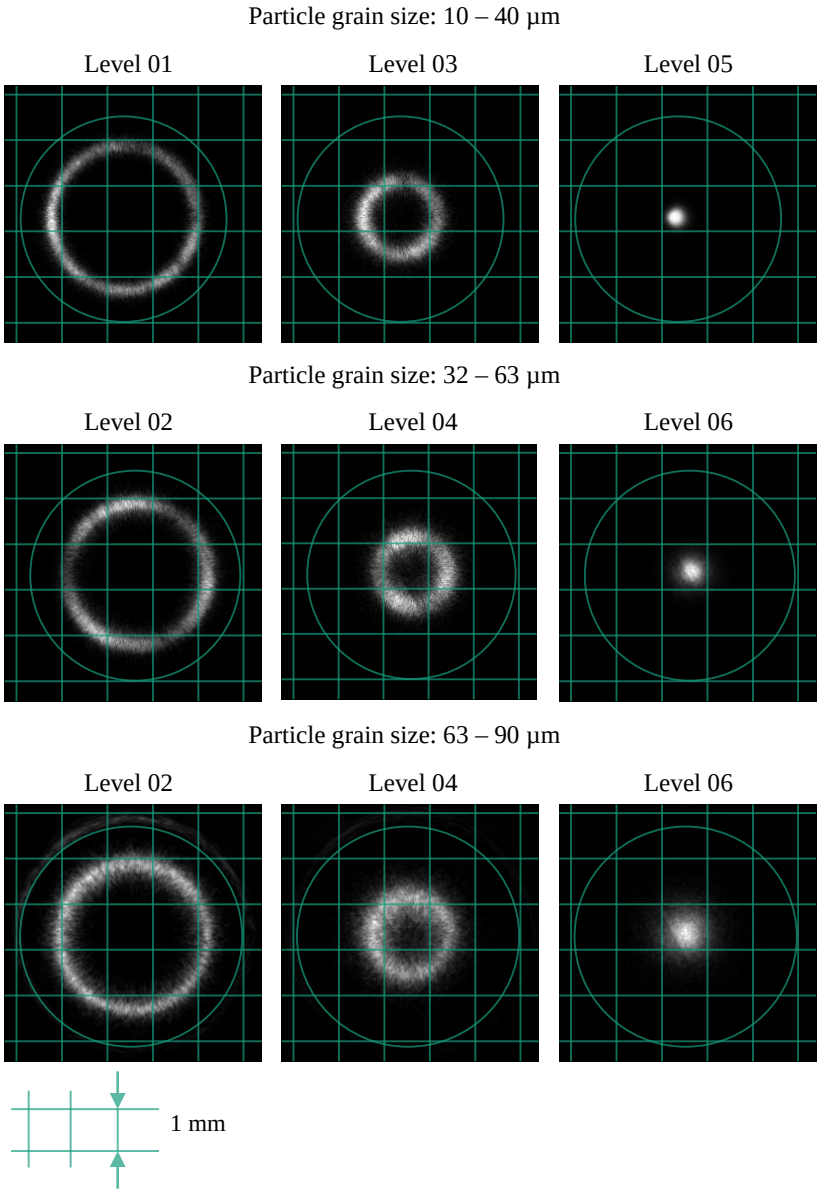

Source: Author.

Changes between each set of images are easily identified. Bigger particles produce larger focus diameter and smaller particles produce denser powder jet focus.

Smaller particles can fit into a small focus easier than bigger ones, producing denser powder jets. During its travel to the melt pool and to the focus level, bigger particles collide and spread from each other, producing, therefore, larger focus diameters and lower particle density distribution.

6 CONCLUSION

For the first time a standardized, automated and reproducible characterization of powder feed nozzles as well as a qualification of a powder jet was possible. This work was part of an important project milestone on searching cost-effective ways for turbomachinery manufacturing and aero engine repair. A measurement system, based on process control techniques was developed and validated through several experiments and intensive research.

The results of a measurement are some relevant images and parameters of the powder jet, which also allow the characterization of the powder feed nozzle. 3D particle density distribution, focus position and diameter are examples of results obtained.

On one hand the system allows the operator to compare and to document the adjustment of nozzles and the resulting powder jet properties. On the other hand, the influence of parameters like powder mass flow, grain sizes or carrier and shielding gas flow to the powder jet can be researched. Even small changes are already detected with satisfactory precision of the image processing algorithms.

It is also interesting to see the way the system was upgraded during time, being automated and utilizing better quality illumination line, through better optics and structure. Its construction as a modular system, being able to be installed in different laboratories or plants turns into a big advantage since it can perform measurements in different laser cells in a factory plant, as it was performed inside the Fraunhofer ILT.

Besides the structure design, the algorithm development and improvement was one of the big challenges of this work. So was it also combining theory of laser beam and powder jet.

Correlating the measurement results and the quality of the produced parts is also important for a continuous improvement of system, its method as well as of the nozzle manufacturing and adjustment procedure and the LMD process itself.

7 FURTHER DEVELOPMENTS

Regarding the technology involved and also the challenging procedure of measuring the powder jet focus parameters in an innovative way, the system of this work still needs improvements in its software and hardware.

The software is going to be more user friendly and will also have its algorithm further developed.

The hardware is going to be modified and simplified, reducing weight and costs so that it could be implemented in LMD machines in the industry.

In order to accomplish these desired improvements, it is necessary to continuously investigate different methods of measurement as well as different equipment.

Technology developments allow the use of smaller and cheaper high-speed cameras, which can produce the same results. New illumination techniques and more efficient lasers are being developed so that new possibilities of applying a laser line to properly illuminate the powder jet and capture more information about the powder particles will appear.

Integrating the system to a laser machine would also be a step further to better automation and also a possibility of implementation of a closed loop control system, detecting errors or process changes live.

At the theoretical area, a quality factor for the powder jet still needs to be validated and assured through more empirical tests and experiments.

REFERENCES

1. ADER, C. et al. **Research on layer manufacturing techniques at Fraunhofer**. Fraunhofer ILT, IFAM and IPT. Germany, p. 12. 2004.
2. GEBHARDT, A. **Rapid Prototyping:** Werkzeuge für die schnelle Produktentwicklung. 2nd Edition. ed. Aachen: Hanser Verlag, v. I, 2000. 409 p. ISBN ISBN-13 978-3446212428.
3. MANN, S.; DE MELO, L.; ABELS, P. **Measurement of particle density distribution of powder nozzles for laser material deposition**. International Congress on Applications of Lasers & Electro-Optics ICALEO. Orlando - US: Laser Institute of America LIA. 2013.
4. MANN, S.; ABELS, P. **Zertifizietung von Pulverdüsen für das Laserauftragschweissen**. Fraunhofer-Institut für Lasertechnik ILT. Aachen, p. 177. 2013.
5. EICHLER, J.; EICHLER, H. J. **Laser:** Bauformen, Strahlführung, Anwendungen. 7th Edition. ed. Berlin: Springer, 2010. 490 p. ISBN ISBN 978-3-642-10462-6.
6. SILFVAST, W. T. **Laser Fundamentals**. 2nd Edition. ed. Cambridge: Cambridge University Press, 2004. ISBN ISBN 0-521-83345-0.
7. SILFVAST, W. T. **Fundamentals of Photonics**. SPIE. Orlando: [s.n.]. 2005.
8. LASERVISION GMBH & CO. KG. **Guide to laser safety**. LASERVISION. Fürth, Germany, p. 52. 2011.
9. PASCHOTTA, R. Encyclopedia. **RP Photonics Encyclopedia**. Disponivel em: <http://www.rp-photonics.com/encyclopedia.html>. Acesso em: 03 fev. 2015.
10. TRUMPF WERKZEUGMASCHINEN GMBH + CO. KG. **Laserbearbeitung: Festkörperlaser**. TRUMPF Werkzeugmaschinen. Ditzingen, p. 120. 2007.
11. SINGH, S. C. et al. Lasers: Fundamentals, Types, and Operations. In: SINGH, S. C., et al. **Nanomaterials:** Processing and Characterization with Lasers. 1st Edition. ed. Weinheim: Wiley-VCH Verlag GmbH & Co. KGaA, v. I, 2012. ISBN ISBN 9783527327157.
12. DEPARTMENT OF MECHANICAL ENGINEERING, COLUMBIA UNIVERSITY. Properties of Laser Beams. **Introduction of Laser Machining Processes**, 2014. Disponivel em: <http://www.aml.engineering.columbia.edu/ntm/level1/ch02/html/l1c02s02.html>. Acesso em: 02 fev. 2015.
13. ION, J. C. **Laser Processing of Engineering Materials:** Principles, Procedure and Industrial Application. 1st Edition. ed. Burlington: Elsevier Butterworth-Heinemann, v. I, 2005. 576 p. ISBN ISBN 0 7506 6079 1.

14. POPRAWE, R. Coherent Light: "From Chips to Ships". **Laser Technik Journal**, Weinheim, v. I, n. 2, p. 31-36, April 2010.
15. POPRAWE, R.; WEBER, H.; HERZIGER, G. **Laser Physics and Applications**. Berlin: Springer, v. 1, 2004. 495 p. ISBN ISBN 978-3-540-00105-8.
16. IEC - INTERNATIONAL ELECTROTECHNICAL COMISSION. **International Standard IEC 60825-1 - Safety of laser products**. IEC. Geneva, p. 122. 2001-08.
17. STEEN, W. M.; MAZUMDER, J. **Laser Material Processing**. 4th Edition. ed. London: Springer Verlag, 2010. ISBN ISBN 978-1-84996-061-8.
18. BELFORTE, D. Laser cladding for difficult-to-access internal contours. **Industrial Laser Solutions for Manufacturing**, 14 abr. 2014. Disponivel em: <http://www.industrial-lasers.com/articles/2014/04/laser-cladding-for-difficult-to-access-internal-contours.html>. Acesso em: 20 jan. 2015.
19. DE LANGE, D. F.; HOFMAN, J. T.; MEIJER, J. **Influence of intensity distribution on the meltpool and clad shape for laser cladding**. Third International WLT-Conference on Lasers in Manufacturing. Munich: Elsevier. 2005. p. 1-5.
20. GASSER, A. Laser Metal Deposition. In: POPRAWE, R. **Tailored Light 2 - Laser Application Technology**. RWTH Edition. ed. Aachen: Springer Verlag, 2011. p. 216-224. ISBN ISBN 978-3-642-01236-5.
21. MEINERS, W. **Direktes Selektives Laser Sintern einkomponentiger metallischer Werkstoffe**. Aachen: Shaker, 1999. 125 p.
22. KOMVOPOULOS, K.; NAGARATHNAM, K. Processing and characterization of laser-cladded coating materials. **Journal of Engineering Materials and Technology**, v. 112, p. 131-143, April 1990.
23. GASSER, A. et al. Laser additive manufacturing. Laser Metal Deposition (LMD) and Selective Laser Melting (SLM) in turbo-engine applications. **Laser Technik Journal**, p. 58-63, 2010.
24. TOYSERKANI, E.; KHAJEPOUR, A.; CORBIN, S. **Laser Cladding**. Boca Raton: CRC Press LLC, 2005. 280 p.
25. COSTA, L.; VILAR, R. Laser powder deposition. **Rapid Prototyping Journal**, Tullahoma, Tennessee, USA, p. 264-279, 2009. ISSN ISSN 1355-2546.
26. MAZUMDER, J. Crystal ball view of Direct Laser Deposition. **JOM - The Journal of The Minerals, Metals & Materials Society**, Michigan, USA, v. 52, n. 12, p. 28-29, 2000. ISSN DOI 10.1007/s11837-000-0063-7.
27. ZEKOVIC, S.; DWIWEDI, R.; KOVACEVIK, R. Numerical simulation and experimental investigation of gas–powder flow from radially symmetrical nozzles in laser-based direct metal deposition. **International**

Journal of Machine Tools & Manufacturing, Richardson, TX, USA, v. 47, p. 112-123, 2007.

28. PINKERTON, A. J.; LI, L. The development of temperature elds and powder ow during laser direct metal deposition wall growth. **Proc. Instn. Mech. Engrs.: Journal Mechanical Engineering Science**, v. 218, n. Part C, p. 531-541, 2004.
29. MAZUMDER, J. et al. Closed loop direct metal deposition: art to part. **Optics and Lasers in Engineering**, Michigan, v. 34, p. 397-414, 2000.
30. AMINE, T.; NEWKIRK, J. W.; LIOU, F. An investigation of the effect of direct metal deposition parameters on the characteristics of the deposited layers. **Case Studies in Thermal Engineering**, v. 3, p. 21-34, jul. 2014.
31. MORVILLE, S. et al. **Numerical Modeling of Powder Flow during Coaxial Laser Direct Metal Deposition – Comparison between Ti-6Al-4V Alloy and Stainless Steel 316L**. COMSOL Conference. Milan, IT: COMSOL. 2012.
32. WANG, F.; MEI, J.; WU, X. Direct laser fabrication of Ti6Al4V/TiB. **Journal of Materials Processing Technology**, Edgbaston, UK, v. 195, n. 1-3, p. 321-326, January 2008.
33. FESSLER, J. R. et al. **Laser Deposition of Metals for Shape Deposition Manufacturing**. Solid Freeform Fabrication Symposium. Austin, Texas - US: The University of Texas at Austin. 1994. p. 1-8.
34. HONG, C. et al. **Advantages of Laser Metal Deposition by Using Zoom Optics and MWO (Modular Welding Optics)**. ICALEO. Orlando, FL: LIA Laser Institute of America. 2011. p. 295-300.
35. WITZEL, J. et al. **Additive Manufacturing of a Blade-integrated Disk by Laser Metal Deposition**. ICALEO 30th International Congress on Applications of Lasers & Electro–Optics. Orlando, FL, USA: [s.n.]. 2011. p. 250-256.
36. IBARRA-MEDINA, J.; VOGEL, M.; PINKERTON, A. J. **A CFD MODEL OF LASER CLADDING:** FROM DEPOSITION HEAD TO MELT POOL DYNAMICS. International Congress on Applications of Lasers & Electro-Optics ICALEO. Orlando, US: Laser Institute of America LIA. 2011. p. 378-386.
37. GU, D. **Laser Additive Manufacturing of High-Performance Materials**. [S.l.]: Springer-Verlag, v. I, 2015. 311 p. ISBN ISBN 9783662460894.
38. TANG, L. et al. Variable Powder Flow Rate Control in Laser Metal Deposition Processes. **Journal of Manufacturing and Engineering**, Rolla, v. 130, p. 11, August 2008. ISSN DOI 10.1115/1.2953074.
39. MEI, H. et al. **The characterization of the performance of a new powder feeder for laser based additive manufacturing**. Southern Methodist University. Richardson, TX, USA, p. 448-457.

40. CANDEL-RUIZ, A. Value from light and dust. Repair and finishing with laser deposition welding. **Laser+Produktion**, 2010.

41. BI, G. et al. Development and qualification of a novel laser-cladding head with integrated sensors. **International Journal of Machine Tools & Manufacture**, n. 47, p. 555-561, July 2006.

42. SCHNEIDER, M. F. **Laser cladding with powder: effect of some machining parameters on clad properties**. University of Twente. The Netherlands. 1998.

43. WEISHEIT, A.; BACKES, G. Alloying and Dispersing. In: POPRAWE, R. **Tailored Light 2 - Laser Application Technology**. RWTH Edition. ed. Aachen: Springer Verlag, 2011. p. 207-215.

44. POPRAWE, R. **Lasertechnik für die Fertigung - Grundlagen, Perspektiven und Beispiele für die innovativen Ingenieur**. 1st Edition. ed. Aachen: Springer Verlag, v. I, 2005. ISBN ISBN 3-540-21406-2.

45. DRAUGELATES, U. **Corrosion and wear protection by CO2 laser beam cladding combined with the hot wire technology**. ECLAT. Oberursel, Germany: DGM Digitalinformationsgesellschaft Verlag. 1994. p. 344-354.

46. STEENBERGEN, M. **Ontwerp en Realisatie van een Draadtoevoersysteem voor Lasercladden**. University of Twente. [S.l.]. 1993.

47. SCHUBERT, E. et al. Laser beam cladding: A flexible tool for local surface treatment and repair. **Journal of Thermal Spray Technology**, Bremen, v. 8, n. 4, p. 590-596, December 1999.

48. OERLIKON METCO. **Laser Cladding in 3D**. Oerlikon Metco. [S.l.], p. 2. 2014.

49. KELBASSA, I. **Qualifizierung des Laserstrahl-Auftragschweißens von BLISKs aus Nickel-und Titanbasislegierungen**. RWTH Aachen University. Aachen. 2006.

50. FRAUNHOFER-GESELLSCHAFT. Fraunhofer-Innovationscluster Turpro - Produkte. **Turpro**, 2010. Disponivel em: <http://www.turpro.de/de/produkte>. Acesso em: 20 mar. 2012.

51. TRUMPF LASER- UND SYSTEMTECHNIK GMBH. **Laserauftragschweißen: Oberflächen optimieren und reparieren**. TRUMPF Laser- und Systemtechnik GmbH. Ditzingen, p. 12. 2008.

52. POEPPEL, S. **Keys to success in Laser Metal Deposition (LMD)**. Joining Technologies, INC. Connecticut, US.

53. LEVY, S. **Two-phase flow in complex systems**. 1st Edition. ed. New York: Wiley, v. I, 1999. 448 p. ISBN 978-0-471-32967-1.

54. GTV VERSCHLEISS-SCHUTZ GMBH. The PF Series of Powder Feeders. **GTV GmbH**, 2015. Disponivel em: <http://www.gtv-

mbh.com/anlagentechnik/pulverfoerderer--dosiersysteme/>. Acesso em: 30 jan. 2015.

55. OERLIKON METCO. Coating Materials: Laser Cladding. **Oerlikon Metco**, 2014. Disponivel em: <http://www.oerlikon.com/metco/en/products-services/coating-materials/laser-pta-weld-overlay/laser-cladding/>. Acesso em: 15 January 2015.
56. SPECIAL METALS. INCONEL ALLOY. **Special Metals**, 2014. Disponivel em: <http://www.specialmetals.com/documents/Inconel%20alloy%20718.pdf>. Acesso em: 22 January 2015.
57. IXUN LASERTECHNIK GMBH. Produkte: Pulverdüsen. **IXUN-Lasertechnik**, 2012. Disponivel em: <http://www.ixun-lasertechnik.de/produkte/pulverzufuhrduesen>. Acesso em: jun. 2014.
58. FRAUNHOFER-INSTITUT FÜR LASERTECHNIK ILT. System Engineering for Powder-Based Laser Cladding. **Fraunhofer ILT**, 2013. Disponivel em: <http://www.ilt.fraunhofer.de/en/publication-and-press/brochures/brochure_System_Engineering_for_Powder-Based_Laser_Cladding.html>. Acesso em: 15 jun. 2014.
59. LIN, J. A simple model of powder catchment in coaxial laser cladding. **Optics & Laser Technology Journal**, 31, n. 1, April 1999. 233-238.
60. PRECITEC GROUP. Processing Heads: Cladding head YC52. **Precitec Group**, 2015. Disponivel em: <http://www.precitec.de/en/products/joining-technology/processing-heads/yc52/>. Acesso em: 10 nov. 2014.
61. FRAUNHOFER CLA. Laser Cladding. **Fraunhofer Center for Laser Applications**, Plymouth. Disponivel em: <http://www.cla.fraunhofer.org/en/laser_cladding.html>. Acesso em: 22 mar. 2014.
62. MAZUMDER, J. et al. **Laser Processing:** Surface Treatment and Film Deposition. Series E: Applied Sciences. ed. Dordrecht: Kluwer Academic Publishers, v. 307, 1996. ISBN e-ISBN 978-94-009-0197-1.
63. HÜGEL, H.; GRAF, T. **Laser in der Fertigung:** Strahlquellen, Systeme, Fertigungsverfahren. Wiesbaden: Vieweg+Teubner, v. 2, 2009. ISBN ISBN 978-3-8351-0005-3.
64. KAIERLE, S.; ABELS, P.; KRATZSCH, C. **Process Monitoring and Control for Laser Material Processing – An Overview**. Proceedings of the Third International WLT- Conference on Lasers in Manufacturing. Munich: [s.n.]. 2005.
65. FRAUNHOFER-INSTITUT FÜR LASERTECHNIK ILT. Process Control in Laser Materials Processing. **Fraunhofer ILT**. Disponivel em: <http://www.ilt.fraunhofer.de/en/publication-and-

press/brochures/brochure_Process_Control_in_Laser_Materials_Processing.html>. Acesso em: 25 abr. 2013.

66. KAIERLE, S.; REGAARD, B. **Optikmodulbaukasten für die Prozessüberwachung und -beobachtung**. Fraunhofer-Institut für Lasertechnik ILT. Aachen, p. 130. 2004.
67. MIKROTRON GMBH. CameraLink(r) - Simple and reliable handling due to technical standards. **Mikrotron**, 2012. Disponivel em: <http://www.mikrotron.de/en/high-speed-camera-solutions/machine-vision-cameras/cameralinkr.html>. Acesso em: 15 jul. 2015.
68. KAIERLE, S. Process Monitoring and Control of Laser Beam Welding. **Laser Technik Journal**, Weinheim, v. I, n. 2, p. 41-43, May 2008.
69. THOMBANSEN, U.; ABELS, P. **Self-optimizing production systems**. Fraunhofer-Institut für Lasertechnik ILT. Aachen, p. 163. 2010.
70. UNGERS, M.; ABELS, P. **Online quality assurance for laser brazing**. Fraunhofer-Institut für Lasertechnik ILT. Aachen, p. 167. 2011.
71. MÜLLER, B. **Einfluss der Pulverkornfraktion beim Extremhochgeschwindigkeitslaserauftragsschweißen (EHLA) von Inconel 625**. FH Aachen - University of Applied Sciences. Aachen, p. 79. 2012.
72. BRUCK, G. J. **Fundamentals And Industrial Applications Of High Power Laser Beam Cladding**. SPIE, Laser Beam Surface Treating and Coating. Dearborn, MI: SPIE. 1988.
73. VILAR, R. Laser Cladding. **Journal of Laser Applications**, v. 11, n. 2, p. 64-79, April 1999.
74. YANG, Y. Microstructure and properties of laser-clad high-temperature wear-resistant alloys. **Applied Surface Science**, 140, n. 1, 1999. 19-23.
75. KATHURIA, Y. P. Laser-cladding process: a study using stationary and scanning CO2 laser beams. **Surface Coatings Technology**, Japan, 97, n. 1-3. 442-447.
76. MANN, S.; ABELS, P. **Measurement of Particle Density Distribution of Powder Nozzles**. Fraunhofer-Institut für Lasertechnik ILT. Aachen, p. 167. 2011.
77. THE MATHWORKS, INC. Products & Services: MATLAB. **MATLAB - The Language of Technical Computing**, 2014. Disponivel em: <http://www.mathworks.com/products/matlab/>. Acesso em: 15 ago. 2014.
78. THE MATHWORKS, INC. Products & Services: Simulink. **Simulink - Simulation and Model-Based Design**, 2014. Disponivel em: <http://www.mathworks.com/products/simulink/>. Acesso em: 15 ago. 2014.
79. THE MATHWORKS, INC. Image Processing Toolbox - Perform image processing, analysis, and algorithm development. **MathWorks -**

MATLAB and Simulink for technical computing, 2015. Disponivel em: <http://www.mathworks.com/products/image/?s_iid=ovp_prodindex_1109924659001-61214_pm>. Acesso em: 15 abr. 2015.

80. THE MATHWORKS, INC. Computer Vision System Toolbox - Design and simulate computer vision and video processing systems. **MathWorks - MATLAB and Simulink for technical computing**, 2015. Disponivel em: <http://www.mathworks.com/help/vision/index.html>. Acesso em: 15 abr. 2015.
81. JOHNSON, S. **Stephen Johnson on Digital Photography**. Sebastopol: O'Reilly Media, v. I, 2006. 305 p.
82. FISHER, R. et al. Glossary. **Hypermidea Image Processing Reference**, 2003. Disponivel em: <http://homepages.inf.ed.ac.uk/rbf/HIPR2/glossary.htm>. Acesso em: 25 maio 2014.
83. IBM. Gray Level Image Technologies. **IBM Research**. Disponivel em: <https://www.research.ibm.com/haifa/projects/image/glt/binar.html>. Acesso em: 25 maio 2014.
84. IRAVANI-TABRIZIPOUR, M. **Image-Based Feature Tracking Algorithms for Real-Time Clad Height Detection in Laser Cladding**. University of Waterloo. Ontario, CA, p. 102.
85. MÖLLENHOFF, M. **Ermittlung von geeigneten Prozessfenstern beim Laserstrahl-Auftragschweißen durch DoE**. RWTH Aachen. Aachen. 2013.
86. PAN, H.; LIOU, F. Numerical simulation of metallic powder flow in a coaxial nozzle for the laser aided deposition process. **Journal of Materials Processing Technology**, Rolla, n. 168, p. 230-244, 2005.
87. WEN, S. Y. et al. Modeling of coaxial powder flow for the laser direct deposition process. **International Journal of Heat and Mass Transfer**, West Lafayette, IN, USA, n. 52, p. 5867-5877, 26 September 2009.
88. ISO 11146-3:2005(E). **Lasers and laser-related equipment - Test methods for laser beam widths, divergence angles and beam propagation ratios - Part 3: Intrinsic and geometrical laser beam classification, propagation and details of test methods**. [S.l.]. 2005.

APPENDIX A – Primary results from standard measurement

Intensity superimposed image

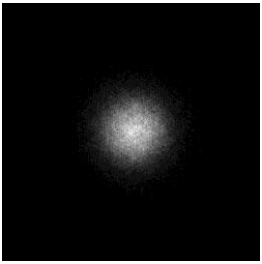

Centroids superimposed image

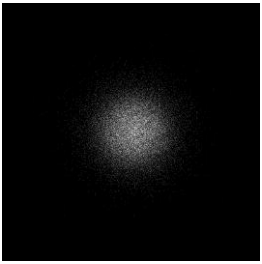

False color superimposed image

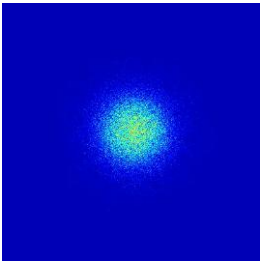

3D superimposed image from centroids

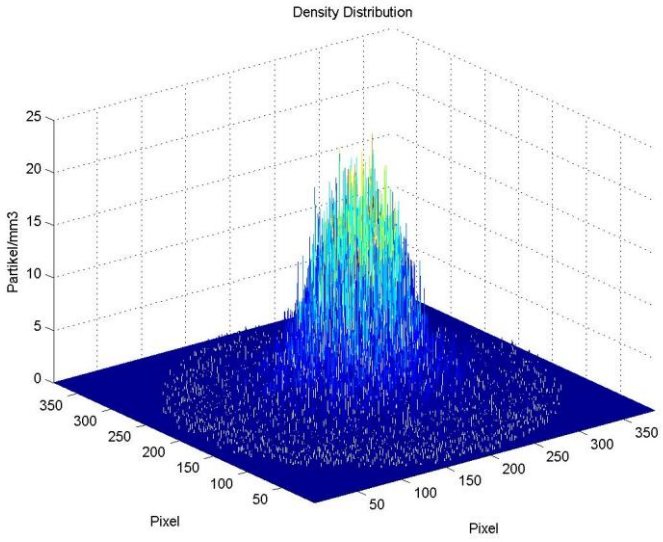

Source: Author.

APPENDIX B – Intensity distribution through levels

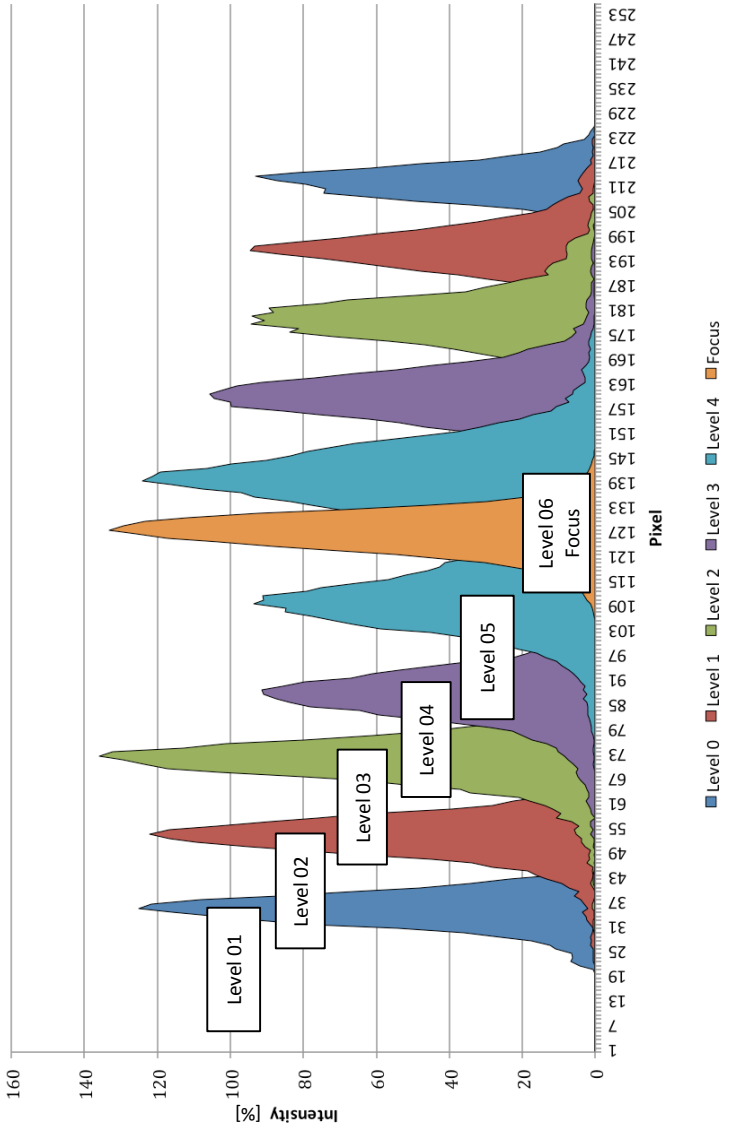

Source: Author.

APPENDIX C – Images of intensity distribution diagram

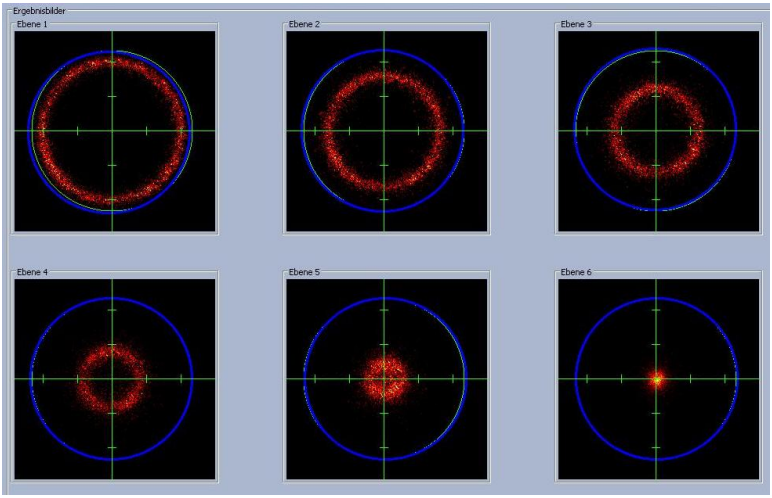

Source: Author.

APPENDIX D - Results of an ILT 3-Jet Nozzle

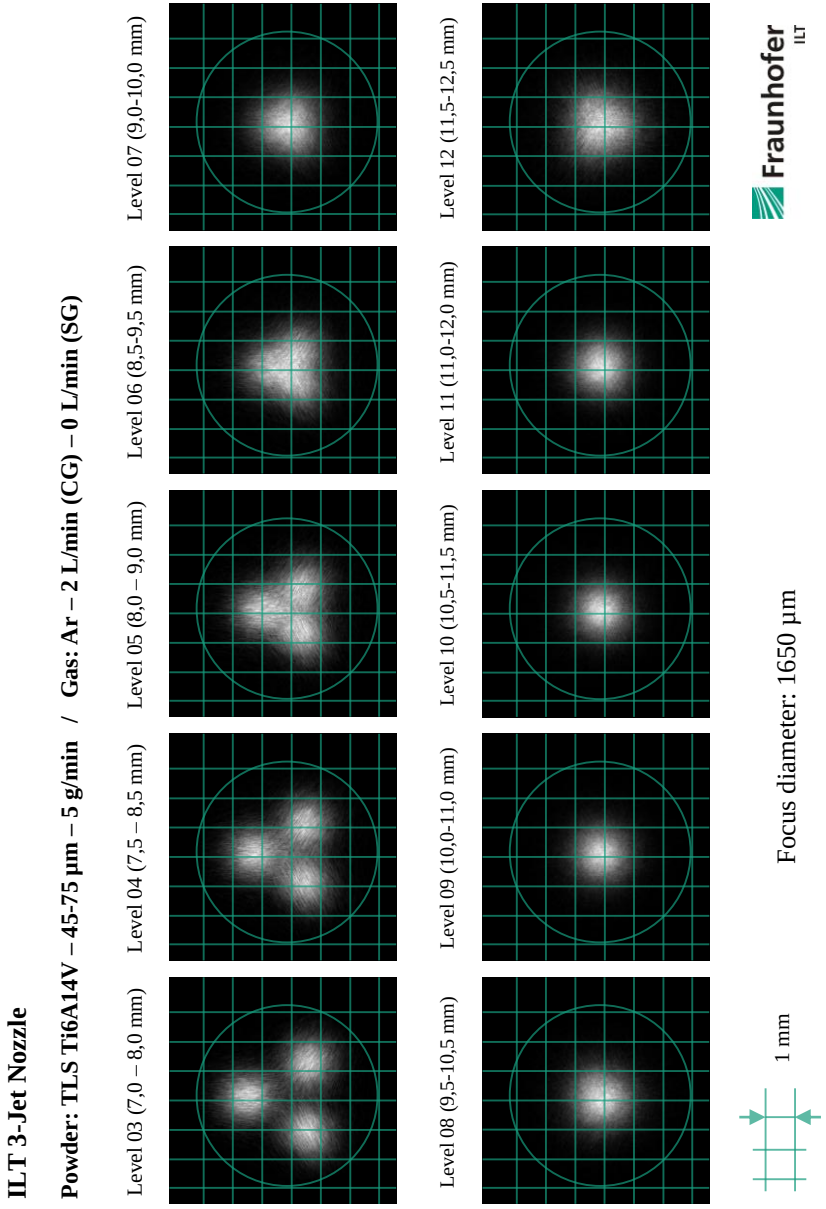

Source: Author.

APPENDIX E - Results of an ILT 3-Jet Nozzle

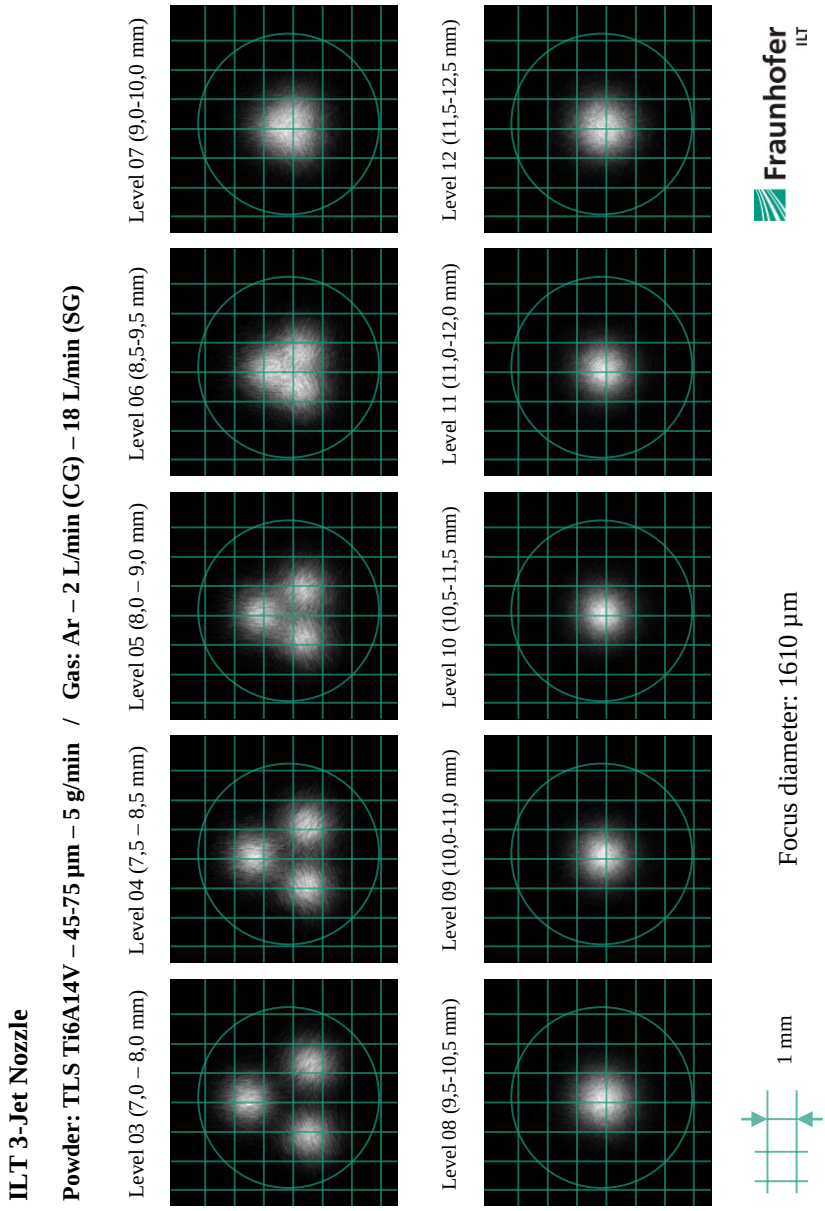

Source: Author.

APPENDIX F - Results of an ILT 3-Jet Nozzle

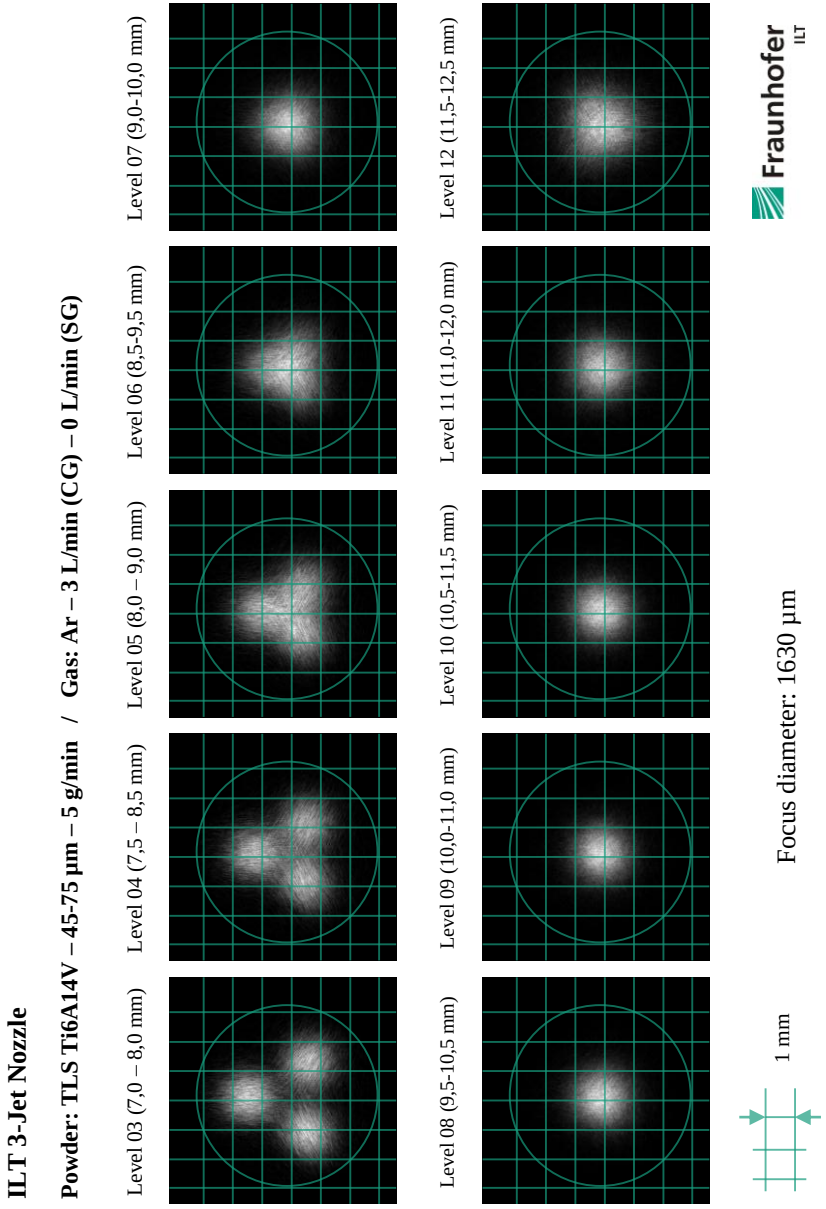

Source: Author.

APPENDIX G – Results of an ILT 3-Jet Nozzle

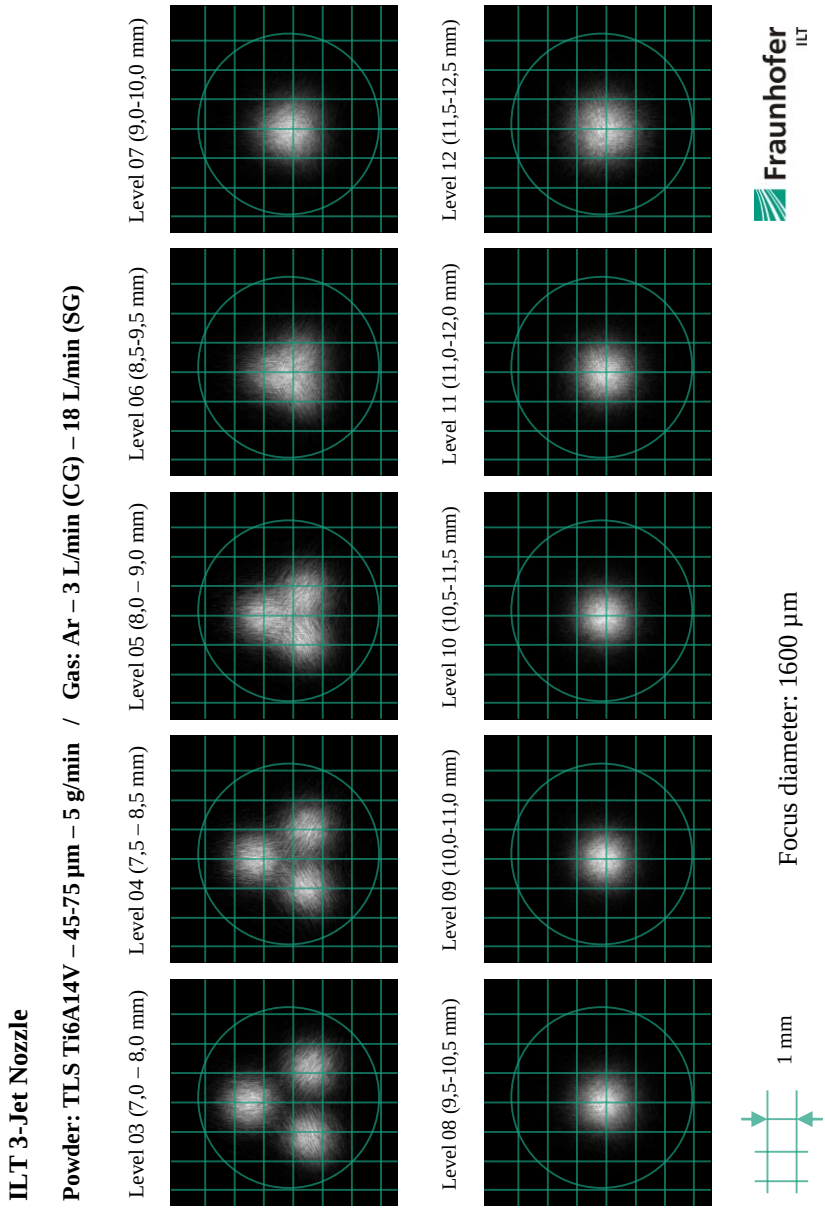

Source: Author.

APPENDIX H – Results of an ILT Ring Nozzle

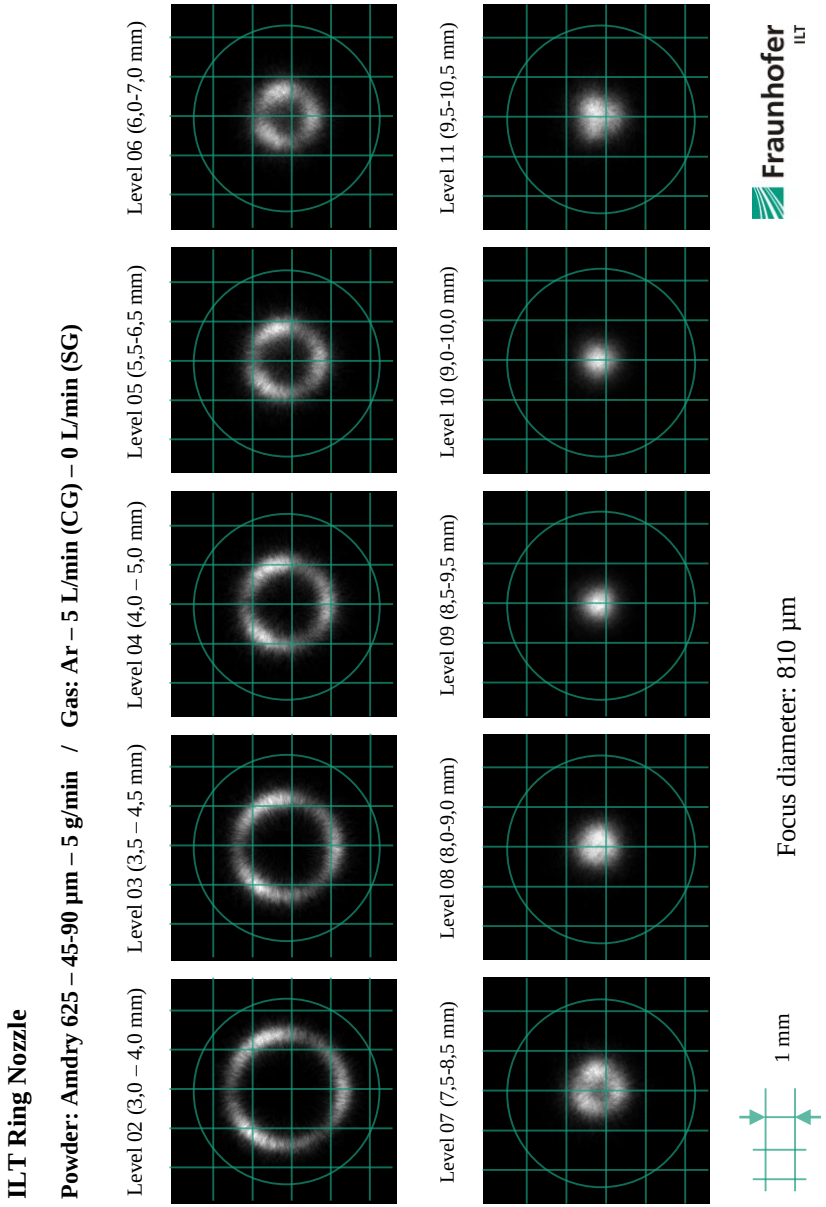

Source: Author.